Investigation into a High Reliability Micro-grid for a Nuclear Facility Emergency Power Supply

Gerard Ratoka Lekhema

A research report submitted to the Faculty of Engineering, University of the Witwatersrand, Johannesburg in partial fulfilment of the requirements for the degree of Master of Science in Engineering

Johannesburg, August 2017

DECLARATION

I declare that this research report is my own unaided work. It is being submitted for the Degree of Master of Science to the University of the Witwatersrand, Johannesburg. It has not been submitted before for any degree or examination to any other University.

Signed on 15 of August 2017

Gerard R. Lekhema

Abstract

The objective of this research work is to investigate the use of a high reliability micro-grid to supply emergency electrical power to a nuclear facility following loss of offsite power (LOOP) accident. Most of the nuclear facilities around the world utilize diesel generators and battery banks as emergency power to back up the grid power supply. This power supply configuration represents the concept of the micro-grid system. The research work proposes reliability improvement of the emergency power supply by introducing diverse energy sources and energy storage systems. The energy sources and storage systems that were investigated include renewable energy sources, decay heat recovery system and large scale energy storage systems. The investigation results presented include information on the suitable energy sources and energy storage system, establishment of the reliable architectural layout and evaluation of the micro-grid system in terms of capacity adequacy and reliability.

To My Family

ACKNOWLEDGEMENTS

Firstly, I would like to thank God for making it possible for me to submit this report.
My sincere gratitude also goes to my wife Lerato and sons, Letuka and Letlotlo for their unconditional love, support and sacrifices.

I am eternally grateful to my supervisor Professor Willem A. Cronje for his guidance, patience and support throughout my research work.

Finally I would like to thank my mentor Dr Ian Korir for his assistance in shaping and reviewing my research work.

Table of Contents

LIST OF FIGURES

LIST OF TABLES

ABBREVIATIONS

AC	Alternating Current
CERTS	Consortium for Electric Reliability Technology Solutions
CSI	Current Source Inverter
CSP	Concentrated Solar Power
DC	Direct Current
DES	Distributed Energy Sources
DFIG	Doubly-Fed Induction Generator
DG/DGs	Diesel Generator / Diesel Generators
EDG	Emergency Diesel Generator
ESS	Energy Storage System
EPS	Emergency Power System
IAEA	International Atomic Energy Agency
IGBT	Insulated-Gate Bipolar Transistor
LOCA	Loss of Coolant Accident
LOOP	Loss of Offsite Power
LPSP	Loss of Power Supply Probability
MCS	Monte Carlo Simulation
MPPT	Maximum Power Point Tracking
PV	Photovoltaic
PWR	Pressurized Water Reactor
RBD	Reliability Block Diagram
RES	Renewable Energy Sources
UPS	Uninterruptable Power Supply
VSI	Voltage Source Inverter
WTG	Wind Turbine Generator

Chapter 1 Introduction

This chapter presents an overview of the research project. The information covered includes background information that motivates the need for research in this area, the research objectives that include the scope of the work, research methodology and research report outline.

1.1 Research Background

In this research work, an investigation is carried out to determine the feasibility of using a micro-grid with renewable energy sources to supply reliable electrical power in a nuclear facility. The nuclear facility is a safety critical application that requires reliable electrical power supply for safe operation. The fundamental safety objective in the nuclear facility is to protect people and environment from harmful effects of ionizing radiation. The safety objective is realized through application of three main safety functions [1]. These functions are control of nuclear reactivity, removal of heat energy from the nuclear reactor core and confinement of radioactive materials [2].

Most of the systems that are used to implement the safety functions require robust and reliable electrical power supply for guaranteed operation. The removal of heat function has high safety significance because after the nuclear reactor is shut down, the irradiated nuclear fuel continues to generate decay heat that requires extended use of cooling systems. The electrical power is required to supply the active cooling systems in standard power reactors (e.g. in nuclear power plants). It should however be noted that small-to-medium size power reactors and non-power reactors rely on passive cooling systems for decay heat removal. In such reactors, the electrical power is crucial mainly for the control and monitoring functions. The unavailability of electrical power to the nuclear facility may hinder the execution of safety functions and this could result in the reactor core meltdown and release of radioactive materials into the environment.

Most of the nuclear facilities worldwide use diesel generators (DGs) and battery banks as emergency backup power sources to ensure uninterruptible power supply following a loss of offsite power (LOOP) accident. The DGs are used as long-term backup power sources (i.e. for up to 72 hours of backup power). The battery banks are normally used to supply low power DC loads and AC loads (through DC-AC converters) for short-term periods (i.e. up to 8 hours) to allow for start-up and loading of the DGs. In order to ensure continuous improvement of safety, operators of the nuclear facilities and various organizations perform periodic safety assessment including research and development (R&D). An international R&D community known as Generation IV International Forum (GIF) is developing advanced next generation power reactors that will possess among others, features such as improved safety and reliability. The routine and periodic safety assessment is normally based on either operating experience or occurrence of nuclear events with high safety significance [5].

One of the nuclear events with high safety significance that has brought about the renewed research interest into the reliability of the electrical power supplies in the nuclear facilities is the Fukushima Daiichi nuclear power plant accident that occurred in March 2011[6]. Organizations, utilities and academics worldwide are currently investigating strategies to improve the reliability of the power supplies in the nuclear facilities [7], [8], [9]. This research work is extensive; however, none of the work is currently investigating the possibility and benefits of using the micro-grid with renewable energy sources.

The micro-grid is a medium-to-low voltage power distribution network comprising distributed energy sources (DES), energy storage devices and controllable loads operated as a single, autonomous grid to reliably supply power either in a host grid connected mode or standalone (islanded) mode [10], [11]. The micro-grid system can offer many advantages in the nuclear installations as compared to the traditional DGs. Progressive developments have demonstrated that the micro-grid systems with renewable energy sources (RES) and energy storage system (ESS) can provide reliable power to safety critical facilities such as hospitals, chemical plants, etc. [12].

The energy sources such as photovoltaic (PV) solar energy and wind energy are attractive environmentally friendly options as compared to the DGs. It is a known fact that fossil fuel reserves globally are continually being depleted and the renewable energy sources are increasingly being introduced into the backup power systems. The renewable sources are not dispatchable. However, the micro-grid system provides a platform for managing the intermittency of the renewable energy sources. Furthermore, the micro-grid system remains online at all times and can autonomously transfer from grid-connected mode to island mode in order to supply emergency power to the nuclear facility. This eliminates the "failure to start" failure mode normally associated with the diesel generators. Under normal conditions, when there is no LOOP accident at the nuclear facility, the electricity generated by the renewable sources can be fed back to the main grid to facilitate recovery of the investment costs.

The above-mentioned benefits portray the micro-grid as an attractive option for use as the emergency power system at the nuclear facilities. However, the established nuclear standards and regulations specify high reliability as the key design basis for the emergency power systems [22]. The reliability of power systems is defined in terms of the ability to operate without failure (reliability) and the ability to supply sufficient power to the load (availability). The micro-grid should be designed to meet these reliability requirements. This makes it indispensable to investigate different technologies and determine the micro-grid layout that conforms to the prescribed reliability requirements.

1.2 Research Objectives and Scope

The main aim of this study is to investigate the micro-grid system that conforms to the reliability requirements of the emergency power supply system at the nuclear facility. The micro-grid with distributed energy sources (DES) that is intended for use in the nuclear facility is defined as a nuclear micro-grid in the context of this research work. The research scope is focused on answering the following key questions:

- What types of distributed energy sources and energy storage systems are suitable for the nuclear micro-grid of high reliability?

- Does the nuclear micro-grid improve the reliability of emergency power system at the nuclear facility?

Koeberg nuclear plant located near Melkbosstrand in Cape Town, South Africa is used as a reference plant in this study.

1.3 Research Methodology

The methodology that is adopted in this study includes: a review of literature to gain understanding of the nuclear facility and micro-grid power systems; suitability analysis of the energy sources, energy storage systems and control strategies to determine the nuclear micro-grid system that conforms to the reliability requirements; and performance evaluation of the nuclear micro-grid in terms of capacity adequacy and reliability.

1.4 The Report Outline

This report details the outcomes of the investigation that was carried out to determine the nuclear micro-grid layout. The information presented contributes to the knowledge of reliability improvement for power systems in the nuclear facilities. The contents of this report are structured as follows:

- Chapter 2 provides a review of literature on the nuclear facilities emergency power supply systems, the design basis for the power systems of high reliability, the micro-grid systems and current research work on nuclear facilities power supply systems.
- Chapter 3 details analysis of the various energy sources to determine their suitability for integration into the nuclear micro-grid system.
- Chapter 4 provides analysis of the various energy storage technologies to determine their suitability for integration into the nuclear micro-grid system.
- Chapter 5 details analysis on control systems and architectural layout that can be utilized to improve the performance and reliability of the nuclear micro-grid.

- Chapter 6 presents capacity sizing analysis of the nuclear micro-grid renewable energy sources and energy storage system to confirm that the nuclear micro-grid has adequate capacity to supply the loads of the safety systems.
- Chapter 7 presents a reliability analysis of the nuclear micro-grid.
- Chapter 8 provides a conclusion of the research work and recommendations for future work.

1.5 Summary

The background information on the research area, research objectives including work scope, research methodology and report outline were presented in this chapter. The next chapter presents a literature review on the emergency electrical power systems at the nuclear facilities, the design basis for emergency power systems, micro-grid systems and the current research work on improvement of the nuclear facilities emergency power supply systems.

Chapter 2 Literature Review

An overview of electrical power systems in the nuclear facilities and the micro-grid systems is presented in this chapter. The information discussed summarizes the design basis for the power systems of high reliability, emphasizes the need for reliable electrical power supply in the nuclear facilities and explores the current research work on improvement of emergency power supply systems in the nuclear facilities.

2.1 Electrical Power in Nuclear Facilitates

Electricity plays an important role in ensuring safe operation of nuclear facilities. Most of the safety systems that carry out functions such as monitoring, reactor protection and removal of heat from the nuclear reactor require reliable electrical supply for guaranteed operation. The electrical power should be available to the safety systems under all operational conditions of the reactor. The operational conditions include normal operation, anticipated operational occurrences, design basis accidents and beyond design basis (severe) accidents. A unique characteristic of the nuclear reactor is that after it has been shut down, it continues to generate decay heat energy. When in operation, the nuclear reactor generates heat from fission of heavy atoms of isotopes such as uranium. The by-products emanating from the fission process are highly radioactive and unstable. The nuclear reactivity is shut down primarily by full insertion of control rods into the nuclear reactor. After shut down, the fission products continue to decay, producing beta particles and gamma rays that generates significant amount of thermal energy.

The decay heat present in the reactor immediately after shut down is about 7% of the thermal power level that the reactor operated at prior to shut down [13]. A 2785 MW power reactor will continue generating approximately 195 MW of thermal power immediately after shutdown. The decay heat follows a logarithmic decay graph over time. This means that the residual heat will be 7% after shutdown, 2% at 1 hour, 1% at 5 hours, 0.5% at 1 day, 0.1% at 10 days and so on [14]. The generated decay heat requires continued operation of the reactor core cooling systems in order to prevent the overheating of the reactor core and nuclear fuel meltdown.

As an example, if the cooling systems are not operational after the 2785 MW reactor is shut down, 40 Giga joules of heat energy would accumulate in 5 minutes after the shutdown. The decay heat is the principal reason of safety concern in the facilities that utilize nuclear reactors. The active and or passive reactor core cooling systems are required to continually remove the decay heat after the reactor has been shut down. The standard power reactors rely mainly on active cooling systems for decay heat removal. The low power reactors (e.g. research reactors, small and medium size reactors, etc.) rely on passive cooling systems. The active cooling systems require reliable electrical power to drive the cooling pumps whereas passive cooling systems rely on gravity, compressed gas, natural circulation and evaporation to transfer heat from the core [15].

Two major nuclear incidents that emphasize the safety significance of decay heat removal and reliable electrical power supply at the nuclear facilities are Three Mile Island (TMI) and Fukushima Daiichi nuclear power plants accidents. The accident at the TMI occurred on 28 March 1979. The plant is comprised of 2 pressurized water reactor units with unit 1 rated at 800 MW (electrical) and unit 2 at 906 MW (electrical). The accident happened at 4 am when the reactor of unit 2 was operating at 97% power level [16]. A malfunction occurred in the secondary cooling circuit and this resulted in automatic shutdown of the reactor. However, a pressure relief valve failed to close and the primary circuit coolant drained out. As a result, the decay heat in the reactor core was not removed and core suffered severe damage. Approximately 43, 000 curies of radioactive krypton-85 gas and 20 curies of hazardous iodine-131 were released into the surrounding environment [17].

The accident at the Fukushima Daiichi took place on 11 March 2011. The Fukushima plant is comprised of 6 boiling water reactors with rated electrical output power of 460 MW for unit 1, 784 MW for units 2-5, and 1100 MW for unit 6 [18]. The accident was initiated by an earthquake of 9.0 magnitude. At the time of the earthquake, units 1 to 3 were operating at full power and units 4 to 6 were on shutdown. The operating units were automatically shut down in response to the earthquake. All offsite power was lost and the onsite emergency diesel generators started automatically. However, about an hour after the earthquake, the plant was hit by two tsunami waves.

The diesel generators, battery banks and electrical switch boards were inundated in water and the electrical power to the monitoring and cooling systems was lost resulting in a condition known as a station blackout. As a result, the decay heat in reactor units 1 to 3 was not removed and the cores suffered significant damage. After the hydrogen explosions, the containment buildings of the 3 units (including unit 4) were damaged and significant radioactive materials were released into the environment. The detailed sequence of the Fukushima accident is documented in International Atomic Energy Agency (IAEA) report [19].

2.2 Design Basis for Emergency Power Supply Systems

Safety in the nuclear facilities is governed and enforced by local and international nuclear safety authorities. The local nuclear authority in South Africa is National Nuclear Regulator (NNR). The role of the NNR is to provide regulatory oversight of safety at the nuclear facilities through establishment of safety standards and regulatory practices. The electrical power systems at the nuclear facilities are designed and maintained according to stringent regulations and standards in order to achieve high reliability and availability. The provisions incorporated into the systems design minimize the possibility of loss of electrical supply to the safety systems during the design basis events and some of the beyond design basis events. The basic layout of the power systems includes normal power supply (offsite grid power) and emergency power supply (onsite back-up power) systems.

The normal power supply is the preferred source of power and supplies both safety and non-safety systems during start-up and shutdown states (in both normal and accident conditions). In most countries, offsite grid power is considered to have higher availability and reliability than onsite backup power because of diverse and multiple generators connected to the offsite transmission system [20]. A minimum of two independent offsite grid transmission lines are required for supplying power to the nuclear facility. Operating experience has shown that extreme eternal events such as hurricanes, tornados, earthquakes and tsunamis have a significant impact on the transmission grid for the offsite power supply.

The emergency power system (EPS) is used as backup to the offsite power and supplies power to the safety loads during a loss of offsite power (LOOP) event. The main power sources of the EPS in the current nuclear facilities (i.e. Koeberg Nuclear Power Plant) are diesel generators and battery banks. The EPS supplies power to AC loads and DC loads. The high power AC loads that allow certain degree of power interruption are supplied directly from the diesel generators. The AC and DC loads that do not permit power interruptions are supplied from the DC bus with battery banks and DC-AC inverters. The general illustration of power supplies for nuclear facility is given in figure 2.1.

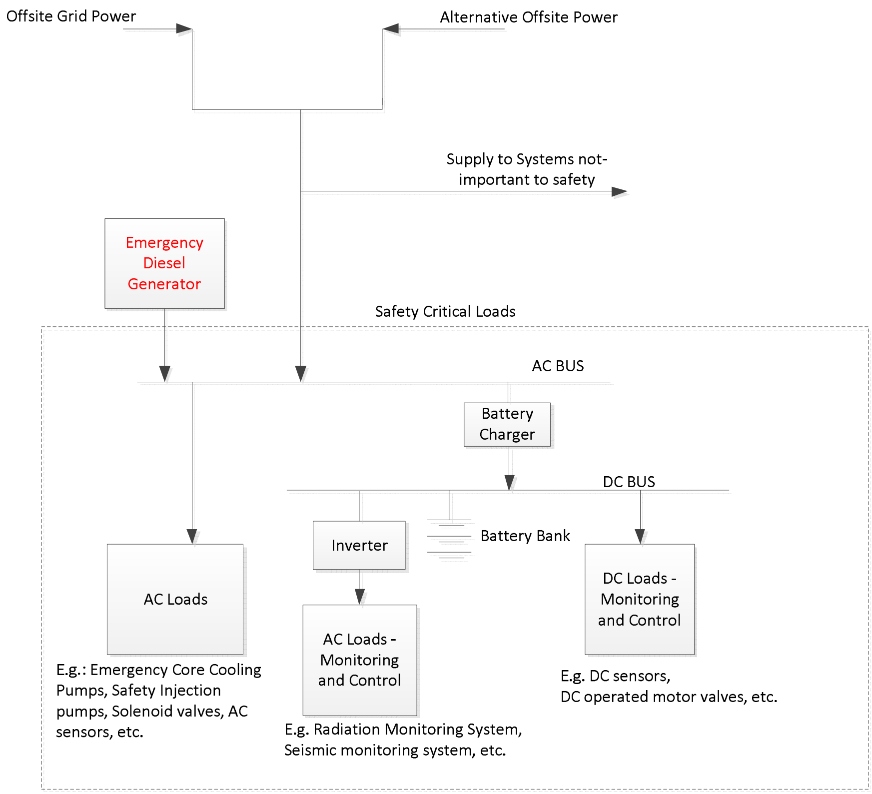

Figure 2.1: Layout of Electrical power supply at the nuclear power plant

The design basis for the EPS of high reliability and availability includes the following requirements [21], [22], [23]:

(a) The effects of common cause failures on the EPS should be addressed during design, maintenance, testing and operation of the EPS. The redundant, diverse and independent power sources and electrical systems should be used to protect the

EPS against common cause failures. The independence of the systems should include physical separation and functional isolation.

(b) The architecture of the EPS should conform to the single-failure criterion requirement. The criterion states that any single detectable failure within the EPS should not result in loss of the capability to supply power to the safety loads. The single failure includes multiple failures resulting from the single failure and spurious actuation of systems. The single failure analysis establishes the minimum redundancy of the EPS such that the supply of electrical power can be accomplished assuming occurrence of a single failure.

(c) The EPS should have sufficient capacity and capability to supply power to the safety loads. The capability of the EPS includes meeting maximum starting power demands during start-up load sequencing. The capacity includes the sufficient supply to all the safety loads and sufficient energy reserves to supply power for the minimum required period. After the Fukushima Daiichi accident, the minimum capacity of the EPS has been increased from 48 hours to 72 hours by most of the nuclear authorities [37].

(d) The EPS should be designed with high quality equipment and incorporate features such as testability, maintainability and fail safe design.

(e) The EPS should be qualified by type tests, previous operating experience and analysis in order to substantiate the capability of meeting the performance requirements. Environmental qualification measures such as seismic qualification and other external environmental conditions should be taken into consideration when designing the EPS.

(f) The EPS should have provisions for periodic testing and inspections. Sufficient instrumentation and control equipment should be provided so that the performance status of the EPS is properly monitored.

(g) The EPS control and protection systems should be provided to limit the performance degradation of the EPS. The protective devices should be properly sized, calibrated and coordinated to protect against electrical faults. The power quality (voltage and frequency) should be controlled such that the performance of the safety loads is not compromised.

(h) Deterministic safety assessment should be carried out to demonstrate the reliability and availability of the EPS. Where reasonable indication exists that the EPS design does not meet the deterministic criteria discussed above [(a) to (g)], then a probabilistic risk (safety) assessment that analyses multiple failures should be carried out.

These design requirements will be used as a basis to establish the layout of the nuclear micro-grid in this study. Figure 2.2 on page 12 illustrates the architecture that implements the ESP design requirements highlighted above. The multiple diesel generators and battery banks illustrated in figure 2.2 show that the EPS is indeed a micro-grid when operating in emergencies (during LOOP accident). The subsequent section provides further information on the micro-grid systems.

2.3 Micro-grid System

The micro-grids have been in existence long before the inception of the traditional (macro) grid. The formal definition and requirements of the micro-grid concept have then been developed in a bit to upgrade the traditional grid into smart-grid with renewable energy sources [3]. The detailed characteristics of the micro-grid system and existing micro-grids are discussed in this section.

2.3.1 Micro-grid System Description

The micro-grid system provides a platform for reliable integration of on-site distributed energy sources (DES), including energy storage system (ESS) and controllable loads.

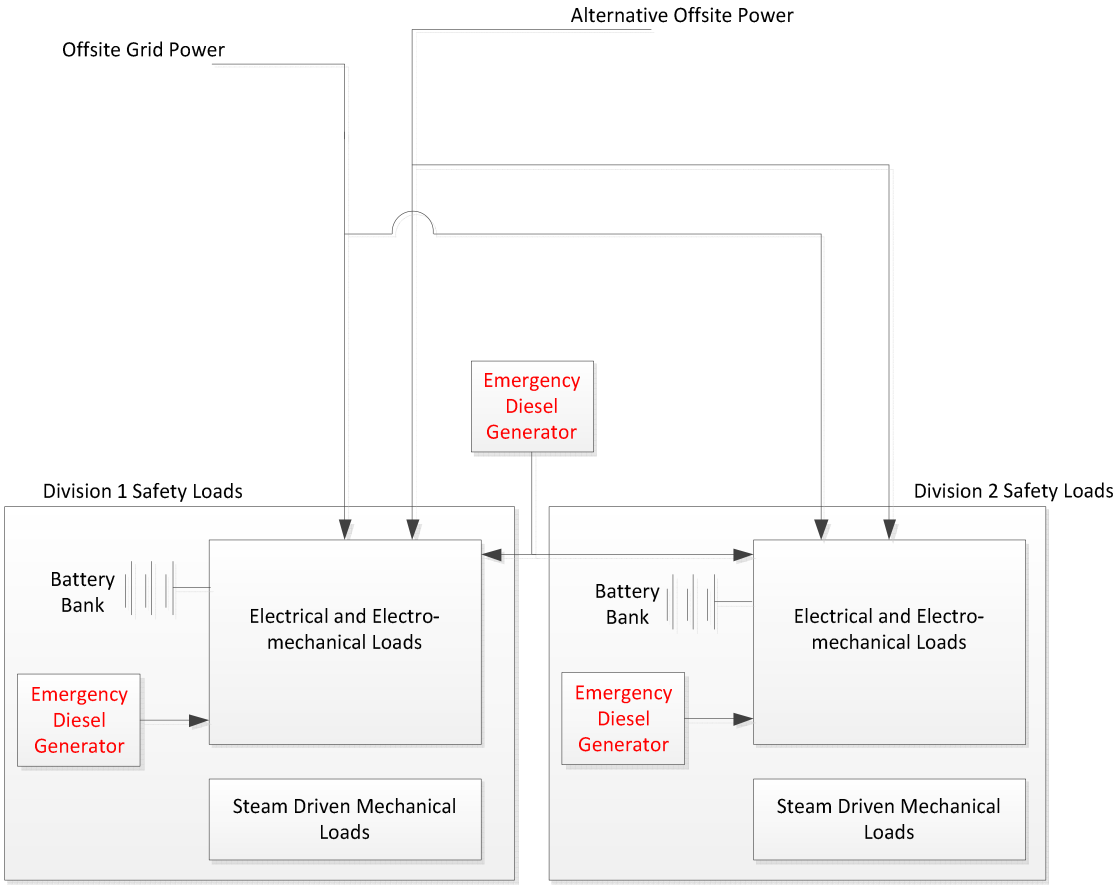

Figure 2.2 Architecture of EPS illustrating redundant and diverse systems

The micro-grid is basically described as a system comprising loads, DES and ESS controlled as a single entity with clearly defined electrical boundaries and connected to the main grid through a single point of common coupling (PCC) [24], [25]. Depending on the dominant type of load supplied, the micro-grid can be configured with either AC or DC grid. The micro-grid can operate in either grid-connected mode or stand-alone (islanded) mode. An important feature of the micro-grid is the provision for seamless transition between the two modes. The disconnection of the micro-grid from the main grid can either be scheduled or unintentional. The scheduled islanding of the micro-grid can occur during scheduled main grid maintenance and also when the power quality of the main grid falls below acceptable thresholds.

The unintentional islanding can occur due to unplanned events such as main grid faults and blackouts. The micro-grid functions as an emergency power supply system in islanded mode. The provision for use of multiple DES in the micro-grid makes it an appealing alternative for integration of the renewable energy sources into the power systems that supply electricity to safety critical applications. The DES in the micro-grid depends on a variety of factors that include location and availability of different technologies. The typical DES include solar energy, wind energy, ocean energy (i.e. wave and tidal), geothermal energy, chemical energy (i.e. hydrogen fuel cells) and heat energy from combustion of fossil and renewable fuels (i.e. micro-turbine, gas-turbine, reciprocating engine, etc.).

The typical ESS used to store electricity generated by DES include batteries (static and flow types), super-capacitors, compressed air, pumped hydro, flywheel and hydrogen (generated through electrolysis). The single line diagram exhibiting the basic architecture of the AC micro-grid is illustrated in figure 2.3, on page 14. The layout of this architecture confirms the fact that the EPS in the nuclear facilities is indeed the micro-grid system that is restricted to islanded operation only. Other systems such as large ships and remote facilities are essentially micro-grids because they are independent grids and operate as single controllable entities.

The integration of multiple DES into the micro-grid introduces several operational challenges for the micro-grid system. The challenges include difficulty in designing protection schemes for the system with bidirectional power flow, stability issues and power quality issues including low inertia effects of the power sources that are interfaced to the grid with power electronics. These issues have been thoroughly investigated by several researches and solutions to address the issues have been developed [26], [27], [28]. Therefore, this research work focuses on the application of the micro-grid in the nuclear facilities.

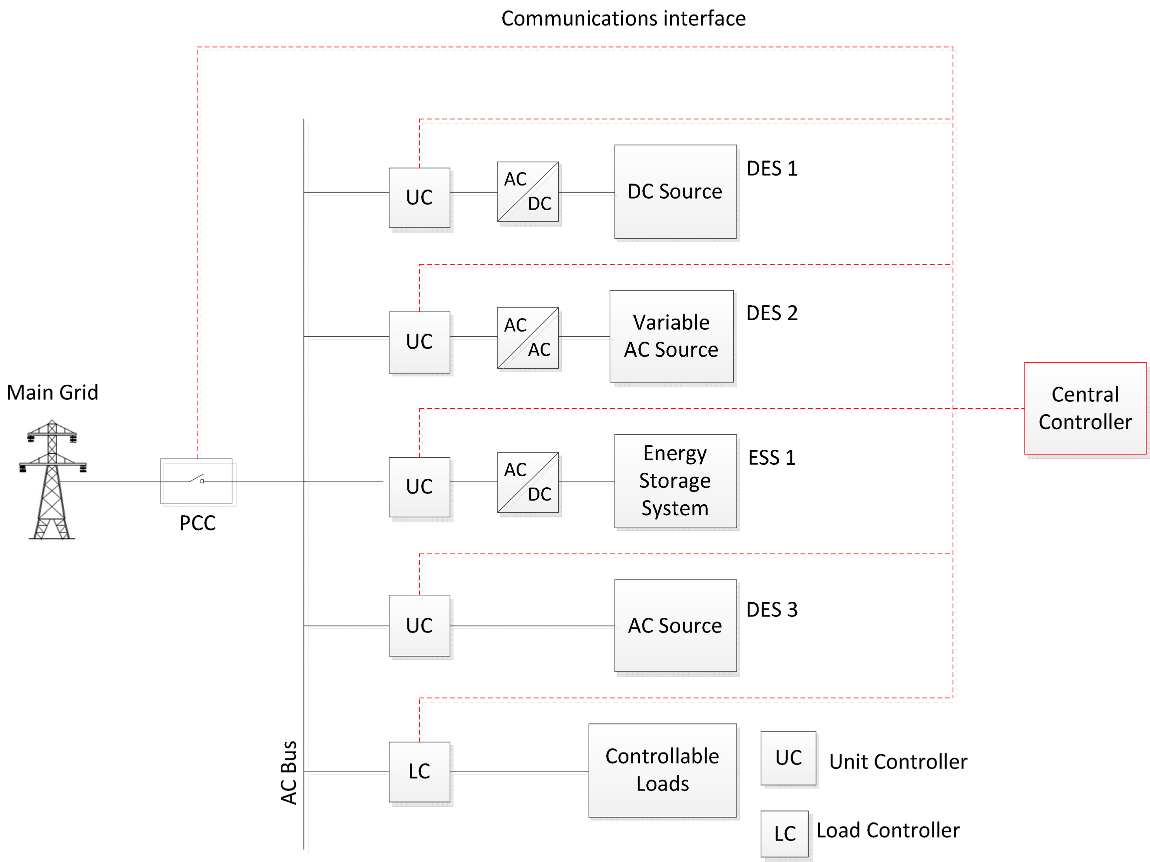

Figure 2.3: Single line diagram illustrating the basic architecture of the 3 phase AC micro-grid system

2.3.2 Examples of Micro-grid System

There are various micro-grid projects that have been developed around the world to demonstrate the reliability and other benefits of the micro-grid system. One of the projects is Consortium for Electric Reliability Technology Solutions (CERTS) micro-grid operating at the Santa Rita Jail. The system is crucial for the safety of officers, staff and inmates and is used to provide reliable power to the jail. It is comprised of 1.2 MW of photovoltaic (PV) power, 1 MW hydrogen fuel cell, 2 MW – 4 MWh Li-ion battery bank and two 1.2 MW diesel generators [30]. Another project is the New Energy and Industrial Technology Development Organization (NEDO) micro-grid operating at the campus of Tohoku Fukushi University in Sendai City in the Tohoku district in Japan.

The micro-grid is comprised of two 350 kW gas engine generators, 250 kW molten carbonate fuel cell, 50 kW (peak) PV power and 600 Ah valve-regulated lead acid battery banks. The loads supplied by the micro-grid include university buildings, a hospital and a high school. The resilience of the micro-grid was demonstrated during the March 2011 earthquake and tsunami. The PV and battery bank power was not lost during the event and the gas generators power was restored within one day [31].

2.4 Current Research on Nuclear Power Supply Systems

Research on the improvement of nuclear power supply system's reliability is an on-going process. The contributing factors to the research include operating experience and safety significant events such as natural disasters (earthquakes, tsunamis, hurricanes, floods, ice storms, etc.). The severe natural and man-made disasters that caused significant damage to grid power infrastructures resulting in long-lasting (up to several months) power outages are documented in [32]. The Fukushima Daiichi nuclear plant accident has also significantly contributed to the renewed interest into the research to improve the backup power supplies in the nuclear facilities. Some of the lessons that were learnt from the accident and the solutions for improvement of the nuclear systems are documented in [33] and [34]. The identified solution for improving the backup power supplies include:

- Diversification of AC backup power sources
- Provision of portable AC emergency power sources and connection points for the power sources.
- Waterproofing and installation of power systems at elevated locations.
- Provision of increased capacity of installed DC power source
- Provision of portable or backup DC power supplies

The nuclear facilities operators and nuclear regulators around the world have adopted differing improvement strategies based on each country's indigenous external hazards. The United States Nuclear Regulatory Commission (US NRC) has adopted diverse and flexible coping strategies (FLEX) that include provision of portable diesel generators, portable DC power supplies and diesel fuel storage for extended supply [35].

Countries such as Finland, South Africa, Japan, France, etc. have also adopted the use of portable diesel generators or gas turbine generators in the existing nuclear facilities. Electrical Research Power Institute (EPRI) conducted a research on the use of hydrogen fuel cells as alternative DC power backup in the existing nuclear facilities. The research includes investigation of different types of fuel cells including the installation footprint of the fuel cells as compared to the battery banks [7]. The research concludes that the proton exchange membrane fuel cell system shows good potential for use as DC-backup power system and should be investigated further.

The use of hydrogen fuel cells in the future new nuclear power plant has previously been investigated in [36]. The investigation assessed the reliability of the fuel cells as compared to the diesel generators and concluded that the fuel cells can provide similar reliability characteristics. None of the research work discussed above has investigated the use of the micro-grid system with environmentally sustainable energy sources (i.e. RES). This is primarily because the RES were not identified as potential improvement solution in references [33] and [34]. Therefore, this research work focuses on addressing this knowledge gap.

2.5 Summary

The detailed background information on electrical power systems at the nuclear facilities and the micro-grid systems was examined in this chapter. The information acquired from existing literature include the importance of electrical power in the nuclear facilities, design basis for nuclear facilities emergency power supply systems, the micro-grid system layout and current research work on improvement of the nuclear facilities emergency power supply systems. The next chapter presents an analysis on energy sources that complies with the design requirements for the nuclear facilities power supply systems.

Chapter 3 Energy Sources Analysis

Energy sources that are suitable for integration into the nuclear micro-grid are analysed in this chapter. The suitable energy sources should be compliant with reliability requirements highlighted in section 2.2. The deterministic methodology used to establish the suitable energy sources include availability assessment, technology maturity assessment, assessment of impact on nuclear safety and environmental sustainability assessment. The mature technologies provide conservative compliance to reliability requirements because their characteristics are well understood. The location of Koeberg nuclear power plant (Melkbosstrand) is used as the reference location for availability assessment of the renewable energy sources (RES).

3.1 Solar Energy

The African continent has the highest level of solar energy density as compared to any other continent on earth. The parameters that are used to measure the solar energy level are insolation level (sunlight intensity) and ambient temperature. The majority of areas in South Africa receive an average of more than 2500 hours of sunlight per year with solar insolation levels of between 4.5 kWh/m^2 and 6.5kWh/m^2 per day [38]. The monthly solar irradiation averages were calculated from the hourly trend for Melkbosstrand recorded in 2009. The monthly average irradiation trend is depicted in figure 3.1. The area has average irradiation level of 228 W/m^2 with maximum of 1235 W/m^2 and minimum average of 131 W/m^2. The 2009 hourly average temperature record for the Melkbosstrand is depicted in figure 3.2. The highest temperature recorded in this area is 37.7 ^{0}C.

The most mature technologies used to convert solar energy into electrical energy are photovoltaic (PV) system and concentrated solar power (CSP) system. The PV system converts solar radiation directly into DC electrical energy using PV cells. The CSP system converts solar energy to electricity indirectly by utilizing reflectors to focus sunlight to heat exchangers that drive turbines to generate electricity.

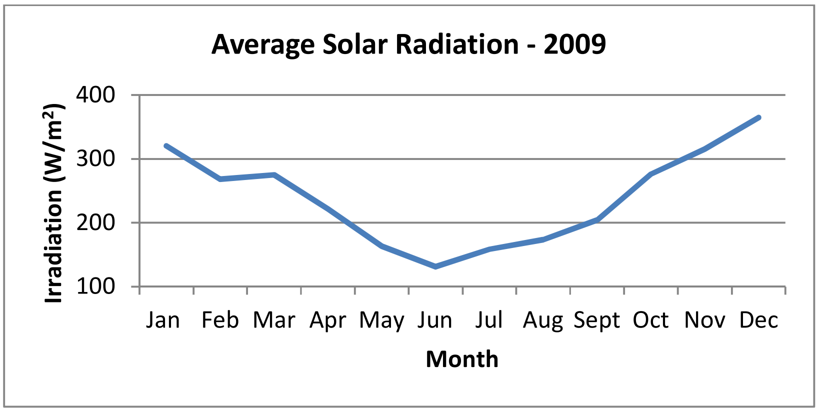

Figure 3.1 Average solar radiation levels for the year 2009

The advantages of the PV system over CSP system include better efficiency, simplified implementation and better reliability [39]. The reliability of the PV system is attributable to direct conversion of solar energy to electricity with no moving parts. Furthermore the PV modules can be installed at onsite area such as rooftops of the nuclear facility whereas the CSP system requires offsite location for installation. The main advantage of the CSP system is the inherent thermal storage feature that is used to generate electricity after sunset or when it is cloudy. On the contrary, PV system usually requires a separate energy storage technology to store electricity. The energy storage options are discussed further in chapter 4.

The PV plants are currently the preferred choice globally with the installed capacity reaching 227 GW in 2015 as compared to 4.8 GW for CSP plants [40]. In South Africa, the installed capacity recorded in February 2016 is 964.98 MW and 200 MW of PV and CSP plants respectively [41]. The South African government plans to install a total capacity of 8400 MW PV power and 1000 MW CSP over a period of 20 years (2010 – 2030). The significant installed capacity of PV systems shows the maturity of the PV technology and provides a wealth of operating experience and continuous improvement of the PV technology. The above mentioned benefits make the PV system the suitable technology for the nuclear micro-grid as compared to the CSP system.

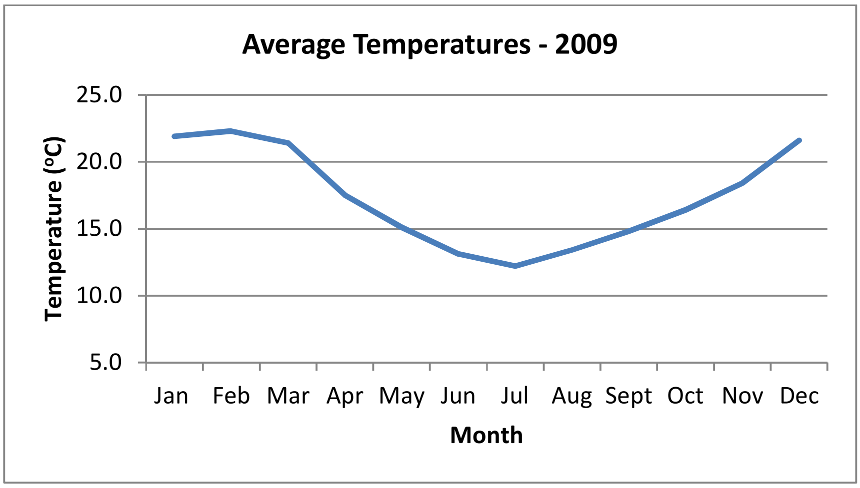

Figure 3.2 Average temperatures for the year 2009

The basic components of the PV system include PV solar arrays and DC-AC inverters to convert generated DC electricity into AC electricity. The PV solar array is composed of PV panels with each panel assembled from several PV modules and each PV module comprised of several PV cells. Efficiency is a crucial factor that needs to be taken into consideration when selecting the PV system for the nuclear micro-grid. High-level guidelines on selection of main PV system components with optimized efficiency are provided as follows:

- **PV panel:** The PV panels with the highest output efficiency, long life-cycle (typically 20 years), with simple and robust architecture should be used for the nuclear micro-grid. The PV module efficiency refers to how efficient is the PV module in converting solar energy into electrical energy. The PV cell efficiency is measured under standard test conditions (STC) of 1000 W/m^2 light intensity and temperature of 25 ^{0}C. The commonly used material for the PV cells is crystalline silicon. The typical commercial single-crystal (mono-crystalline) silicon modules exhibit low-complexity of cell architecture and a robust production process. These modules have typical efficiencies of about 16-18% [42]. The improved silicon PV module has been developed by Fraunhofer, Germany and has module efficiency of 25.1 ± 0.5 % with designated illumination area of 4.01 cm^2 [43].

The poly-crystalline and ribbon silicon modules are slightly less expensive but at the expense of reduced efficiency. The other types of PV cells are thin-film, group III-V multi-junction, tandem, and organic polymer cells [44]. The output efficiency of the PV module is normally improved by using optical concentrators and cell cooling methods (active and passive). The optical concentrators such as Fresnel lenses direct more sunlight onto the PV module. The output of the PV module is inversely proportional to the ambient temperature. Melkbosstrand does not have a hot climate as depicted in figure 3.2 and therefore, the PV cell cooling methods are not necessary for the nuclear micro-grid. The most efficient PV module with efficiency of 43% is constructed with high efficiency PV cells (46%) and high efficiency Fresnel lens (95%) [45]. However, the technology used in this PV module is at early stage of development and therefore considered not yet suitable for the nuclear micro-grid.

- **PV array installation area:** A detailed analysis should be made for the installation area of the PV array. The required total installation area is dictated by the type of PV panels used (power density in watts per square meter) and the maximum power rating of the PV system. The increase in PV module efficiency results in decrease in the total surface area of the PV panel per watt.

- **Tilt angle and orientation for PV panels:** The PV panels should be oriented towards the solar window in order to receive maximum amount of solar radiation during different seasons of the year. Various researches conclude that north oriented PV panels receive higher solar radiation for countries in the southern hemisphere [46], [47]. Three options used for PV panels tilt angle are fixed tilt angle, monthly adjustable tilt angle and solar tracking system. The PV array with fixed angle of about 30^0 (with reference to installation area latitude) provides optimum power output as supported by [48]. The monthly adjustable tilt angle improves PV system output energy by about 6% [49]. The solar tracking system exist in either mechanical (passive) or electronic (active) options. The passive trackers have drawbacks of losing the sun direction during cold weathers [34].

The active trackers improve the PV system output by about 13% for single-axis trackers and about 25% for dual axis trackers. Although, the adjustable tilt and sun tracking systems increase the PV system output, but the main drawback is that they also increase the complexity of the PV arrays as compared to fixed-tilt arrays [46]. Therefore the most suitable option for the nuclear micro-grid is considered as the fixed-tilt PV system in order to reduce the inherent failure modes of the system.

3.2 Wind Energy

Availability of wind energy depends on the geographical location of various regions globally. The region around equator receives highest level of heat from the sun as compared to the rest of the world. This uneven heating of the Earth's surface results in air pressure difference that causes air to circulate from regions of high pressure to regions of low pressure. The amount of kinetic energy available in the circulating air (wind) depends primarily on the wind speed. Wind turbines are used to convert the kinetic energy into useful form of energy such as electrical energy. The rate of energy transfer (power) from the wind to the wind turbine is determined using equation 3.1 [50].

$$P = \frac{1}{2}\rho A V^3 \qquad (3.1)$$

Where P is the mechanical power in the moving air (watts), ρ is air density (kg/m^3), A is area swept by the rotor blades and V is air velocity (m/s)

South Africa has a good wind energy potential mainly along the coastal regions of Western Cape and Eastern Cape as portrayed on the wind atlas of South Africa (WASA) [51]. Figure 3.3 shows the average monthly wind speed calculated from the annual hourly wind speed record for Melkbosstrand, Cape Town. The wind speeds frequency distribution portrayed in figure 3.4 shows 4 – 8 m/s as the most prominent wind speed at Melkbosstrand. The speed threshold that determines the potential for wind to generate electricity is determined by the specifications of the wind turbine. These specifications are cut-in speed, rated speed and cut-off speed.

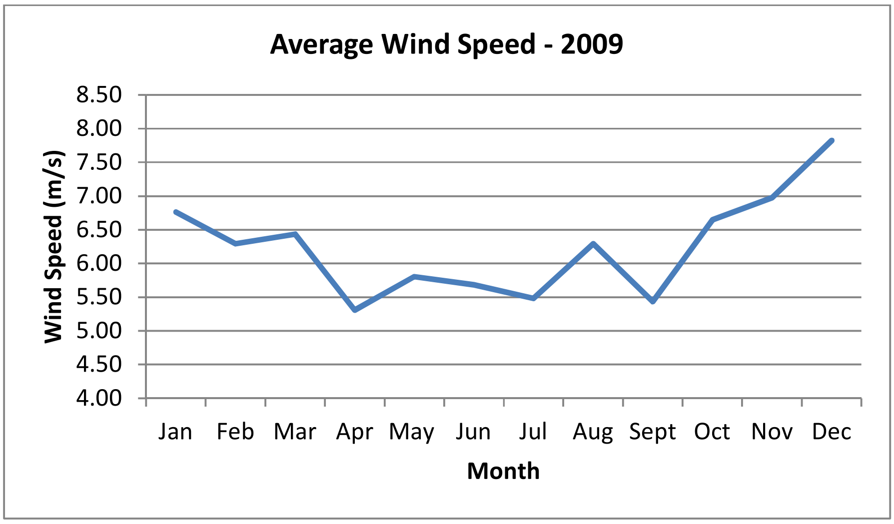

Figure 3.3: Average wind speed for the year 2009

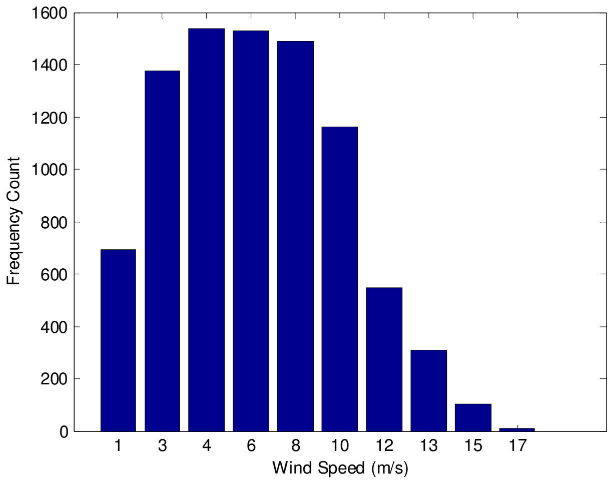

Figure 3.4: Frequency distribution of prominent wind speeds for 2009 wind speed record

The cut-in speed is the minimum speed at which the wind turbine starts rotating and depends on the turbine aerodynamic specifications and electrical output power specification. The rated speed is the speed at which the wind turbine generates the rated output power and the cut-off speed at which the wind turbine is shut off to prevent damage to the turbine.

A typical 2.3 MW wind turbine is rated at wind speed of 12 – 13 m/s with cut-in speed of 3 – 4 m/s and cut-off speed of 25 m/s [52]. The wind turbines can be installed either onshore or offshore. Although wind speeds are much higher at offshore locations, however, the onshore wind turbines are considered to be the most mature and cost-effective of all renewable energy technologies [30]. The wind power is the second most utilized renewable energy source after hydropower. The total global installed capacity of electrical power from wind turbines reached 433 GW in 2015.

In South Africa, the installed capacity recorded in February 2016 is 969.98 MW and the South African government plans to install the total capacity of 8400 MW onshore wind turbines over a period of 20 years (2010 – 2030) [31]. The availability of wind energy in Melkbosstrand and the technology maturity of onshore wind turbines confirm the suitability of wind energy as the energy source for the nuclear micro-grid. The basic components of a typical horizontal axis wind turbine are a tower structure, a rotor with two or three blades attached to the hub, a yaw mechanism (i.e. tail vane) and a nacelle that houses a shaft with mechanical gears, an electrical generator and power control system. High-level guidelines for determination of the wind turbine sitting are provided as follows:

- For optimal generation of electricity, the wind turbines must be installed at a high altitude and away from objects that can cause wind flow obstruction. The height of the wind turbine is usually the combination of the tower structure height and the installation area altitude.
- The site of the wind farm must be far enough from the nuclear facility to minimize noise interference and yet close enough to reduce the length of cabling from the farm to the nuclear facility.
- The optimum spacing of the wind turbines in the wind farm must be ensured in order to harvest optimum wind energy annually. Recommendations provided in [40] suggest the spacing between two turbines in the wind direction must be 8 to 10 rotor diameters apart and 2 to 4 rotor diameters apart in the cross-wind direction.

- The wind turbine hub should be protected against direct and side lightning flashes according to the requirements specified in IEC 62305 standards [127].

3.3 Ocean Energy

Melkbosstrand is located close to the Atlantic Ocean and hence ocean energy is a potential option for use as one of the nuclear micro-grid energy sources. Ocean energy includes all forms of renewable energy sources that can be harnessed from the ocean by means of ocean waves, ocean tides, ocean currents, temperature gradients and salinity gradient. The wave and tidal energies are the only commercialized forms of ocean energy. The ocean waves are basically caused by water absorbing the wind kinetic energy. Several wave power systems with power ratings from 40 kW up to 0.5 MW have been installed and connected to the grid in countries like United Kingdom, United States of America and Spain [53]. In South Africa, a wave energy converter with maximum generating capacity of 770 MW was developed by University of Stellenbosch but has not been implemented for commercial power generation [54].

Tidal energy is a form of hydropower that results from rise and fall of sea levels due to the tides and water movement caused by gravitational attractions between the earth and the moon. The tidal energy is highly predictable and has much higher energy density as compared to wind [30]. The two largest projects that utilize tidal energy are a 254 MW power plant in Republic of Korea that commenced operation in 2011 and a 240 MW power plant in France that commenced operation in 1966 [30]. The commercial implementation of ocean energy technology is still not yet fully developed because most of the technologies are still in various prototype and demonstration stages. The harsh ocean environmental conditions are some of the main challenges that are hindering progress in development of the ocean energy. It is therefore concluded that the ocean energy is not a suitable energy source option for the nuclear micro-grid at the current stage.

3.4 Decay Heat Recovery System

The nuclear reactor continues to generate significant amount of decay heat after it has been shut down. The detailed discussion on this nuclear reactor characteristic is provided in section 2.1. The decay heat is a potential energy source that can be used as one of the nuclear micro-grid energy sources. The decay heat can be used after reactor shut down to supply power to the safety loads that are required to safely bring the reactor to a cold shut down condition. To determine the feasibility of utilizing the decay energy in the nuclear micro-grid, the available quantity of the decay heat in the nuclear reactor must first be established. The Koeberg pressurized water reactor technology rated at 2785 MW thermal and 929 MW electrical is used as a reference plant to calculate the available quantity of decay heat.

The pressurized water reactor (PWR) plant is normally operated at maximum power for a period of 18 – 24 months before being shut down for refuelling. The thermal power (rate of energy release) emanating from decaying fission products at time t_s after the reactor shutdown is depended on the maximum operating power (P_0) of the reactor. The ratio of decay power P (t_s) to maximum thermal power P_0 at time t_s is approximated using equation 3.2 [55].

$$\frac{P(t_s)}{P_0} = 0.066[(t_s)^{-0.2} - (t_s + t_0)^{-0.2}] \quad (3.2)$$

Where P (t_s) is the decay power at time t_s, t_s is the time after reactor has been shut down, P_0 is the maximum reactor thermal power (2785 MW), t_0 is the time the reactor has been operating before shutdown (taken as 18 months).

The logarithmic decay pattern of the decay heat after the reactor is shut down is illustrated in figure 3.5. As shown in figure 3.5, it takes more than 100 years for the decay heat power to decay down to a very insignificant value.

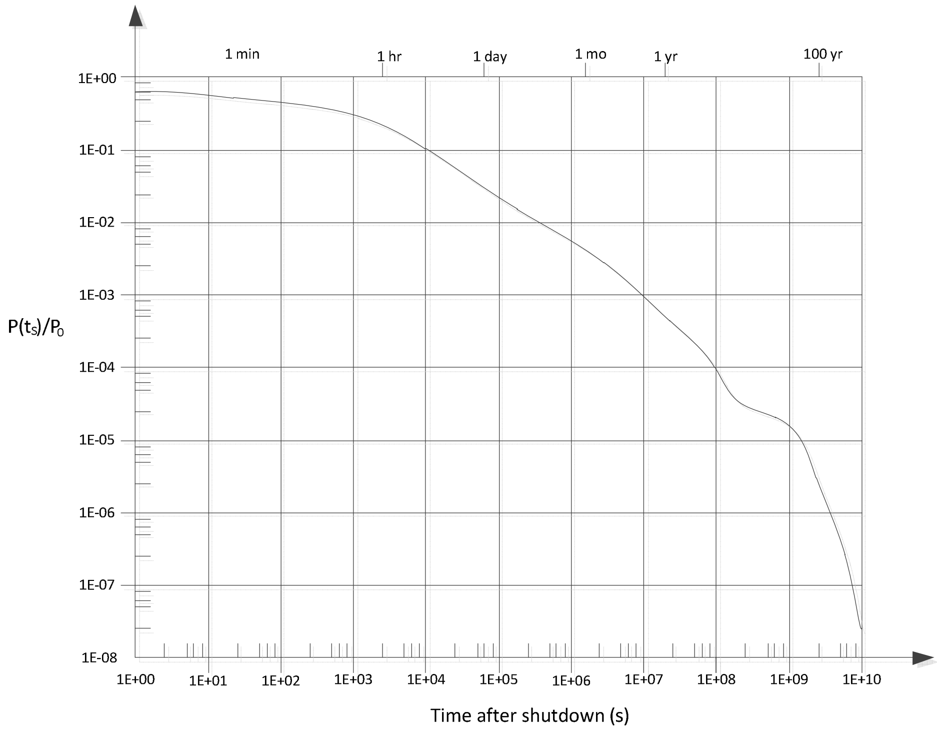

Figure 3.5: Decay power ratio as a function of time after shutdown (ANS-2005 standard for Decay Heat Power in Light Water Reactors)

The decay heat can be converted into electrical power using either steam-turbine electricity generator or solid-state thermal-to-electric converters. The use of these two options in the nuclear micro-grid is analysed further in the subsequent sections.

3.4.1 Steam-Turbine Generator

The PWR utilizes steam turbines to generate electricity. A typical 900 MW (electrical) Westinghouse PWR is comprised of three steam generators used to produce steam that drives the steam turbine to generate electricity. These components are designed to operate efficiently at maximum thermal power (2785 MW). The decay heat recovery system requires a separate system with lower power rating specifications.

The required components for the recovery system are illustrated in figure 3.6.The Westinghouse PWR has an approximate heat to electricity conversion efficiency of about 33%. Figure 3.7 shows the decay power to electrical power conversion graphs using the steam turbine generator with efficiency of 33%. The nuclear micro-grid should be able to supply electricity to the nuclear facility for a period of at least 72 hours as demonstrated by the sequence of events that occurred during the Fukushima Daiichi accident (see sections 2.1 and 2.2). As portrayed in figure 3.7, the electrical power available immediately after shut down of the nuclear reactor is 13.8 MW and it goes down to 3.26 MW after 72 hours. The total electrical energy that is available from the decay heat for the 72 hour period is 1.15×10^3 Giga Joules (318 MWh electrical). This translates to average electrical output of 4.42 MW per hour.

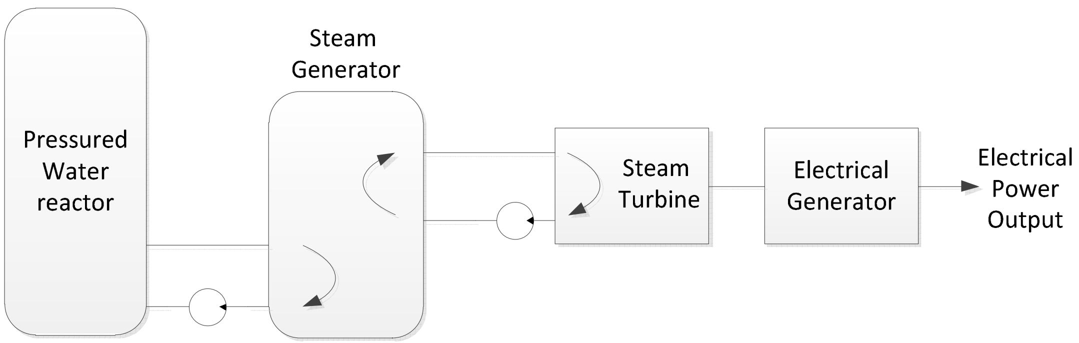

Figure 3.6: General illustration of decay heat recovery system

The energy demand of the safe loads during the LOOP accident is 156.8 MWh as calculated in appendix A. The auxiliary loads of the decay heat recovery plant will consume about 5 – 8% of the total generated electrical power which is a typical consumption percentage for the nuclear power plants auxiliary loads [20]. The steam-turbine decay heat recovery system thus has the capability to supply 100% of the total energy required by the safety loads for a period of 72 hours during LOOP accident only. During LOOP combined with loss of coolant accident (LOCA), the energy demand of the safety loads is 302.8 MWh (appendix A) and hence the steam-turbine heat recovery system is insufficient to meet this demand.

The other energy sources in the nuclear micro-grid can be used to balance the energy deficit. The main advantages of the heat recovery system are safety improvement and environmental sustainability because of using the waste decay heat to supply power during the LOOP accident. The system combines safety and efficiency by removing the hazarding decay heat while using it at the same time to generate power. The system however has two main drawbacks. Firstly, during the LOOP accident combined with LOCA, the system will become unavailable due to the loss of pressure that will be caused by LOCA. Secondly, the implementation of the system involves modification to the PWR pressure boundary conditions.

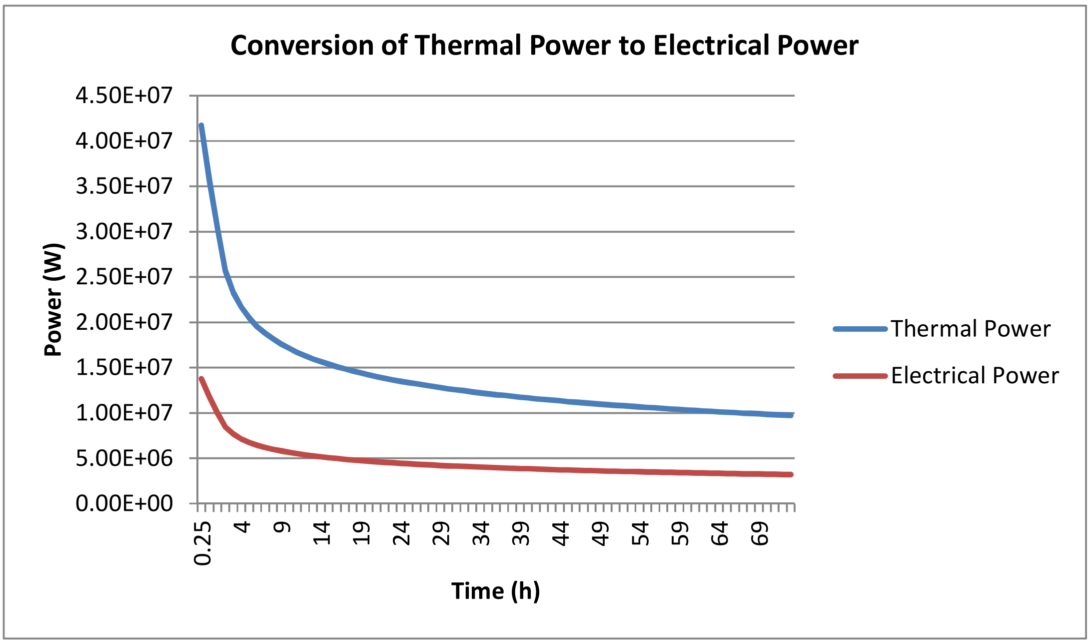

Figure 3.7: Decay thermal power to electrical power conversion

This introduces additional failure modes to the PWR system and can compromise the overall safety of the PWR system. It is clear that drawbacks for the steam-turbine heat recovery system outweigh the benefits of the system. It is therefore concluded that the steam-turbine decay heat recovery system is not a suitable energy source option for the nuclear micro-grid. However there is a room for further research into the safety implications of the steam-turbine heat recovery system.

3.4.2 Solid-State Thermal-to-Electric Converters

Thermionic and thermoelectric generators are used to convert thermal energy directly into electrical energy. The thermionic generator converts thermal energy into electricity based on the principle of thermionic emission [56]. A typical thermionic generator is constructed with two metallic plates separated by a vacuum. To generate electricity, one metallic plate is heated while the other is kept at a lower temperature. The temperature difference between the two plates results in a flow of electric charge, where electrons are emitted from the hot plate (cathode) and travel through the vacuum to the cold plate (anode) where they condense. This concept has been known since the late 1950's but its application has been inhibited mainly by a space charge problem [57].

The thermoelectric generator converts thermal energy into electrical energy based on the thermoelectric effect principle called Seebeck effect [59]. The thermoelectric generator is constructed with N-type and P-type semiconductors that are electrically connected in series and thermally connected in parallel. When heats is applied across the thermal couple, electrons at the N-leg and holes at P-leg move from the heat source and conduct the heat to the cold end. This creates potential difference across the legs and drives electric current across the external electrical circuit. The thermoelectric generator applications include extra low power (mill-micro watts) devices such as thermocouples and low power devices (kilo watts) deployed in space missions [60]. They have also been used in space missions utilizing nuclear reactor as a heat source [46].

The thermionic and thermoelectric devices generate electricity without any moving parts. They are therefore more reliable and durable as compared to conventional heat-to-electricity technologies. Their main drawbacks when used as power generators include low conversion efficiency (around 5%) and low power rating (up to few kilo watts). Studies conducted by [61] indicate that combining thermionic and thermoelectric generators to form a single generator results in slight improvement of the efficiency and power rating.

However, based on the drawbacks mentioned above and the fact that the technology improvements have not yet matured, it is concluded that the thermionic and thermoelectric generators are not yet suitable technologies for use as part of the energy sources for the nuclear micro-grid. Further developments of this technology may make it a viable option in the future.

3.5 Diesel Generator

Most of the existing nuclear facilities utilize diesel generators as standby emergency power sources. The diesel generators have proven to supply reliable electrical power during loss of offsite power accidents and they play a critical role in ensuring the safe operation of the nuclear facilities. However, the use of diesel generators alone is severely constrained as compared to the distributed energy sources of the nuclear micro-grid. The main drawbacks of the diesel generators are listed as follows:

- The diesel generators are designed as standby sources that cannot be used for continuous operation. This implies that they cannot operate or be fully tested while the main grid power is available. This presents the risk of failure-to-start and failure-to-run situations as compared to the nuclear micro-grid sources that remain on-line at all times.
- There is a risk of fuel contamination for fuel stored onsite and this makes storage of large quantities of fuel onsite not a recommended option. However, natural or man-made disasters can inhibit delivery of fuel to the nuclear facility. The Fukushima Daiichi nuclear power plant accident demonstrated that delivery of additional fuel to the nuclear facility can be inhibited by damage to access roads. Furthermore fuel management programs that include procedures such as fuel inspections, testing, fuel circulation, regular online fuel usage and complete replacement of deteriorated fuel are recommended in applicable standards and regulatory guides [62], [63].
- Diesel is not an environmentally friendly energy source. The continual depletion of fossil fuels and increasing greenhouse gases emission has initiated various researches into alternative clean energy sources.

> It is an invertible fact that crude oil reserves will eventually get depleted. Currently there is about 1.48 – 1.64 trillion barrels of crude oil reserves globally [64], [65]. It can be argued that the development of biodiesel has reached maturity; however, the biodiesel still emits a certain percentage of pollutants [66].

Despite the above-mentioned drawbacks, the diesel generators are still used as the main backup power sources for the nuclear facilities. It is therefore concluded that the existing diesel generators in the nuclear facilities should form part of the energy sources for the nuclear micro-grid. It is possible that the future nuclear facilities will use mainly the energy sources analysed in this chapter with less focus on the diesel generators. The use of the diesel generators can contribute to reduction of energy storage system capacity and hence reduce the overall costs of the nuclear micro-grid.

3.6 Summary

The potential energy source options were discussed in this chapter. Table 3.1 summarizes the suitability assessment outcome based on the rationale discussed in this chapter. The solar energy, wind energy and diesel generators have been determined to be the most suitable energy sources for the nuclear micro-grid. The energy sources that have impact on the nuclear safety have been ruled out of potential energy options. The concept of solid-state heat-to-electricity conversion using thermionic and thermoelectric converters can provide a robust decay heat recovery system for the nuclear micro-grid. Further research and development of this technology is required in order to improve it for future use in the nuclear micro-grid. The next chapter presents an analysis on energy storage technologies that complies with the design basis for the nuclear facilities power systems.

Table 3.1: Summary of suitability assessment for potential energy sources

Energy Source	Energy Resource Availability	Technology Maturity	Impact on Nuclear Safety	Environmental Sustainability
Solar	Available	Mature	No impact	Sustainable
Wind	Available	Mature	No impact	Sustainable
Ocean	Available	Under development	No impact	Sustainable
Steam-turbine Decay heat recovery	Conditionally available	Mature	Impact on primary systems	Sustainable
Solid-state decay heat recovery	Available after reactor shutdown	Under development	No impact	Sustainable
Diesel Generator	Available	Mature	No impact	Not Sustainable

Chapter 4 Energy Storage System Analysis

Energy storage technologies that are suitable for the nuclear micro-grid are investigated in this chapter. The suitable technologies should be compliant with reliability requirements highlighted in section 2.2. The deterministic selection criteria used to establish suitable technologies include capability to meet the power and energy requirements of safety loads, technology maturity, siting considerations and the type of storage medium. The mature technologies provide conservative compliance to reliability requirements because their characteristics are well understood.

4.1 Electrical Energy Storage Options

The energy storage system (ESS) improves the reliability of the renewable energy sources (RES), by mitigating their intermittency and ensuring dispatchable energy supply. The ESS can provide additional benefits for the nuclear micro-grid as compared to the diesel fuel storage medium. This can be achieved by utilizing the ESS in grid ancillary services (i.e. spinning reserve, frequency regulation, reactive power and voltage support, grid stabilization, load levelling and energy arbitrage) in conjunction with storing and supplying energy during emergency operation of the nuclear micro-grid. The energy storage technologies are commonly classified in terms of energy storage form and in terms of energy storage duration (response time) [4], [68], [69].

The electrical energy can be stored directly in its original form or indirectly by converting it to other forms of energy (i.e. mechanical, chemical or thermal energy). The storage medium with moving parts (i.e. mechanical) is considered to be more complex and less reliable as compared to storage medium without moving part (i.e. static chemical) [69]. The direct electrical energy storage mediums include electrostatic mediums (capacitors and super-capacitors) and electromagnetic mediums (superconducting Magnetic Energy Storage). The forms of mechanical energy used to store electricity are kinetic energy storage (flywheels) and potential energy storage (pumped hydroelectric storage and compressed air energy storage).

The forms of chemical energy storage options include electrochemical energy storage (static and flow batteries), chemical energy storage (hydrogen used in fuel cells) and thermochemical energy storage (solar hydrogen, solar metal, solar methane and solar ammonia). The thermal energy storage options include low temperature energy storage (acquiferous cold energy storage and cryogenic energy storage) and high temperature energy storage (steam/hot water accumulators, hot rocks and concrete and latent heat systems) [70], [71]. The storage mediums performance is affected mainly by conversion efficiencies of electricity-to-storage and storage-to-electricity processes. The classification of energy storage technologies based on their energy storage durations is divided into 2 categories which are short-term storage duration (few seconds or minutes) and long term storage duration (minutes, hours or days). The short-term response storage devices are primarily used to improve power quality by maintaining voltage stability during short duration transients [68].

The long-term storage devices are more prevalent in power systems with the renewable energy sources where they regulate the frequency fluctuations associated with the intermittent energy sources. They supply or absorb the electrical energy in the power system and contribute to the energy management and grid congestion management [68]. Table 4.1 summarizes the various short and long term energy storage mediums. The short-term energy storage mediums do not meet the 72 hour energy supply requirement of the nuclear micro-grid (see section 2.2 (c)). The long-term energy storage mediums that are analysed further in the subsequent subsections include pumped hydroelectric, compressed air, hydrogen and large scale battery.

The storage duration of thermal storage is usually limited to a few hours while the thermochemical storage technology is still at earliest stage of development. Therefore, the thermal and thermochemical energy storage mediums are not analysed further. The maximum power and energy requirements are 4.21 MW and 302 MWh as analysed in appendix A and the suitability analysis is therefore focuses on the ESS with capability to meet these requirements.

Table 4.1: Summary of short term and long-term energy storage mediums

Short term Energy Storage Medium	Long-term energy Storage Medium
Capacitor and super capacitor	Pumped hydroelectric storage
Super-conducting magnet	Compressed air energy storage
Flywheel	Hydrogen energy storage
Battery	Large scale battery
	Thermal energy storage
	Thermochemical energy storage

4.2 Pumped hydroelectric storage

The pumped hydroelectric storage (PHS) is the most commercially implemented large-scale ESS with long operational history and high technical maturity. The typical PHS plant is comprised of two reservoirs located at different elevations, water pumps and turbine-generator sets. Water is pumped into the reservoir at higher elevation to store electricity as potential energy of water. The amount of energy stored depends on the height of reservoir and the amount of water stored. When electricity demand arises, the water flows from higher to lower elevation reservoirs thereby driving the turbines to generate electricity. The PHS plants have cycle efficiency of about 70 – 80 % with more than 40 years life span [70]. The PHS accounts for about 97% of global energy storage capacity with the installed capacity reaching 145 GW in 2015. [40] South Africa currently has two operational PHS plants (Drakensberg with capacity of 1000 MW for 10 hours and Palmiet with capacity of 400 MW for 25 hours) and one plant under construction (Ingula with capacity of 1 332 MW for 16 hours) [67].

The PHS is a mature technology and allows for large scale energy storage with storage duration of up to several years [70]. It can be used as ESS for the nuclear micro-grid and can concurrently be designed to provide grid ancillary services such as frequency regulation, voltage control, operating reserves, etc. [72]. However, PHS depends on a specific geographical location. It can only be implemented in locations with high water head, large area for reservoirs and waterways.

The locations with these features are very scarce and definitely cannot be established within the site of the nuclear facility. Furthermore, the implementation of PHS involves long construction time and high capital investments. Based on the disadvantages of the PHS, it is concluded that PHS system is not a suitable ESS for the nuclear micro-grid.

4.3 Compressed Air Energy Storage

The compressed air energy storage (CAES) is another type of commercially available ESS technology. It is comprised of a motor/generator pair coupled with clutches to engage either compressors or turbines, air compressors with cooling units, high and low pressure turbines and a cavity/container for storing the compressed air. The electricity storage operation involves coupling the motor to the compressors to store electricity in the form of elastic potential energy of compressed air. To extract the stored energy, the CAES system is coupled to the gas turbine plant, where the compressed air is heated and passed through the high pressure turbine which recovers some of the energy in the compressed air. The air is then mixed with fuel, combusted and passed through the low pressure turbine. The turbines are coupled to the electricity generator. The CAES plant has storage efficiency of about 70 – 89%. There are two existing CAES units in the world [71]. The CAES meets the power and energy requirements for the ESS of the nuclear micro-grid. However, it is not a suitable option mainly because it is not an independent system and forms part of the gas turbine plant for electricity generation. Furthermore, the implementation of CAES is reliant on the geographical location because the container/cavity is usually in the form of underground rock caverns, salt caverns or water-bearing aquifers [70].

4.4 Hydrogen Energy Storage

Hydrogen energy storage (HES) systems are receiving increasing attention recently with much of the research focused on their integration with renewable energy sources [73]. The HES system is basically comprised of a water electrolyser, compressed hydrogen gas storage tanks and a fuel cell as shown in figure 4.1. Electricity is used to generate hydrogen from water using the electrolysis process.

The hydrogen is then stored in high-pressure tanks. This storage method provides limited storage capacity of about few MWh [74]. The other hydrogen storage mediums that can provide better storage capacity include underground caverns, solid phase storage and liquid phase storage. The properties of these storage mediums are discussed in [72]. The stored hydrogen is channelled to the hydrogen fuel cell to generate electricity when the demand arises. The fuel cell combines hydrogen and oxygen from air to generate electricity and water plus heat energy as by-products.

The main types of hydrogen fuel cells include proton exchange membrane, alkaline, phosphoric acid, molten carbonate and solid oxide fuel cells. The fuel cells differ based on the type hydrogen fuel used, operating temperature and type of construction material. Detailed information on their technical characteristics, advantages and disadvantages is provided in [75].

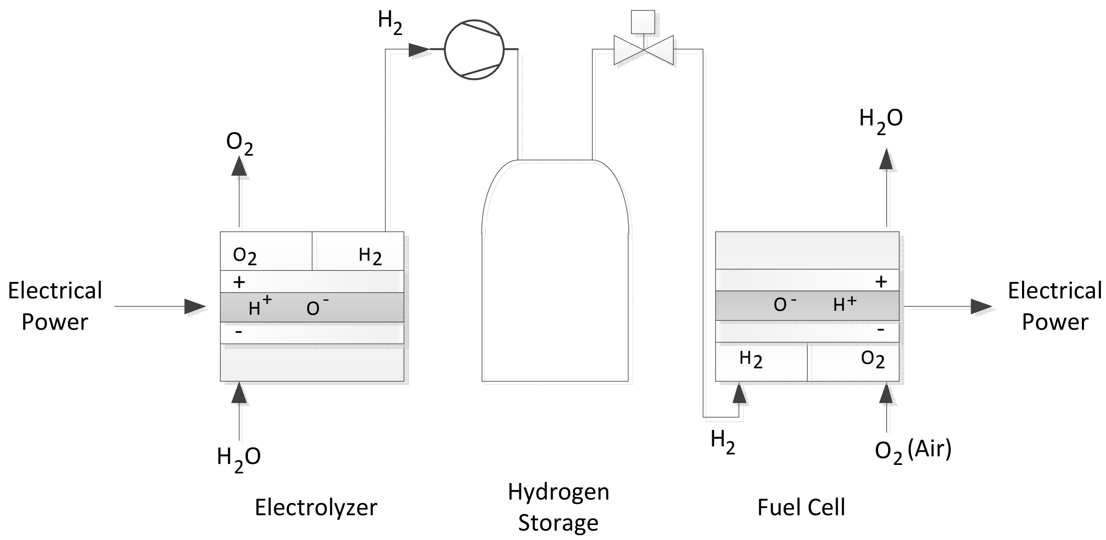

Figure 4.1: The basic components of a hydrogen storage system

The round trip efficiency of the HES system is around 50% [71]. The storage capacity of HES system depends on the storage medium. The use of large underground caverns can provide very large storage capacity of up to 100 GWh of electricity [74]. The HES system with the fuel cell technology is currently in the development and demonstration stages.

The research conducted by [36] concludes that the hydrogen fuel cell technology will be ready for deployment in the nuclear facilities by the year 2030 while the research conducted by [7] indicates that the proton exchange membrane fuel cell technology can be used to provide DC backup power at the nuclear facilities in the near future.

It is therefore concluded that the HES is still under development and not yet suitable for deployment as the ESS for the nuclear micro-grid.

4.5 Battery Storage

Rechargeable batteries are the oldest and most widely used form of electrical energy storage technology. The structure of the battery includes electrochemical cells that are immersed in an electrolyte. Each cell is comprised of a pair of electrodes forming an anode and cathode. The electrical energy is stored in the battery (as electrochemical energy) by charging the electrolyte to create electrically charged ions. The electrical energy is released by discharging the electrolyte. In static batteries, the electrolyte is stationery whereas in flow batteries, the electrolyte is stored in external tanks and pumped through the stack of cells for charge/discharge operations.

4.5.1 Static Battery Storage

The main barriers associated with implementation of static batteries in the high power, large scale battery storage application include short life cycle (5 – 20 years), high maintenance costs, excessively high capital costs, low energy densities (75 – 315 watts/kg) and limited discharge capabilities. The batteries however, have round-trip efficiency of 60 – 90% and self-discharge per day rates of 0.1 – 0.6 % (except for 5 – 20% of nickel-metal hydride battery) [76], [69]. Despite the barriers, the static batteries have continuously been improved for use in high power applications such as standby power quality systems (UPS), grid ancillary services and integration in renewable energy applications.

The batteries that exhibit high power and energy storage capabilities are lead-acid, nickel-cadmium, lithium-ion and sodium-sulfur batteries. Their characteristics are discussed further as follows:

A. Lead-acid Batteries

The lead-acid batteries are the most commonly used type of energy storage technology. The battery cell is comprised of lead oxide (PbO_2) as cathode, lead (Pb) as anode and sulfuric acid as electrolyte. They are available in either flooded or valve regulated types. The lead-acid batteries are uncomplicated, easy to install, low cost and mature type of technology. Their disadvantages include low energy density (around 30 Wh/kg), limited number of charge/discharge cycles and toxic environmentally hazardous materials (lead and sulfuric acid). The lead-acid batteries require large area for high power and energy applications because of the low energy density. Enhancements have been made through the use of lead-carbon electrodes to improve their cycle life and discharge capabilities (deep-cycle lead-acid batteries) [69]. A high power and energy reference application that utilizes the lead-acid batteries is a 10 MW/40 MWh storage facility in Chino, California, USA that is used to provide ancillary services [70].The lead-acid technology meets the power requirements of ESS for the nuclear micro-grid. The suitable energy sizing methodology is discussed in chapter 6.

B. Nickel-cadmium Batteries

The nickel-cadmium (NiCd) batteries use nickel hydroxide for anode, cadmium hydroxide for cathode and aqueous alkali solution (potassium hydroxide or lithium hydroxide) for electrolyte. The NiCd batteries exhibit higher energy densities (50 – 80 Wh/kg) as compared to lead-acid batteries [70]. However, they are more expensive, have high self-discharge rate (up to 10%), use toxic heavy metals (cadmium and nickel) and suffer from memory effect as compared to the lead-acid batteries [77], [70]. The NiCd batteries are popular for providing standby power in harsh environmental conditions. One commercial application that utilizes NiCd batteries is a 27 MW/6.75 MWh storage facility in Golden Valley, Alaska, USA that is used as ancillary service for spinning reserve and reactive power compensation [76].

The NiCd batteries are currently not researched further for high power and energy applications due to the above-mentioned disadvantages [70]. The high self-discharge rates and memory effect issue of NiCd batteries makes this technology not a suitable option for the nuclear micro-grid.

C. Lithium-ion Batteries

A lithium-ion (Li-ion) battery cathode is made of lithium metal oxide (such as $LiCoO_2$), and the anode is made of graphitic carbon. The electrolyte is made up of lithium salts (such as $LiClO_4$) dissolved in organic carbonates [71]. The Li-ion batteries have higher energy density (150 – 200 Wh/kg) and high cycle efficiencies (up to 97%) as compared to lead-acid and NiCd batteries. The batteries however cannot be deep-cycled and require electronic protection circuit to protect the cells against under/over charge. The Li-ion batteries are used extensively in small portable device applications but their application in high power and energy system is constrained by the high capital costs due to the electronic protection circuits. Progressive research work has been focused on reducing the capital costs of the Li-ion batteries and the current application with the highest power and energy ratings is the 40 MW/40 MWh storage facility in Tohuku, Japan that is used for renewable energy sources integration [78].

Other planned lithium-ion storage projects include a 20 MW/80 MWh Tesla Powerpack system at the Southern California Edison Mira Loma substation [80] and the 100 MW/400 MWh AES storage system for Alamitos Power Center at Long Beach in California [81]. Safety concerns associated with Li-ion batteries is the thermally unstable metal oxide electrodes that decompose at elevated temperatures producing oxygen that can lead to a thermal runway situation. This safety issue has been resolved with the improved Lithium-ion phosphate (LFP) battery. LFP battery shows stable thermal characteristics and does not degrade when subjected to variable and incomplete charging cycles in renewable energy applications [79]. Another improvement has been made by Tesla using a combination of lithium, nickel, cobalt and aluminium oxide as the cathode [82] The Li-ion technology meets the power and energy requirements of ESS for the nuclear micro-grid.

D. Sodium-Sulfur Batteries

Sodium-sulfur (NaS) battery is comprised of molten sulfur and sodium used as anode and cathode respectively. The electrodes are separated by solid beta alumina ceramic electrolyte. The battery operates at high temperatures (300 – 350 ^{0}C) that is required to keep the electrolytes in liquid (molten) form. The NaS batteries have high energy densities (150 – 300 Wh/L), almost zero self-discharge rate and are made from inexpensive and non-toxic materials. The primary limitation of the NaS battery is the requirement for thermal management to ensure the correct operating temperature and this result in high operational costs [70]. There are several large-scale energy storage projects that have been implemented using the NaS battery technology. A reference example is a 40 MW/244.8 MWh in Rokkasho, Japan that is used for wind power fluctuation mitigation. Furthermore, there is NaS storage plant under construction since 2012 in Mexico with a storage capacity of 1000 MW for up to 6 hours (6 GWh). The facility is expected to be completed in 7 years and will be used to support the renewable energy sources in both USA and Mexico [69], [83]. The NaS technology meets the power and energy requirements of ESS for the nuclear micro-grid.

E. Other Types of Static Batteries

The other types of static batteries that are not suitable for the ESS of the nuclear micro-grid are nickel-metal hydride (NiMH), nickel-zinc (NiZn), Sodium Nickel Chloride (also known as ZEBRA battery) and metal-air batteries. The NiMH and NiZn batteries are not a preferred choice due to high self-discharge rate (up to 20%) and sensitivity to deep-cycling [70]. The ZEBRA batteries have low energy density, takes up to 15 hours to heat-up after solidification and only one company in the world is involved with the development of the battery and the technology is still at early stage of development (demonstration stage). The metal-air batteries are the most compact and potentially least expensive type of batteries. They are however difficult and inefficient to recharge. The rechargeable metal-air batteries are still under development and currently exhibit low charge/recharge cycles and low cycle efficiencies [71]. It is therefore concluded that the battery technologies discussed above are not suitable options for the nuclear micro-grid.

Table 4.2 summarizes the advantages and limitations of the static battery technologies that are suitable for the nuclear micro-grid.

Table 4.2: Key characteristics of the suitable static battery technologies

Battery Type	Advantages	Disadvantages
Lead-acid	- Simple mature technology. - Low capital cost. - Relatively high cycle efficiency (approx. 90%).	- Low energy density makes them bulky for high power/energy applications. - Susceptible to temperature degradation. - Low depth of discharge (approx. 50%). - Low number of charge/discharge cycles (up to 1500). - Use Lead metal that is toxic to environment.
Lithium-ion	- Commercialized technology. - High energy density. - High cycle efficiency (approx. 98%). - High charge/discharge cycles (up to 5000). - Improved safety in LFP with no thermal runaway risk.	- High capital cost. - Complex overcharge protection circuit for each cell.
Sodium-Sulfur	- Commercialized technology. - Energy density higher than Li-ion. - Good cycle efficiency (approx. 86%). - High charge/discharge cycles (up to 4500).	- Capital cost higher than Li-ion. - Operates at high temperatures and requires thermal energy management system. - Has long term corrosion problem on cathode containers.

4.5.2 Flow Battery Technology

The flow battery is made up of two liquid electrolytes contained in external tanks, an electrochemical cell that is comprised of a cathode, an anode and a membrane separator. The electrical energy storage/discharge operations are carried by pumping the two electrolytes through the electrochemical cell stack. During charging operation, one electrolyte is oxidized at the anode, while the other electrolyte is reduced at the cathode and during discharge operation, the process is reversed. The main advantages of the flow battery over the static battery are high energy capacity (achievable by use of large storage tanks), long life cycle, low maintenance, and very deep discharge capabilities [70]. The main drawback of the flow battery is the increased system complexity due to pumps, sensors, flow regulation and containment vessels. The flow battery also has low energy density and this result in large active area of cell stack causing uneven distribution of electrolyte charge. The uneven distribution of charge affects the overall efficiency of the flow battery. The three types of flow batteries that have been tested at utility scale (high power and energy) applications are discussed as follows:

A. Vanadium Redox Flow Battery

The vanadium redox (reduction-oxidation) flow battery (VRB) is considered the most successful flow battery technology. The VBR utilizes two electrolyte solutions stored in separated tanks. The electrolyte solutions are made up of vanadium ion couples (V^{2+}/V^{3+} and V^{4+}/V^{5+}) each dissolved in mild sulfuric acid solution [70]. During charge/discharge operations, the hydrogen ions are exchanged between the two electrolyte tanks through the selective ion membrane to produce about 1.4V across each cell. The illustrative diagram of VRB is shown in figure 4.2. The VRB exhibits fast response time (about 0.001 s), high efficiency (up 85%), high number of cycles (more than 16, 000) and continuous power discharge capabilities (more than 24 hours). A reference high energy and power application that utilizes VRB technology is a 2 MW/12 MWh energy storage facility in Ireland used to mitigate wind power fluctuations and grid stabilization [70].

The current VRB have low energy and power densities. Improvements have been made by increasing the ion-membrane active area. However, the large area causes uneven distribution of current density across each cell section. This produces electrical field current inside conductive electrodes resulting in induced shunt currents that further reduces the overall efficiency of the system [84].

The VRB technology shows promising features for large scale deployment. It is therefore concluded that the VRB technology is currently not suitable for the ESS. However, after further developments, it will become the most suitable option for the nuclear micro-grid in the future.

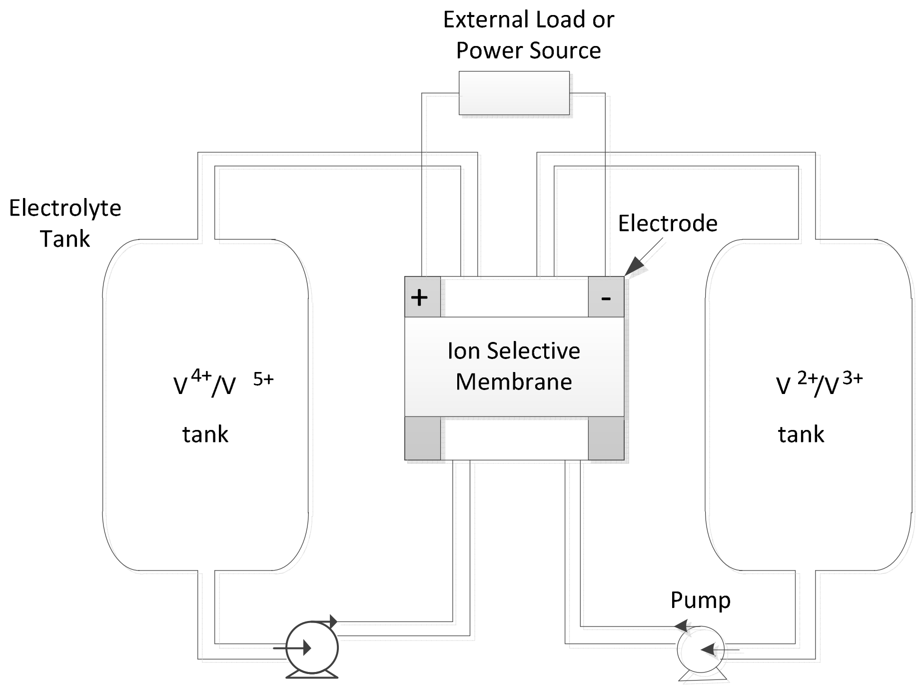

Table 4.2: General illustration of the Vanadium Redox Battery technology

B. Zinc Bromide (ZnBr) flow Battery

The ZnBr flow battery is hybrid flow battery comprised of zinc based electrolyte in one tank, bromine based electrolyte in the other tank and a carbon-plastic composite electrode. During discharge Zn and Br combine into zinc bromide generating about 1.8V across each cell and during the charge operation, metallic zink is plated as thin film on one side of the composite electrode. The ZnBr flow batteries have relatively lower cycle efficiencies (65 – 75%) and are prone to material corrosion as compared to VRB [70].

The utility scale application of ZnBr is still at early demonstration stage. A reference large scale ZnBr plant is a 0.5 MW/2.8 MWh in USA being tested for grid ancillary services. It is therefore concluded that the ZnBr battery technology is currently not an option for ESS. However, the current research work shows that it will be suitable for the nuclear micro-grid in the future after further developments.

C. Polysulfide Bromine (PSB) Flow Battery

The PSB flow battery is a regenerative fuel cell type of flow battery that utilizes sodium bromine and sodium polysulphide as salt solution electrolytes and a polymer membrane as electrodes. The electrolytes solutions undergo a reversible electrochemical reaction as they are brought close together in the battery cells with the polymer membrane separating the solutions. The membrane allows only sodium ions to pass through it, generating about 1.5 V across the membrane. The PSB is at an early demonstration stage. A reference large scale PSB plant is a 15 MW / 120 MWh energy storage facility in Tennessee Valley in USA. The Plant is still incomplete due to engineering and financial constraints [70]. There is currently no indication showing that the PSB technology will be a suitable option for the nuclear micro-grid in the future. It is therefore concluded that the PBS technology is not a suitable option for the ESS of the nuclear micro-grid.

4.6 Summary

The various energy storage technology options were discussed in this chapter. Table 4.3 summarizes the suitability assessment outcome based on the rationale discussed in this chapter. The static battery technologies that are suitable for the nuclear micro-grid are Lead-acid, Lithium-ion and Sodium-sulphur batteries. Their advantages and limitation are listed in table 4.2. The technologies that are still in development and yet showing promising characteristics for deployment as energy storage system in the nuclear micro-grid are hydrogen energy storage system, vanadium redox flow battery and Zinc Bromide flow Battery. The next chapter presents an analysis on control strategies and architectural layout that comply with the design basis for the nuclear facilities power systems.

Table 4.3: Summary of suitability assessment for potential energy sources

Energy Source	**Energy & Power Capability**	**Technology Maturity**	**Siting Considerations**	**Storage Medium**
Pumped Hydroelectric	Capable	Mature	Geographically dependent	Mechanical energy
Compressed air	Capable	Mature	Geographically dependent	Mechanical energy
Hydrogen	Capable	Under development	Not Geographically dependent	Chemical energy (Mechanical drive)
Static Battery	Capable	Commercialized (Lead-acid mature)	Not geographically dependent	Chemical energy
Flow Battery	Capable	Under development	Not geographically dependent	Chemical energy (Mechanical drive)

Chapter 5 Control Systems and Architecture

Clear and systematic control strategy is essential for the reliable performance of the nuclear micro-grid as specified in section 2.2 (g). The architectural layout of the micro-grid is usually established from the type of control scheme used and the design-for-reliability requirements highlighted in section 2.2. The control system and architectural layout that are suitable for the reliable performance of the nuclear micro-grid are analysed in this chapter.

5.1 General Control Concepts of Micro-grid Systems

The micro-grid system is controlled to ensure proper power sharing among energy sources and to regulate the bus voltage magnitude and frequency. Either centralized or decentralized control architecture can be used to control the micro-grid system. The centralized architecture involves a central controller that monitors and controls the system parameters in real time. Extensive communications are required between the central controller and controlled units (DES, ESS and loads) for collection of measured information and dispatch of set points. The decentralized architecture is comprised of local controllers that control each unit in the micro-grid using local information without any communications interface with other units.

The centralized architecture provides a more efficient power management platform but comes at a higher cost and complexity as compared to the decentralized architecture. The detailed advantages and limitations of the two architectures are discussed in [10] and [85]. A balanced control scheme is achieved by combining the two control architectures to form a hierarchical control scheme that is comprised of primary, secondary and tertiary control levels [10], [86]. The primary control level is further partitioned into voltage-current (V-I) control loop and power sharing control loop. The V-I control loop utilizes only local measurements to provide the fastest control response to each unit. The power sharing control loop establishes power sharing (active and reactive power) among the DES and ESS of the micro-grid and provides voltage and current references to the V-I control loop.

The secondary control level is used to compensate for the voltage amplitude and frequency deviations caused by the primary control level in the islanded micro-grid. The secondary level has a slower control response as compared to the primary level and can be implemented either locally or in a centralized controller. The tertiary control level is usually referred to as a central energy management system (EMS) and is used to manage parameters such as capacities of DES, state of charge of ESS and forecasting of non-dispatchable DES. Most of the DES and ESS units are interfaced to the AC grid via power electronics and therefore the control algorithms are applied in the interfacing inverters. The V-I control loop is implemented with voltage-source inverter (VSI) or current-source inverter (CSI) configurations depending on the control objective. In grid-connected mode, the inverters are configured in grid-following mode with CSI supplying maximum active power while the voltage magnitude and frequency are regulated by the main grid.

This is based on the fact that the main grid is usually a stiff AC system that has multiple synchronous generators connected in parallel. The synchronous generators exhibit high inertia that maintains constant system frequency and utilize automatic voltage regulators to maintain constant voltage magnitude. Therefore the CSI configuration with maximum power point tracking (MPPT) algorithm is normally adopted for the micro-grid sources operating in grid-connected mode [87], [88], [89].

In islanded mode, the interfacing inverters are configured in grid-forming mode with single or multiple VSI acting as master controllers to control the voltage magnitude and frequency while also regulating the flow of the active power and reactive power. It is crucial to maintain uniform voltage across all the inverters connected in parallel because a mismatch in voltage amplitude, phase angle or frequency between any of the units in the micro-grid can result in relatively high circulation current [10], [88], [89]. In the single master operation mode, one inverter is configured in grid-forming mode (VSI) while the rest of the inverters in the micro-grid are configured in grid-following mode (CSI). In the multiple master mode, several inverters are configured as VSI while the remaining inverters are configured as CSI. The power sharing control is implemented in VSI using either non-droop or droop-based based control methods.

The non-droop based control technique involves a centralized approach and is implemented in a centralized controller [24]. The droop-based control technique involves the control of the VSI by emulating the droop characteristics of the conventional synchronous generators. The droop control is derived from the fact that active power (P) depends predominantly on power angle and reactive power (Q) depends predominantly on voltage magnitude as illustrated in equations 2.1 and 2.2. The equations assume that the micro-grid network is inductive. The phase angle is dynamically controlled by controlling the frequency of the power system.

$$P = \frac{EV}{X} \sin \delta \qquad (2.1)$$

$$Q = \frac{E}{X} (E - V cos\, \delta) \qquad (2.2)$$

Where E is the inverter output voltage, V is the micro-grid bus voltage, X is the reactance coupling the inverter to the micro-grid, and δ is the phase angle across X.

The droop control allows for sharing of P and Q among the DES and ESS according to predefined frequency and voltage magnitude droop characteristics determined by the capacity rating of each unit. The power sharing prevents the possible overloading of inverters during load transients while maintaining stable bus voltage magnitude and frequency. The maximum voltage magnitude deviation of 5% and frequency deviation of –5% to +3% are predefined by IAEA standard for the nuclear facilities [20]. The relationship between active power-frequency and reactive power-voltage can be expressed with equations 2.3 and 2.4 [29]. Figure 2.3 illustrates the droop behaviour of an energy source based on its rated P and Q capacities.

$$f = f_0 - k_P \times P \qquad (2.3)$$

$$V = V_0 - k_Q \times Q \qquad (2.4)$$

Where P and Q are active power and reactive power, k_P and k_Q are droop slopes and f_0 and V_0 are reference frequency and voltage values.

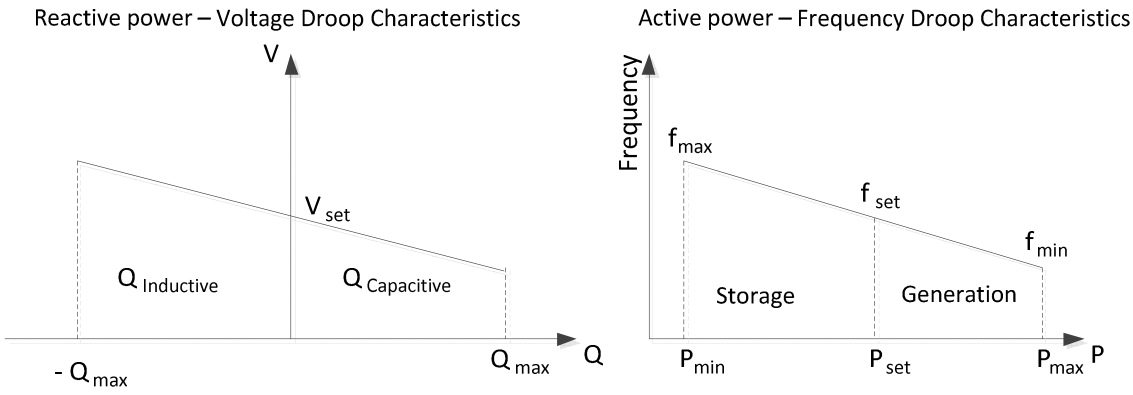

Figure 5.1: Illustration of Q – V and P – f droop characteristics

The droop control algorithm relies on AC-bus voltage magnitude and frequency signals and is implemented with no requirement for communication links to the central controller [90]. The CSI operating in islanded mode supply the maximum active power using MPPT algorithm and cannot deliver the reactive power from the energy sources. As a result the VSI normally experience increased demand for reactive power resulting in reduced capacity for active power. One way to overcome this limitation is through the use of the central controller to adjust the active/reactive power references for the CSI using additional communications links as discussed in [91].

Another option is to use a reverse droop control algorithms (V – Q and f – P) for the CSI as proposed in [92]. The reverse droop control is implemented with not communications links and this reduces the complexity of the system and improves overall system reliability. The reverse droop control strategy is still at early stage of development and further tests and demonstrations are required before it can be considered for use in the nuclear micro-grid.

5.2 Nuclear Micro-grid Control System

The nuclear micro-grid is required to operate in normal mode (grid-connected mode), emergency mode (islanded mode) and have the ability to seamlessly transfer between these two modes. The seamless transition and emergency operations are the most crucial operation modes that ensure supply of reliable backup power to the safety loads.

In order to determine the proper control system for the nuclear micro-grid, the circuit parameters and characteristics must first be established. The circuit parameters include the distributed energy sources (DES), energy storage system (ESS), power distribution network and the safety loads. Chapters 3 and 4 provide information on the DES and ESS for the nuclear micro-grid. Appendix A provides a detailed list of different types of safety loads. The safety loads are mainly comprised of inductive loads (e.g. three phase motors for pumps), non-linear loads (e.g. power electronics for battery chargers and uninterruptible power supplies) and resistive loads (e.g. electric heaters). The distribution network for the islanded mode is assumed to be mainly resistive because the power distribution cables cover short distances within the nuclear facility.

Various individuals and organizations have carried out and documented reviews on the micro-grid control strategies that offer optimum reliability and stability under various operational conditions [10], [85], [93], [94]. The control scheme that is suitable for the nuclear micro-grid system is summarized as follows:

- The hierarchical control scheme with three control levels (primary, secondary and tertiary) is the most suitable option for the nuclear micro-grid. The primary and secondary levels should be implemented in distributed local controllers and control the nuclear micro-grid under emergency mode with no requirement for communication among the local controllers. The tertiary level should be implemented in a central controller and manage all micro-grid units under grid-connected operational mode.
- The voltage-source inverter (VSI) configuration is recommended by communities such as IEEE and CERTS for the grid-forming inverters in the nuclear micro-grid because it provides a stable operation in grid-connected and emergency modes of operations and allows for seamless transition between the two modes without the need for fast island detection control system [88], [95]. This reduces the complexity of the system as well as minimizes the additional failure modes that can be introduced by the island detection system. It is preferable that the ESS is connected with grid-forming inverters because they can provide enough power reserve that compensates for the power mismatches between the RES and loads.

The ESS should also be configured as multiple master units such that should one unit fail, the other units will continue regulating the bus voltage.

- The current-source inverter (CSI) configuration is recommended for the grid-following inverters in the nuclear micro-grid. It is preferable that the RES are connected as grid-following units because the power generated by CSI can be implemented with MPPT so that the maximum power can be generated by the RES according to the prevailing environmental conditions.
- The droop control algorithm should be implemented in the grid-forming inverters. The droop control strategy allows for even power (active and reactive) sharing among the grid-forming units in order to maintain a stable bus voltage magnitude and frequency during load transients in the islanded nuclear micro-grid. It has been established in [98] that nonlinear loads that generate significant harmonic currents may result in uneven sharing of harmonic power among the micro-grid units if the conventional droop control strategy is used. However, the conventional droop control strategy will provide adequate control of the VSI in the nuclear micro-grid because the safety loads are mainly inductive and the harmonic currents due to nonlinear loads (battery chargers) are insignificant (see appendix A).
- Coordinated control of ESS should be implemented in islanded operational mode in order to maintain the ESS state of charge (SoC) within acceptable limits. The ESS should charge when the load power (P_{Load}) is less than the power of all the RES in the micro-grid (P_{MES}). The ESS should discharge and supply balance of power (P_{ESS}) when P_{Load} is greater than the P_{MES}. Normally the ESS has acceptable maximum state of charge (SoC_{Max}) and minimum state of charge (SoC_{Min}). The charging and discharging of the ESS should not exceed these maximum and minimum values. When the SoC_{Min} of the ESS is reached, then the system should switch over to the diesel generators which are configured as backup to the RES. The coordinated control strategy of the ESS is illustrated graphically in figure 5.1 as adopted from [97].

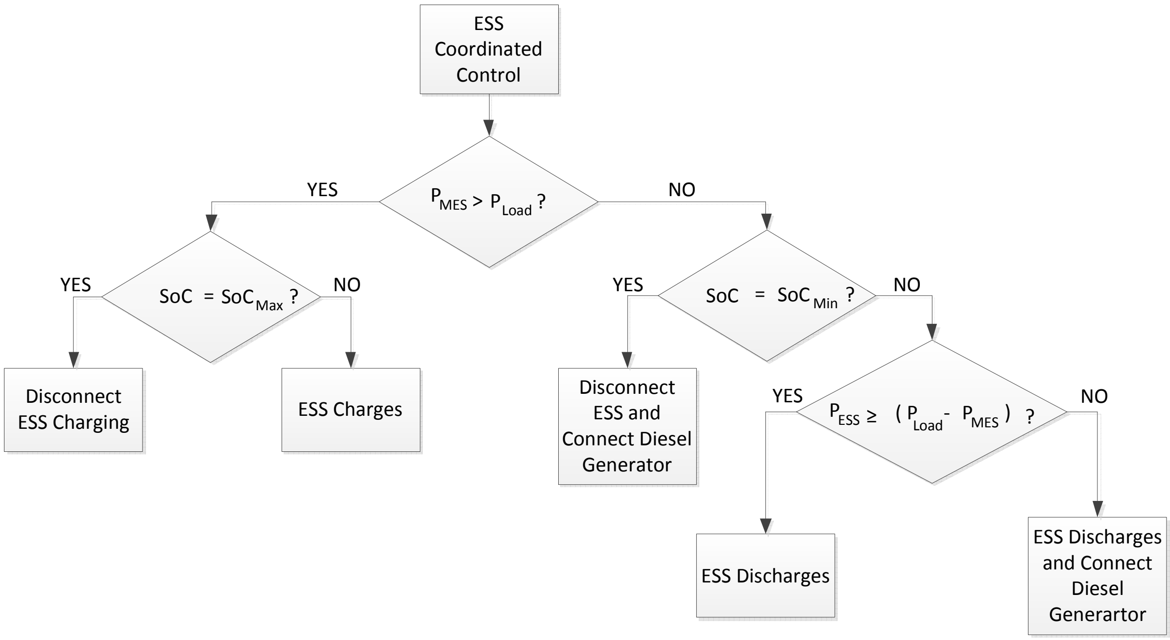

Figure 5.2: Coordinated control illustration of ESS

5.3 Nuclear Micro-grid architecture

The architectural layout of the nuclear micro-grid is analysed with reference to the main subsystems (RES, ESS and safety loads), taking into account the control scheme specifications and the design-for-reliability requirements. The redundant, diverse and independent RES and ESS (analysed in chapters 3 and 4) conform to the common cause failure and single failure criterion reliability requirements (highlighted in (a) and (b) of section 2.2). The AC loads are the main type of loads for the safety systems (see appendix A) and therefore an AC micro-grid is the most suitable configuration for the nuclear micro-grid system. The layout of each subsystem is analysed in this section in order to establish the overall architectural layout of the nuclear micro-grid.

A. Photovoltaic System

The photovoltaic (PV) system is mainly comprised of PV panels and DC/AC inverters. The PV system can be implemented using either a central inverter with a string of series-and-parallel-connected PV panels or micro-inverters that are dedicated to individual PV panels.

The reliability of the PV system is usually constrained by the inverters because the inverters exhibit high failure rates. Faults are likely to occur in subcomponents such as IGBTs, diodes, capacitors, inductors, etc. The central inverter configuration is therefore not a reliable option because the failure of the inverter results in the failure of the entire system. On the other hand, the micro-inverter configuration achieves high redundancy and improves safety and reliability [99], [100], [101]. The improved reliability is attributable to the use of low power electronics that operate at low temperature and the elimination of the electrolytic capacitors. The micro-inverter layout is therefore the most suitable option for the PV system. Each micro-inverter is configured as the current-source inverter (CSI) with MPPT algorithm.

B. Wind Turbine Generator System

The wind turbine generator (WTG) system is mainly comprised of wind turbine assembly, electrical generator and/or power converter electronics (AC/DC & DC/AC). The WTG can be configured in either fixed speed or variable speed arrangements. The fixed speed arrangement utilizes an induction generator (squirrel cade or wound-rotor induction generators) that is directly coupled to the AC network through a transformer. The variable speed arrangement utilizes electrical generator (induction generator, doubly-fed induction generator, synchronous generator or permanent magnet synchronous generator) that is interfaced to the AC network via the power converter electronics. The variable speed is an improvement of the fixed speed arrangement in such a way that the wind speed is decoupled from the AC network frequency and the wind turbine speed can be maintained at the best flow geometry in order to harvest maximum wind power [102].

The variable speed system with doubly-fed induction generator (DFIG) is able to supply active and reactive power as compared to the variable speed system that uses a single-fed induction generator [103]. Furthermore, the DFIG system utilizes power electronics with reduced power ratings (approx. 30% reduction) as compared to permanent magnet synchronous generator (PMSG) configuration. The power electronics with lower power rating makes the DFIG system more reliable and less expensive as confirmed in research work such as [104] and [105].

The DFIG can be configured with either a three-stage gearbox or single-stage gearbox. Performance analysis conducted in [106] shows that the configuration with single-stage gearbox has lower losses. Furthermore analysis conducted in [105] shows that the doubly-fed reluctance generator (DFRG) has no brushes and slip rings and this increases system reliability and reduce maintenance requirements. However, there is limited number of commercially available systems that utilize single-stage gearbox or the DFRG. The DFIG drive train utilizes industrially standardized components that yield benefits in cost and reliability. The DFIG drive train is therefore considered as the most suitable option for the WTG system. The grid-side power inverter should be configured as the CSI with the MPPT algorithm.

C. Battery Storage System

The battery storage system (BSS) is mainly comprised of a battery bank and power electronics (AC/DC and DC/AC). The battery technologies that are suitable for the nuclear micro-grid have been analysed in chapter 4. The BSS should be configured as an uninterruptible power supply (UPS) and partitioned into multiple master units to allow for redundant voltage-source inverters that regulate the bus voltage magnitude and frequency. The UPS systems have traditionally been interfaced to the medium voltage network through a step-up transformer.

An improved transformer-less UPS that exhibits higher efficiency as compared to traditional UPS has also been developed. The traditional UPS has a wealth of operating experience that has proved it to have high inherent reliability due to lower number of components used and simplified maintenance requirements [107]. The lack of field experience for the transformer-less UPS systems is usually compensated with intensive product testing to predict their future reliability. However, the transformer based UPS system is considered as the most suitable option for the nuclear micro-grid.

D. Emergency Diesel Generators

Most of the current nuclear facilities (i.e. Koeberg Nuclear Power Plant) have 2 or 3 emergency diesel generators (EDG) installed onsite.

The EDG are configured to automatically start when the loss of power is detected on the safety bus. The introduction of the nuclear micro-grid system will ensure uninterrupted supply of electrical power to the safety bus when the LOOP event is experienced. Therefore, the EDG will act as backup source for the nuclear micro-grid system. A single-line diagram showing a simplified architectural layout of the nuclear micro-grid is exhibited in figure 5.3.

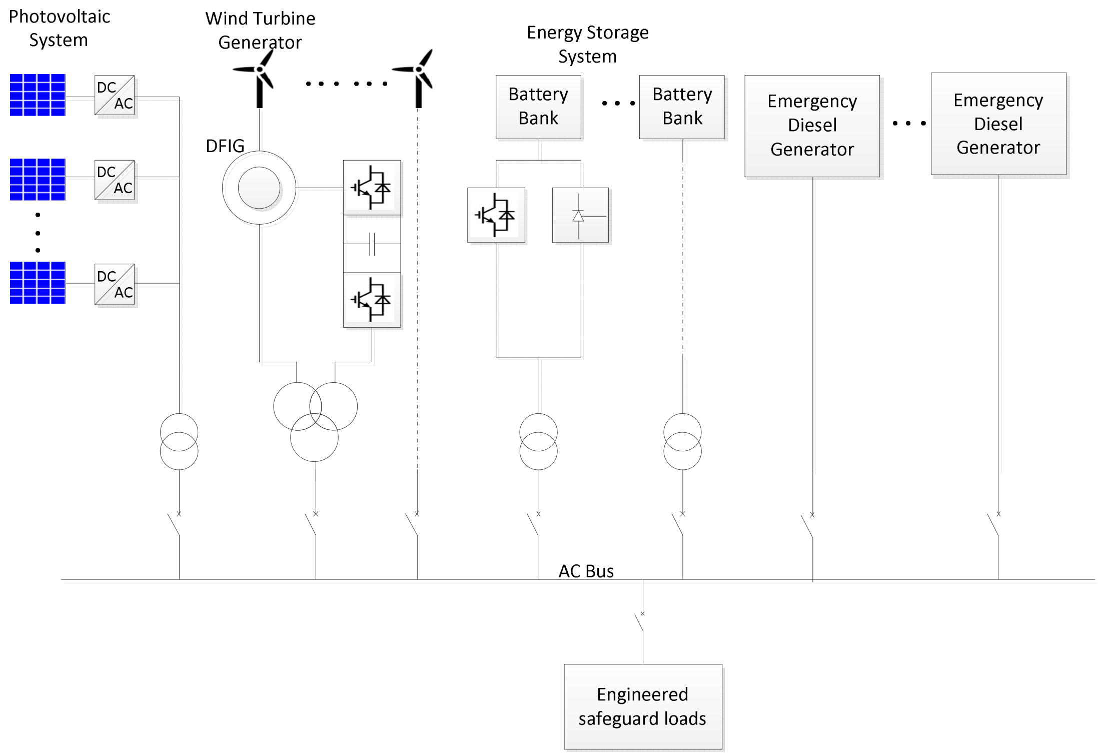

Figure 5.3: Simplified architectural layout of the nuclear micro-grid

5.4 Summary

The control scheme and architectural layout of the nuclear micro-grid were analysed in this chapter. The hierarchical control scheme with voltage-source inverter (VSI) configuration for grid forming inverters and current-source inverter (CSI) configuration for grid following inverters was determined to be the suitable control schemes for the nuclear micro-grid.

The traditional droop control algorithm was suggested for VSI and maximum power tracking algorithm suggested for CSI. The coordinated control strategy was suggested for the energy storage system. The architectural layout was established with reference to the suggested control system and the design-for-reliability requirements. The next chapter presents a methodology that is used to establish the energy capacities of the nuclear micro-grid subsystems.

Chapter 6 Nuclear Micro-grid Capacity Sizing

Sufficient capacity is another reliability requirement for the emergency power supply system as specified in section 2.2 (c). A methodology used to determine the sufficient energy capacities of the nuclear micro-grid subsystems is discussed in this chapter. The analysis focuses on the renewable energy sources (RES) and energy storage system (ESS) because the capacity of the diesel generator is well established at the existing nuclear facilities. The information covered in this chapter includes details of the capacity sizing methodology and the application of the methodology.

6.1 Capacity Sizing Methodology

The suitable distributed energy sources (DES) and ESS that were determined in chapters 3 and 4 are solar energy, wind energy, diesel generators and static battery storage system. The diesel generator supplies dispatchable power that is determined by the engine power rating and constrained by the amount of available fuel (energy quantity). The diesel generator is therefore considered as the fixed backup supply for the RES and ESS. The photovoltaic (PV) and wind turbine generator (WTG) are considered as the preferred power sources for the nuclear micro-grid. However these sources generate intermittent power and should be adequately sized together with the ESS in order to ensure 100% availability of electrical power under all postulated design basis conditions.

The sizing methods that have been investigated in various research works (i.e. [93] and [97]) focus on optimization of the RES and ESS capacities while minimizing the investment. On the contrary, the benefits of sufficient capacity are considered to outweigh the cost factor for the nuclear micro-grid system because safety is a primary objective in the nuclear facilities. Therefore the sizing methodology considered in this study, focuses only on the capacities that achieve 100% power availability.

The methodology for sizing the capacities of PV, WTG and ESS is defined as follows:

1. Determine the mathematical models of the subsystems that can be used to estimate the performance of the PV, WTG and ESS under fluctuating weather conditions.
2. Determine the historical weather information that includes average solar irradiation levels, temperatures and wind speed. The weather information is used together with the mathematical models to calculate the output performance of the nuclear micro-grid.
3. Determine the specifications of the commercially available PV, WTG and ESS components.
4. Develop an algorithm for sizing the capacities of PV, WTG and ESS based on the weather information.
5. Analyse the capacities of the subsystems using the algorithms and taking into account the system constraints such as availability of installation area, availability of existing reference technology, system costs, etc.

6.2 Application of the Methodology

The above-mentioned sizing methodology is applied to the reference plant (Koeberg Nuclear Power Plant) in order to evaluate the performance of the nuclear micro-grid.

6.2.1 Mathematical Models of RES and ESS

The mathematical models of the PV, WTG and ESS are analysed in this subsection.

A. Photovoltaic System Model

The output of the PV panel is directly proportional to the available solar radiation and inversely proportional to ambient temperature. Other factors that affect the PV panel output include wiring losses, DC-AC inverter conversion losses, dust accumulation and shading. The simplified performance model of the PV panel is given in equation 6.1 taking into consideration that the PV system inverter is configured with maximum power point tracking (MPPT) algorithm [108], [109].

$$P_{PV} = f_{PV} P_{M0} \frac{G_a}{G_0} [1 + \mu_{TM} (T_M - T_0] \qquad (6.1)$$

Where P_{PV} is maximum power generated by the PV panel

f_{PV} is the de-rating factor due to dust, shading, wiring & converter losses

G_a and G_0 are solar radiation at operation and standard condition respectively

P_{M0} is the maximum power generated at standard condition

T_M and T_0 are module temperature at operating and standard condition

μ_{TM} is the temperature coefficient of maximum power

The operation temperature T_M depends on the solar radiation G_a and ambient temperature as given in equation 6.2.

$$T_M = T_a + G_a \left[\frac{NOCT - 20}{800}\right] \qquad (6.2)$$

Where *NOCT* is the normal operating cell temperature

T_a is the ambient temperature

T_M is substituted in equation 1 to get the maximum output power as given in equation 6.3.

$$P_{PV} = f_{PV} P_{M0} \frac{G_a}{G_0} \left[1 + \mu_{TM} \left(T_a + G_a \frac{NOCT - 20}{800} - 25\right)\right] \qquad (6.3)$$

The total energy generated by the PV panels is the calculated using equation 6.4.

$$E_{PV}(t) = N_{PV} \sum_{t=1}^{t=N} P_{PV}(t) \qquad (6.4)$$

Where N is the total number of hours in one year

N_{PV} is the total number of PV panels

B. Wind Turbine Generator Model

The rate of energy transfer from wind to the wind turbine is proportional to the density of air, the turbine rotor area and the cube of the wind speed as given in equation 6.5 [110].

$$P_{Con} = \frac{1}{2}\rho A \lambda V_w^3 \qquad (6.5)$$

Where P_{Con} is the converted power; ρ is the air density; A is the swept area of the rotor disc; λ is dimensionless performance coefficient; V_w is wind speed

The simplified model for output power of wind turbine can be determined using the turbine's output power characteristics. Figure 6.1 shows a typical power curve of a wind turbine [110].

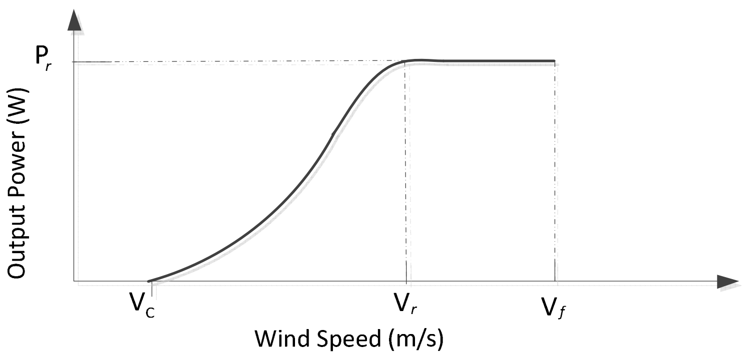

Figure 6.1: Wind turbine output power characteristics

Using figure 6.1, the simplified output power of the wind turbine can determined using expressions in equation 6.6.

$$P_{WT} = \begin{cases} P_r\left(\frac{V^2 - V_c^2}{V_r^2 - V_c^2}\right) & V_c \leq V \leq V_r \\ P_r & V_r \leq V \leq V_f \\ 0 & V < V_c \ \ or\ V > V_f \end{cases} \qquad (6.6)$$

Where P_{WT} is the output electrical power, P_r is the rated power, V_c is the cut in speed, V_r is the rated speed of the turbine and V_f is the cut-out speed.

The total electrical energy generated by the wind turbine (for N_W number of wind turbines) is determined using equation 6.7.

$$E_{WT}(t) = N_W \sum_{t=1}^{t=N} P_{WT}(t) \qquad (6.7)$$

The wind speed increases with increasing altitude. If the height at which the wind speed is measured is different from the height of the wind turbine hub, then equation 6.8 is used to estimate the wind speed at the turbine hub height.

$$V_2 = V_1 \left(\frac{h_2}{h_1}\right)^{\propto} \qquad (6.8)$$

Where V_2 is the estimated wind speed at turbine height (h_2), V_1 is the measured wind speed at height h_1 and α is the ground surface friction coefficient

The ground surface friction coefficient is taken as 0.1 for ocean surface or smooth hard ground [110].

C. Battery Storage System Model

The static battery technology has been identified in chapter 4 as the most suitable energy storage medium. Therefore, the characteristics of the static battery storage (lithium-ion) are applied to establish the model of the battery storage system. The battery bank stores net energy when generation from RES is greater than the load (E_L). Whenever the generation is insufficient, the battery bank supplies the net energy to the load. The net energy (NetE) at any time instance is determined using equation 6.9 and can either be positive or negative.

$$NetE(t) = E_{PV}(t) + E_{WT}(t) - E_L \qquad (6.9)$$

The capacity of the battery bank is constraint by power and energy limits (amp-hours). The battery energy limit is measured by a state of charge (SOC) and this should always be maintained within the minimum (SOC_{min}) and maximum (SOC_{max}) in order to prevent overcharging and over-discharging of the battery bank. At any time instance, the available energy (E_B) in the battery bank is determined from the state of charge conditions as illustrated in expression 6.10.

$$E_{Bmin}(t) \leq E_B(t) \leq E_{Bmax}(t) \qquad (6.10)$$

The charging efficiency and discharging efficiency are normally provided by the manufacturer as a single value called round-trip efficiency (approx. 96% for lithium ion batteries). Other factors that affect the efficiency of the battery are ambient temperature, humidity, etc.

6.2.2 Historical Weather Information

The electrical output characteristics of PV panels and wind turbines rely on weather conditions and therefore one year (8760 hours) historical weather information (measured at Koeberg weather station) is used to establish their capacities. The use of historical weather information does not guarantee 100% electricity availability but it provides a reasonable engineering solution based on statistical information. The hourly solar irradiation, temperature and wind speed trends for Melkbosstrand, Cape Town recorded for one year (2009) are provided in figure 6.2 (a), (b) and (c) respectively. Detailed analysis on the weather data has been provided in chapter 3. The solar irradiation and wind speed usually exhibit complimentary characteristics from the fact that solar radiation is available during clear day hours and higher wind speed are mostly experienced during cloudy or night hours.

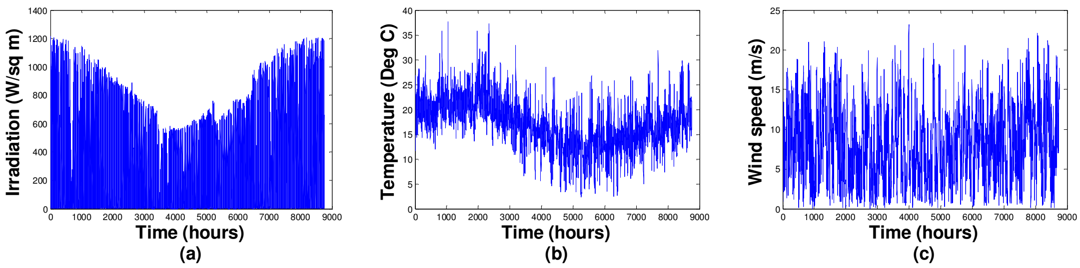

Figure 6.2: Annual weather data of Melkbosstrand, Cape Town

6.2.3 Specifications of Subsystems

The specifications of the PV, WTG and ESS are determined from the commercially available datasheets. The deciding factors for selection of the PV panel are maximum output power of the panel under standard test conditions (STC) and the efficiency.

The selection of the wind turbine is based on the lowest wind speed (including the frequency of occurrence for the lowest wind speed) as recorded for the Melkbosstrand.

The lowest wind speed must have a high frequency of occurrence in order to limit the mechanical wear that may arise from frequent start-up of the wind turbine generator. Figure 3.4 in chapter 3 shows the speed of 3 m/s as the lowest wind speed with relatively high frequency of occurrence. Therefore, the wind turbine with cut-in speed of 3 m/s is selected. The lithium-ion battery is selected based on arguments that were presented in table 4.2 of chapter 4. The parameters of the selected PV panel, WTG and battery are provided in table 6.1.

Table 6.1: Parameters of PV Panel, wind turbine and battery [111], [112], [113]

PV Panel: SunPower P17 SPR-P17-355-COM	**Wind Turbine: Nordex N117/2400**	**Battery: Tesla PowerPack**
Nominal Power: 355 W	Rated Power:2.4 MW	Rated power: 50 kW
Efficiency: 17.2 %	Cut-in speed: 3 m/s	Capacity: 210 kWh
Rated Voltage: 43.4 V	Rated Speed: 11 m/s	Rated voltage: 480V, 3Phase
Rated Current: 8.18 A	Cut-off speed: 20 m/s	Depth of Discharge: 100%
Open-Circuit Voltage: 51.9 V	Min. hub height: 91 m	Round-trip efficiency: 89%
Short-Circuit Current: 8.68 A	Rotor diameter: 117 m	No. of Cycles: 5,000
Power temp. Coef.: -0.37%/ ^{0}C	Warranty: 20 years	Warranty: 10 years
Dimensions (L×W×D): 2.067×0.998×0.046 m	Capital Cost: $1,160/kW	Dimensions including inverter (L×W×H): 2.3×2.1×4.4 m
Warranty: 25 years		Capital Cost: $526.4 / kWh
Capital Cost: $ 882 /kW		

6.2.4 Capacity Sizing Algorithm

The capacities of the PV arrays, WTGs and battery banks depend on the system parameters (table 6.1), the mathematical models (section 6.2.1) and the annual weather information (section 6.2.2). An algorithm that calculates the capacities based on the above information was developed. The algorithm is partitioned into two modules.

The first module is termed availability algorithm and is used to calculate the availability of electrical power to the safety loads. The second module is termed sizing algorithm. The sizing algorithm incorporates the availability algorithm to calculate the number of PV panels, WTGs and the battery bank capacity. The flowchart for the availability algorithm is illustrated in figure F.1 of appendix F. It has been modified from [114] to incorporate the wind energy source.

The flowchart for the sizing algorithm is illustrated in figure F.2 of appendix F. The system constraints that restrict the size of the nuclear micro-grid are factored into the sizing algorithm. At each calculation step, either the number of PV panels or WTGs are incremented based on the specified system constraints. MATLAB code that was used to implement the algorithms is provided in appendix C. The algorithms are applied in the next subsections to calculate the capacities of the subsystems based on the specific system constraints and the desired electrical power availability.

6.2.5 Analysis of Subsystems Capacities

The availability of installation area is the main constraint associated with capacity evaluation of the nuclear micro-grid for new and existing nuclear facilities. The maximum power and energy requirements for the safety loads are 4.21 MW and 302.8 MWh as calculated in appendix A. It is expected that the nuclear micro-grid should have the adequate capacity to meet the safety loads requirements while taking into consideration the space constraints and fluctuating weather conditions. It is further expected that the total annual energy generated from PV and WTGs should be equal or greater than the annual safety loads energy demand of 36.8 GWh (4.205 MW×8760hrs).

The constraints that are analysed in this subsection are the installation area of PV system and restrictions on battery bank capacity based on existing reference applications. Other constrains such as wind turbines installation area are excluded for future work. The objective of the analysis is to establish the capacities of the subsystems that achieve 100% availability of electrical power to the safety loads with no required intervention from the backup diesel generators.

A. PV Installation Area Constraint

The PV panels for the nuclear micro-grid can be installed on the building rooftops or on flat surfaces that are adjacent to the buildings. The surface area required for the installation of the PV system depends on many factors such as individual panel dimensions, tilt angle, their spacing in the array, fire codes, accessibility, wind loads, etc. Before the capacity of the PV system can be established, the available installation area must first be determined. Using Koeberg plant as reference, an installation area of 107,100 m^2 (equivalent to 15 soccer fields) is selected for evaluation purposes.

This area translates to a maximum number of 51,915 PV panels calculated using the dimensions of PV panels in table 6.1 (space de-rating factors are ignored for simplicity). The 51,915 PV panels translate to peak power of 18.4 MW. It should however be noted that the actual installation area is unique for each installation site and should be evaluated before the PV array capacity analysis is conducted. The hourly wind speed was recorded at 85m height and it has been converted to the turbine hub height of 91m using equation 6.8. The converted wind speed trend and frequency distribution graphs are shown in figures B.1 and B.2 of appendix B. Availability and sizing algorithms were used for the calculation of the number of WTGs and battery bank capacity with the number of PV panels fixed at 51,915.

The battery bank capacity was gradually incremented until the number of WTGs that achieve 100% power availability was established. Table 6.2 shows the results of the simulation. It is observed that the battery capacity of 20 – 40 MWh achieves power availability of 99.99% under the specified space constraint. This translates to 21 hours of power unavailability.

The 50 – 60 MWh bank achieves 99.999% availability that translates to 2 hours of power unavailability. This implies that the storage capacity of 20 – 60 MWh is insufficient for the 100% availability requirement. This was confirmed by calculating the total annual energy generated by the PV panels, WTGs with the battery storage capacity of 20 – 60 MWh. The calculation results are tabulated in Table 6.3. It can be seen from table 6.3 that the total annual energy is much higher than the safety loads annual demand. However there is insufficient capacity to store the excess energy and ensure 100% power availability. The battery bank capacity that achieves 100% availability under the specified constraint is 80 MWh with 10 wind turbines (rated at 24 MW_{Peak}). It is observed from table 6.2 that increasing the battery bank capacity beyond 130 MWh does not results in any further reduction in the number of wind turbines. This is attributable the pattern of the historical weather information that was used in the simulation. Therefore the 130 MWh is considered as the maximum permissible battery storage capacity for the nuclear micro-grid under the specified system constraint. As the capacity of the battery bank is increased, the number of deep discharges is reduced as illustrated in figure 6.5. The reduction in deep discharges of the battery bank can increase the lifespan of the battery bank and this can increase the overall reliability of the nuclear micro-grid.

Table 6.2: Capacity evaluation of the micro-grid under fixed capacity of PV system

Battery Bank Capacity	**No. of Wind Turbines**		
	99.99%	99.999%	100%
20 MWh	684	-	-
30 MWh	184	-	-
40 MWh	17	-	-
50 MWh	8	152	-
60 MWh	5	12	-
70 MWh	4	8	12
80 MWh	4	7	10
90 MWh	3	6	8
100 MWh	3	5	6
110 MWh	3	4	5
120 MWh	2	3	4
130 MWh	2	3	3
140 MWh	2	3	3

Table 6.3: Annual energy generated by PV and WTGs for 20 – 60 MWh storage capacity

Battery Bank Capacity	No. of Wind Turbines	Achievable Availability	Annual Energy Generated by PV and Wind (GWh)
20 MWh	684	99.99%	7,590
30 MWh	184	99.99%	2,067
40 MWh	17	99.99%	222
50 MWh	152	99.999%	1,710
60 MWh	12	99.999%	167

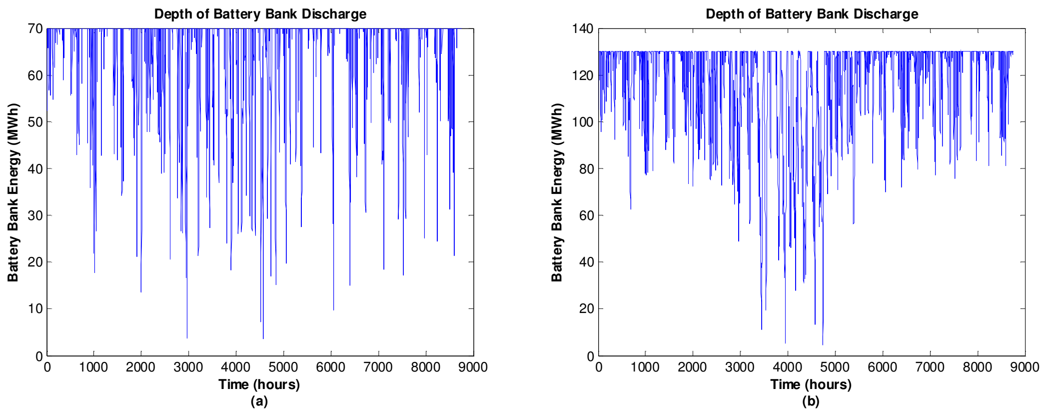

Figure 6.3: Depth of discharge for: (a) 70 MWh battery and (b) 130 MWh battery

B. Consideration of battery bank capacity

The calculations in the above subsection show that the minimum capacities that achieve 100% power availability are 70 MWh battery bank, 51,915 PV panels and 12 WTGs. However, the largest existing lithium-ion storage application is rated at 40 MW / 40 MWh as mentioned in section 4.5.1. It is therefore a good engineering approach to curb the battery storage capacity within the tried and tested limits. The battery bank with capacity of 50.5 MWh is therefore selected for simulation purposes The 50.5 MWh capacity can supply the safety loads of 4.21 MW for a period of 12 hours, during a loss of offsite power (LOOP) event with solar and wind energy unavailable. The availability and sizing algorithms are used to simulate the capacities of the subsystems.

The expected simulation results are the number of PV panels and wind turbines that achieve 100% availability of electrical power with the battery bank of capacity of 50.5 MWh. It is further expected that the total annual energy generated from PV and WTGs should be greater than the annual safety loads energy demand of 36.8 GWh (4.205 MW×8760hrs). Table 6.3 shows the simulation results that include various combinations of the PV panels and WTGs and the annual energy generated by PV and WTGs. It is observed that the lowest number of 247,901 PV panels is achievable with 13 wind turbines. Increasing the number of WTGs beyond 13 does not results in further reduction of the number of the PV panels.

This is attributable to the pattern of the weather information that was used in the simulation. It is further observed that the various combinations of PV panels and wind turbines generate annual energy that is much higher than the safety loads annual demand for all various combinations. As the number of wind turbines increase, the number of battery discharges decreases while the depth of discharge (DOD) for the battery remains approximately the same. This is confirmed by the battery bank DOD graphs in figure 6.6 where (a) represents 1 wind turbine and (b) represents 14 wind turbines. The reduction in number of battery discharges can increase the lifespan of the battery bank and this can in turn increase the overall reliability of the nuclear micro-grid.

Table 6.4: Simulation results for battery bank fixed at 50.5 MWh

No. WTGs	No. of PV Panels	Annual Energy (GWh)
1	2,613,001	1,748
2	1,407,001	957
3	1,226,101	848
4	1,179,201	828
5	743,701	550
6	596,301	462
7	582,901	465
8	576,201	471
9	549,401	464
10	455,601	413
11	361,801	362
12	268,001	311
13	247,901	308
14	247,901	319

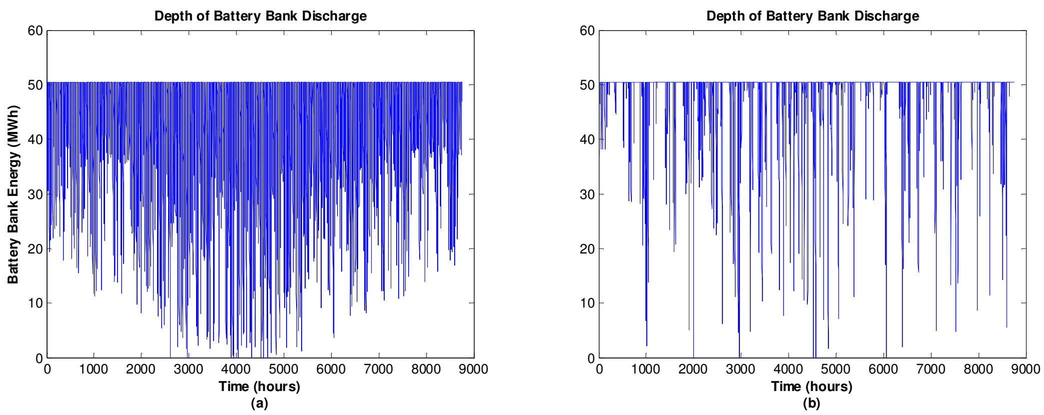

Figure 6.4: Battery bank depth of discharge for (a) 1 wind turbines and (b) 14 wind turbines

6.3 Summary

In this chapter, the methodology that is used to calculate the capacities of the RES and battery bank storage was presented. The steps of the capacity sizing methodology were explained in details. The application of the methodology included the use of capacity sizing algorithms together with the mathematical models of subsystems, historical weather information and the parameters of subsystems to calculate the capacities of PV arrays, WTGs and battery bank. The impact of system constraints on the overall capacity was also investigated. The simulation results confirm that the preferred energy sources (RES and ESS) of the nuclear micro-grid can be configured with sufficient capacity to supply 100% of electrical power for any desired duration without the intervention of the backup diesel generators. The next chapter presents a reliability assessment of the nuclear micro-grid to determine the system's ability to supply power without failure.

Chapter 7 Nuclear Micro-grid Reliability Analysis

The architectural layout of the nuclear micro-grid was established with multiple, diverse and independent energy sources and energy storage system as discussed in chapter 5. The diverse energy sources can either improve the system reliability or reduce it due to additional potential failure modes as a result of increased system complexity and intermittent energy sources. In this chapter, a reliability analysis is carried out to assess the robustness of the nuclear micro-grid system when operating in emergency mode. The analysis addresses the probabilistic risk assessment requirement specified in section 2.2 (g).

7.1 Reliability Analysis Concepts

Reliability is defined as the probability that an item will perform a required function under stated conditions and for a stated period of time [118]. The reliability study of power systems in general provides insights into the potential failure modes including service life estimate and is important during both design and operational stages. The main reliability evaluation methods include Fault Tree Analysis (FTA), Event Tree Analysis (ETA), Markov Process (MP), Reliability Block Diagram (RBD), Monte-Carlo simulation (MCS), etc. The analysis conducted in [119] shows that these evaluation methods yield approximately equal reliability indices.

The FTA is one of the most commonly used tools in industries such as nuclear power plants and space missions. It involves specifying an undesired event and analysing the system in the context of defined conditions to find all realistic ways in which the undesired event can occur [118]. ETA is used to define the probability of failures/accidents as a result of a single or multiple initiating events. MP models the stochastic behaviour of a system using a Markov space state diagram. The system components at any given time are represented by either an operational state or a failed state [99].

The RBD involves representing the physical system components graphically with blocks linked in series or parallel depending on their effects on overall system reliability. The MCS can be used to approximate solution to a quantitative problem through statistical sampling. The reliability analysis process can be divided into two broad categories, namely qualitative and quantitative analyses. The qualitative analysis uses graphical models (i.e. FTA, ETA, RBD, etc.) to verify the various failure modes and causes that contribute to the unreliability of the system. The quantitative analysis includes the use of reliability indices in conjunction with mathematical models to determine quantitative estimates of system reliability. The most commonly used reliability index is mean-time-to-failure (MTTF) for items that cannot be repaired or mean-time-between-failures (MTBF) for repairable items.

The first step in evaluating the reliability indices is to determine a probability density function (denoted as *f(t)*) of failures for each subsystem. The *f(t)* can be defined using distributions such as Gamma, Weibull, Exponential, etc. [118]. Using *f(t)*, the failure probability of the subsystem within time interval [0,t] can be calculated using equation 7.1 [116].

$$F(t) = \int_{0}^{t} f(\tau)d\tau \qquad (7.1)$$

The reliability function can then be defined using equation 7.2

$$R(t) = 1 - F(t) \qquad (7.2)$$

The mean-time-to-failure (MTTF) can be calculated from *R(t)* using equation 7.3

$$MTTF = \int_{0}^{\infty} R(t)dt \qquad (7.3)$$

The failure rate $\lambda(t)$ of component can then be determined as the ratio of failure probability density function to the reliability function as given in equation 7.4

$$\lambda(t) = \frac{f(t)}{R(t)} \quad (7.4)$$

The exponential distribution is widely used for modelling time to failure [118] and will be used in this study. Taking a constant failure rate value, the exponential distribution function is determined from equation 7.5 [121].

$$f(t) = \lambda e^{-\lambda t} \quad (7.5)$$

The reliability function can then be calculated using equation 7.6

$$R(t) = e^{-\lambda t} \quad (7.6)$$

The MTTR is then determined from equation 7.7

$$MTTF = \int_{0}^{\infty} e^{-\lambda t} dt = \frac{1}{\lambda} \quad (7.7)$$

Taking the repair rate as μ, then the mean-time-to-repair (MTTR) can be determined in a similar manner to MTTF using equation 7.8

$$MTTR = \frac{1}{\mu} \quad (7.8)$$

The risk assessment of the emergency diesel generators used in the nuclear power plants is normally evaluated in terms of reliability and availability. The availability is defined as the probability that an item will perform a required function under stated conditions in a stated moment of time [118]. The availability (A) can be calculated from MTTF and MTTR using equation 7.9.

$$A = \frac{MTTF}{MTTF + MTTR} = \frac{\mu}{\mu + \lambda} \quad (7.9)$$

7.2 Nuclear Micro-grid Components Modelling

The reliability block diagram (RBD) model is used for analysis in this study in order to get a graphical representation of the nuclear micro-grid subsystems.

Each subsystem is modelled individually using the failure rate and repair rate indices. The components failure and repair rates are sourced from field data recorded in a number of publications. The manufacturers' warranty is also used to estimate the failure rates of components whose performance data cannot be sourced from existing publications. The failure modes associated with communication systems and island detection systems have been excluded from the models based on the nuclear micro-grid control system discussed in section 5.2.

A. Photovoltaic System

The RBD model of the photovoltaic (PV) system components is shown in figure 7.1. The typical failure modes of PV panels include internal failures (i.e. open circuits, short circuits and back-sheet delamination), external failures (i.e. fractured glass) and degradation due to weather conditions [120]. The DC/AC inverter is the most vulnerable component in the PV system due to the semiconductor modules and capacitors. This vulnerability can be improved through the use of the micro-inverter as discussed in section 5.3 A. The transformer is an essential component for the reliability of the power system. The common causes of transformer failures include power surges, poor manufacturer workmanship, insulation deterioration, overloading, moisture, etc. The failure modes of circuit breakers include failing-to-open, failing-while-in-service, damage-while-successfully-opening, etc. [121].

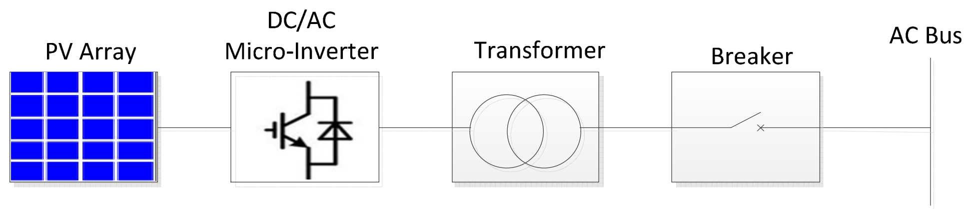

Figure 7.1: Reliability block diagram model of the PV system components

Table 7.1 summarizes shows the failure rates (λ) in failures per hour (f/h) and repair rates (μ) in repair per hour (r/h) for the components of the PV system. The values have been sourced from manufacturers datasheets, publications and standards (IEEE std. 439) [100], [111], [121].

Table 7.1: Failure and Repair Rates of the PV system components

Component	λ (f/h)	µ (r/h)	Component	λ (f/h)	µ (r/h)
PV Module	4.57×10^{-6}	1.39×10^{-2}	Power cables	1.61×10^{-7}	2.19×10^{-3}
Micro-inverter	4.57×10^{-6}	1.39×10^{-2}	Circuit Breaker	5.93×10^{-7}	1.72×10^{-1}
Transformer	6.73×10^{-7}	3.36×10^{-3}			

B. Wind Turbine Generator System

The architectural layout of the wind energy system has been discussed in section 5.3. The simplified RBD model of the wind turbine generator system components is shown in figure 7.2. The wind turbine subsystem is comprised mainly of blades, hydraulics for pitch control and brake system. Both the turbine and gearbox components are subjected to mechanical stresses and their failure modes include cracking, scuffing, lubricant contamination, bearings failure and hydraulic system failure. The doubly-fed induction generator system is subjected to both mechanical and electrical failures.

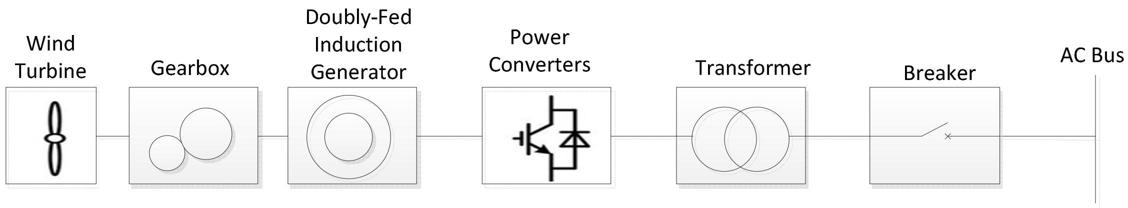

Figure 7.2: Reliability block diagram model of the wind energy system components

The Nordex wind turbine (N117/2400) used as reference in this study is designed to operate for a period of 20 years. The failure and repair rates recorded by various sources are exhibited in table 7.2 [124], [125], [104], [121].

Table 7.2: Failure Rates of the Wind Turbine Generator system components

Component	λ (f/h)	μ (r/h)	Component	λ (f/h)	μ (r/h)
Wind Turbine	2.85×10^{-5}	1.67×10^{-2}	Power Converters	1.21×10^{-5}	2.19×10^{-3}
Gearbox	1.43×10^{-5}	1.67×10^{-2}	Transformer	6.73×10^{-7}	3.36×10^{-3}
Generator	1.4×10^{-5}	3.06×10^{-2}	Power cables	1.61×10^{-7}	2.19×10^{-3}
Circuit breaker	5.93×10^{-7}	1.72×10^{-1}			

C. Battery Storage System

The simplified RBD model of the battery storage system components is shown in figure 7.3. The lithium-ion battery technology with nickel-manganese-cobalt alloy cathode manufactured by Tesla is used as reference in this study. The main failure mode of safety concern is short-circuiting of Li-ion cells. The short circuit can be caused by repeated over-charging and failure of the protection circuit. The protection circuit is normally designed to fail in an open position (fail-safe).

Other factors that can cause the degradation and failure of the Li-ion are operating at higher than rated temperature and frequent deep cycling beyond the rated depth of discharge. The Tesla PowerPack Li-ion battery is designed to operate for a period of 10 years with more than 5000 charge/discharge cycles [82]. However, the battery bank for the nuclear micro-grid is expected to be cycled only during loss of offsite power event. This condition has been factored into the failure rate of the battery bank. The envisaged future use of the battery bank for grid ancillary services has been set aside in this analysis. The failure and repair rates of the battery storage system components are exhibited in table 7.3 [82], [121].

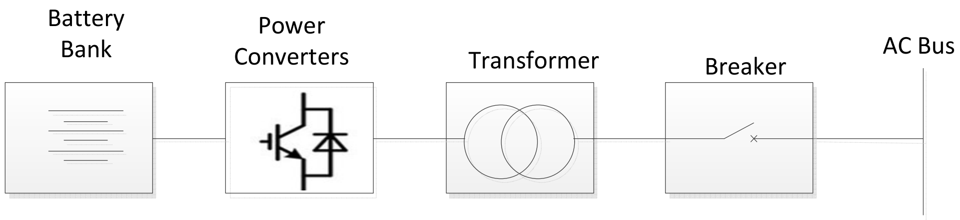

Figure 7.3: Reliability block diagram model of the battery storage system

Table 7.3: Failure Rates of the battery storage system components

Component	**λ (f/h)**	**μ (r/h)**	**Component**	**λ (f/h)**	**μ (r/h)**
Battery Bank	1.14×10^{-5}	3.06×10^{-2}	Circuit breaker	5.93×10^{-7}	1.72×10^{-1}
Power Converters	1.21×10^{-4}	9.34×10^{-3}	Power cables	1.61×10^{-7}	2.19×10^{-3}
Transformer	6.73×10^{-7}	3.36×10^{-3}			

D. Diesel Generator

The main subsystems of diesel generators (DGs) include diesel engine, generator, exciter, voltage regulator and output breaker [58]. The failure data on these DGs is continuously and accurately recorded by standards organizations, utility companies as well as the nuclear regulatory bodies (i.e.US NRC). The main failure modes associated with the DGs include failure-to-start, failure-to-run and maintenance-out-of-service. Approximately 70% of the diesel generators unreliability is attributed to maintenance being performed on the generator at the time of unplanned demand [126]. However, the recovery from maintenance-out-of-service failure mode can be swiftly achieved within minimum time frame. The two-unit nuclear facilities (i.e. Koeberg Nuclear Power Plant) require a minimum of 2 out of 3 DGs to be operational. For simplicity, one diesel generator is used for reliability analysis in this study. The failure rate of diesel generators recorded from field data in updated NUREG/CR-5500 is 2.74×10^{-3} failures/hour as calculated from unreliability with no recovery of 2.17×10^{-2} over an 8 hour run period [126]. The repair rate is 3.23×10^{-4} as calculated from failure-to-start unavailability of 1.47×10^{-2}.

7.3 Reliability Evaluation

The nuclear micro-grid can fail to supply power either due to physical components failure or unavailability of renewable energy sources. The reliability evaluation is carried out to assess the effects of physical components failures and the effects of multiple failures (physical components failures combined with unavailability of RES). The objective of the analysis is to assess the extent to which the nuclear micro-grid improves the reliability of the emergency power systems.

7.3.1 Physical Components Failures

The reliability block diagram (RBD) models, failure and repair rates analysed in section 7.2 are used to evaluate the reliability and availability of the nuclear micro-grid with respect to physical components failures. The evaluation compares three configurations which are the sole operation of diesel generators (configuration at the current nuclear facilities); the RES and storage without the DGs; and the RES and storage with DGs. The PV, wind turbine generator and battery bank models analysed in section 7.2 show series-connected components. The overall reliability of the system containing n number of series components can be calculated using equation 7.10

$$R(t) = R_1(t) \times R_2(t) \times \dots\dots\dots R_n(t) \qquad (7.10)$$

The simplified RBD model of the overall micro-grid system is comprised of four parallel systems as illustrated in figure 7.4. For the system with n number of subsystems connected in parallel, the overall system reliability can be calculated using equation 7.11, taking the system input reliability as 1 (100%). The total availabilities are calculated by substituting reliability functions with availabilities in equations 7.10 and 7.11.

$$R(t) = 1 - [(1 - R_1(t)) \times (1 - R_2(t)) \times \dots\dots\dots (1 - R_n(t))] \qquad (7.11)$$

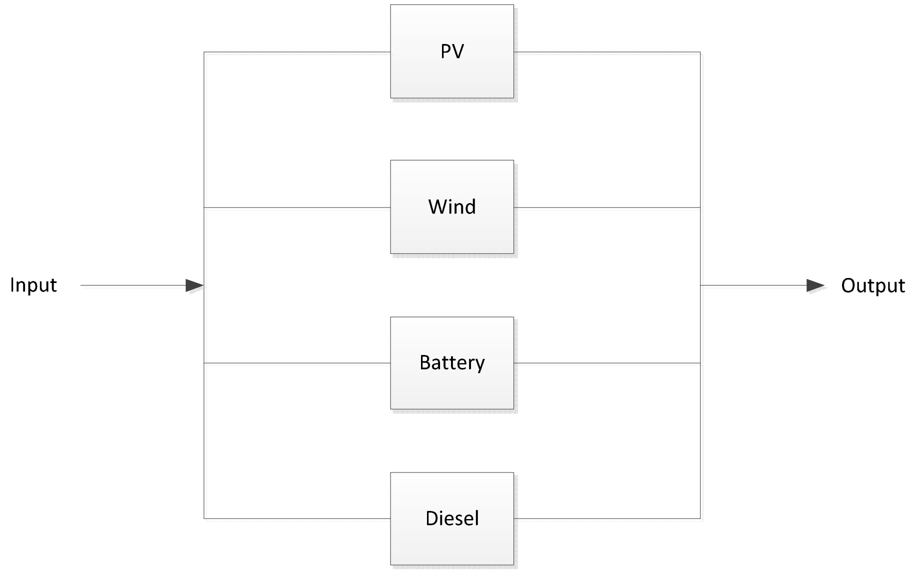

Figure 7.4: The reliability block diagram of the overall nuclear micro-grid system

During normal operational mode, the renewable energy sources are expected to export power to the main grid with battery bank providing grid ancillary services while the diesel generators are in standby mode. The battery bank ancillary services feature, the renewable energy sources always-online feature and the diesel generators standby operational mode are set aside in the analysis carried out in this subsection. A statistical value for the always-online feature and standby operational mode will be applied in the next subsection. During emergency mode, the nuclear micro-grid is expected to deliver electrical power for a period of 72 hours. Therefore, reliability analysis is carried out for a 72-hour mission.

The results of the analysis are tabulated in table 7.4. It is evident from the results that the nuclear micro-grid indeed improves the reliability and availability of the emergency power systems in the nuclear facilities. This is attributable to the architecture that was selected (section 5.3) and the control system that excludes failure modes associated with communications and island detection systems (section 5.2). The lower reliability and availability of the diesel generator are attributable to the failure-to-start and failure-to-run failure modes associated with the power sources that are configured in standby mode.

Table 7.4: Reliability and Availability Analysis Results

Configuration Description	Reliability	Availability
Diesel Generator (DG)	0.991	0.985
Renewable Energy Sources (RES) plus Battery Storage (BS)	0.997	1.00
Nuclear Micro-grid (RES + BS + DG)	1.00	1.00

7.3.2 Multiple Failures

The coordinated control strategy discussed in section 5.2 indicated that the diesel generators (DGs) are configured as the backup supply to the renewable energy sources (RES). The output power of RES (solar and wind) is intermittent and uncontrollable. Therefore, there exists a possibility that the components failures of RES and DGs can occur concurrently with unavailable RES. This subsection analyses the nuclear micro-grid reliability in terms of the loss of power supply probability (LPSP) with respect to multiple failures. The multiple failures considered in the analysis are the micro-grid components failures and intermittency of the wind or solar energies.

The topic of the micro-grid reliability analysis considering these types of multiple failures has previously been evaluated in several research works such as [96], [115], [117] and [123]. Reference [115] applied sequential Monte Carlo Simulation (MCS) to evaluate a micro-grid that is comprised of DG, micro gas turbine, wind turbine generator (WTG) and photovoltaic (PV). The work concludes that WTG and PV are more unreliable as compared to conventional sources due to their dependence on the weather conditions. However, the work did not evaluate the benefits that could be harnessed by the addition of sufficient RES and the ESS to the micro-grid. References [96], [117] and [123] apply Markov Process model to the micro-grids that are comprised of PV-Wind-Storage, PV-Storage and PV respectively. The conclusion drawn in these studies is that the distributed sources (PV and Wind) increase power supply availability at the expense of increased failure frequency. On the contrary, it is expected that reduced failure frequency of the PV and Wind can be achieved through the use of robust control systems and architecture that have been discussed in chapter 5.

The reliability analysis in terms of Loss of Power Supply Probability (LPSP) is carried out using sequential Monte Carlo Simulation (MCS) in this study. The demand for emergency operational mode can occur concurrently with multiple failures at any instance during the life-time of the nuclear micro-grid. Therefore, the analysis should takes into account the operational duration of the RES and DGs which are defined in procedures and standards. The life-time of the RES can be estimated using the manufacturer warranties. The IEEE 387-1995 standard specifies minimum operational requirements for the DGs in the nuclear facilities as 4000 starts and 6000 hours [58]. The following random occurrences are factored into the simulation:

- The hourly weather index is selected randomly from the annual weather data. The random index is then used to select the corresponding weather data and then calculate the capacities of the renewable sources at the instance of the emergency mode demand.
- The duration in service is selected randomly within the service life of each subsystem. The duration is then used to calculate the reliability of each subsystem at the instance of the emergency mode demand.

The PV, wind and battery bank capacities that achieve 100% power availability (51,915 panels - 18.4 MW peak, 10 wind turbines - 24 MW peak and 80 MWh battery bank) calculated in section 6.2.5 A. are used in the simulation. The reliability functions of the subsystems are computed using the models established in section 7.2. The flow chat for MCS algorithm is outlined in appendix D. The complete MATLAB code for the MCS algorithm is provided in appendix E. The algorithm was executed with 1 million sampling done to simulate the Loss of Power Supply Probability (LPSP) for five different configurations of the nuclear micro-grid. The descriptions of the configurations are listed in table 7.5.

Table 7.5: Description of the five identified configurations of the Nuclear Micro-grid

Configurations	**Description**
1	PV + Wind + Battery-storage + Diesel-Generator
2	Wind + Battery-storage + Diesel-Generator
3	PV + Wind + Battery-storage
4	PV + Battery-storage + Diesel-Generator
5	Diesel Generator

The simulation results are given in figure 7.5. The results show that the addition of the renewable energy sources (RES) and battery storage (BS) indeed reduces the LPSP for the nuclear micro-grid. It is also observed that the use of RES and the BS without the diesel generator (DG) results in lower LPSP as compared to the sole use of the DG. This is attributable to the fact that the sufficient capacities of the RES and BS were calculated in chapter 6 using the historical weather data of the site used as reference in this study (Melkbosstrand, Cape Town). It is further noted that the wind energy (conf. 2) has a much higher impact on the LPSP as compared to solar energy (conf. 4). This is attributable to the fact that the location of the selected site has higher wind resource compared to solar resource.

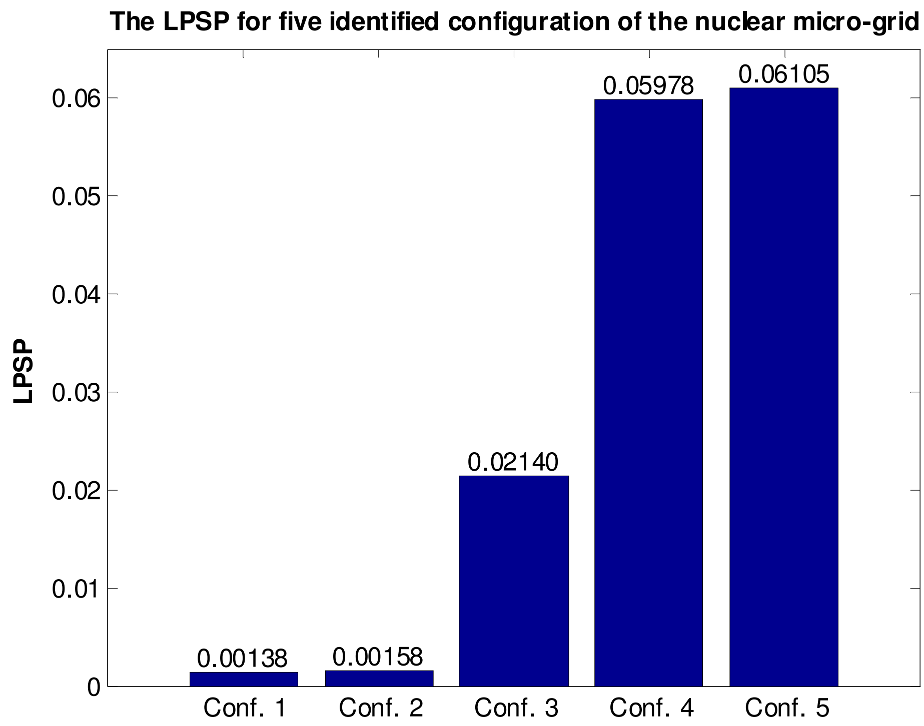

Figure 7.5: LPSP for various configurations of the Nuclear Micro-Grid

7.3 Summary

Reliability analysis of the nuclear micro-grid was carried out in this chapter. The background information on reliability principles was first introduced. The nuclear micro-grid was then modelled with reliability block diagrams using failure and repair rates for each subsystem. The reliability evaluation was then carried out to assess the effects of physical components failures and the effects of multiple failures (physical components failures combined with unavailability of the RES). The Monte Carlo Simulation algorithm was developed and used to evaluate the effects of multiple failures. The results show that the reliability and availability of the emergency power supply is significantly increased by the used of the nuclear micro-grid. Furthermore, the nuclear micro-grid reduces the loss of power supply probability significantly. The next chapter presents the conclusion of the research work and includes recommendations for future work.

Chapter 8 Conclusions and Recommendations

8.1 Key Findings

The reliability requirements for emergency power supplies in the nuclear facility were established through the literature review. The micro-grid with distributed energy sources and energy storage system that is intended for use in the nuclear facilities has been termed a nuclear micro-grid in the context of this study. The energy sources that meet the high reliability requirements are solar energy, wind energy and diesel generators. The static battery technology was established as the energy storage system that adheres to the reliability requirements as well as power and energy requirements of the safety loads. The technologies that are in development stage and yet exhibit potential for use in the nuclear micro-grid were also discussed.

Information on the control strategies and architectural layout of the nuclear micro-grid was also discussed. The capacity sizing analysis revealed that the selected renewable energy sources and energy storage system have the capacity and capability to supply power to the safety loads without the intervention of the backup diesel generators. The reliability analysis shows that the nuclear micro-grid significantly increases the reliability and availability of the emergency power systems in the nuclear facility. The loss of power supply probability is also significantly reduced.

8.2 Recommendations for Future Work

The design-for-reliability requirements (section 2.2) that were not addressed in this research work were set aside for analysis in the future work. Furthermore, the following additional recommendations are proposed for the future work:

- Modelling and performance assessment of the nuclear micro-grid to establish the performance when subjected to varying operational conditions of the safety loads.
- Reliability assessment of the nuclear micro-grid under severe weather conditions.
- Economic analysis of the nuclear micro-grid.

The aim of modelling and performance assessment will be to investigate the performance of the established micro-grid architecture when subjected to inductive, resistive and non-linear safety loads during transition from grid-connected to islanded mode. The severe weather conditions such as the earthquake and tsunami that occurred in Japan can render the nuclear micro-grid inoperable. Therefore the performance of the nuclear micro-grid will be investigated under such conditions. The economic analysis will provide insight into the economic benefits associated with the use of the nuclear micro-grid instead of the diesel generators alone for the emergency power supply in the nuclear facilities.

9. Appendix A: Energy and Power Requirements of the Safety Loads

1. Introduction

Loss of offsite power (LOOP) accident is an event where all offsite AC power (grid power) to the nuclear facility is lost. The LOOP accident is classified as a design basis condition II event. During the LOOP accident, electrical power to the main reactor coolant pumps is lost. The reactor is then shut down using emergency feed-water system and residual heat removal system. These safeguards loads are powered from the onsite backup power supply system (diesel generators in current nuclear facilities). The probabilistic risk assessment establishes that the LOOP accident can occur concurrently with other accidents (i.e. loss of coolant accident).

The loss of coolant accident (LOCA) is an event where there is a pipe break in primary coolant loop or secondary coolant loop and this result in reduced or total loss of reactor coolant water in pressurized water reactors. The LOCA is considered as a condition IV event because it can rarely occur but when it occurs; there is high probability of core meltdown. The emergency core cooling system is used to remove heat from the core following a LOCA. If LOOP occurs concurrently with LOCA, then the onsite emergency power should be able to power the emergency core cooling loads.

The energy requirements of the safety loads required during LOOP and during LOOP with LOCA are analysed in the subsequent sections.

2. Safety Loads Energy Requirements - LOOP Accident Only

The systems that are used to remove heat from the pressurized water reactor after the loss of offsite power (LOOP) accident are the emergency feed-water system and the residual heat removal (RHR) system. The electrical components of the emergency feed-water system include auxiliary feed-water pump, motor-driven valves and steam valves as shown in figure A.1 (highlighted with green dotted line). Each system is comprised of two or three pumps/components for redundancy, but one pump/component shown for each system in the figure A.1 is for illustrative purposes only. After the LOOP accident, natural circulation of water is continued in the reactor primary coolant loop. The stream generators generate steam that is dumped to the atmosphere through steam dump valves. The auxiliary feed-water tank is used to replenish water level in the steam generators. This operation is carried out for 6 hours.

After 6 hours, heat removal through stream generators is no longer effective. The heat removal is then continued through the residual heat removal (RHR) system. The RHR system is comprised of RHR pump, heat exchangers, component cooling pump, essential service water pump and valves. The RHR system is shown in figure A.1 (highlighted with blue dotted line). The RHR system should continue cooling the reactor for minimum period a maximum period of 72 hours as learnt from the Fukushima Daiichi nuclear power plant accident.

Table A.1 shows the energy requirements for the emergency feed-water system loads. After 6 hours, the emergency feed-water system is stopped and the residual heat removal system is started. Table A.2 shows the additional energy requirements for the residual heat removal system. Figure A.2 shows the total energy requirements for safety loads during a LOOP accident only.

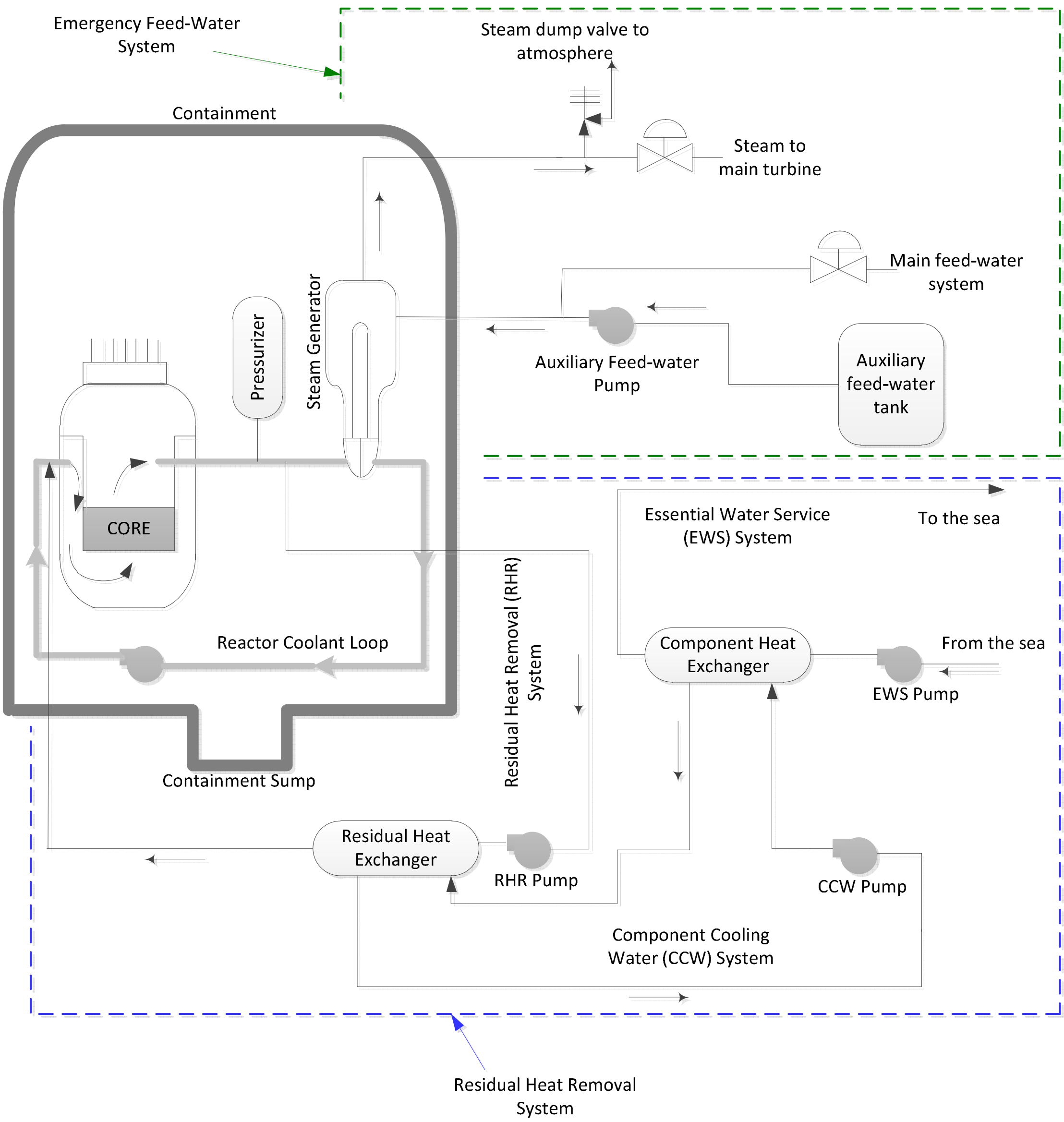

Figure A.1: Emergency feed-water system and residual heat removal system for pressurized water reactor

Table A.1 Energy requirements of emergency feed-water system (6 hour period)

No.	Description of Safeguard Loads	Power Rating
1	DC Loads Battery chargers	194 kW
2	Auxiliary Feed-water System (AFS) Pump	315 kW
3	Nuclear Island Chilled Water (NICW) System Pumps and Compressors set 1	416.7 kW
4	Air conditioning, elevator, lubrication pumps, exhaust fans	255 kW
	Total kW	1 180 kW

Table A.2 Additional energy requirements for residual heat removal system (72 hour period)

No.	Description of Safeguard Loads	Power Rating
1	Active loads after emergency feed-water system is stopped	915.7 kW
1	Residual Heat Recovery (RHR) system Pump	355 kW
2	Nuclear Island Component Cooling (NICC) system Pump	450 kW
3	Essential Service Water (ESW) System Pump	250 kW
4	System valves, motor cooling fans, lubrication pumps	110 kW
	Total kW	2 080.7 kW

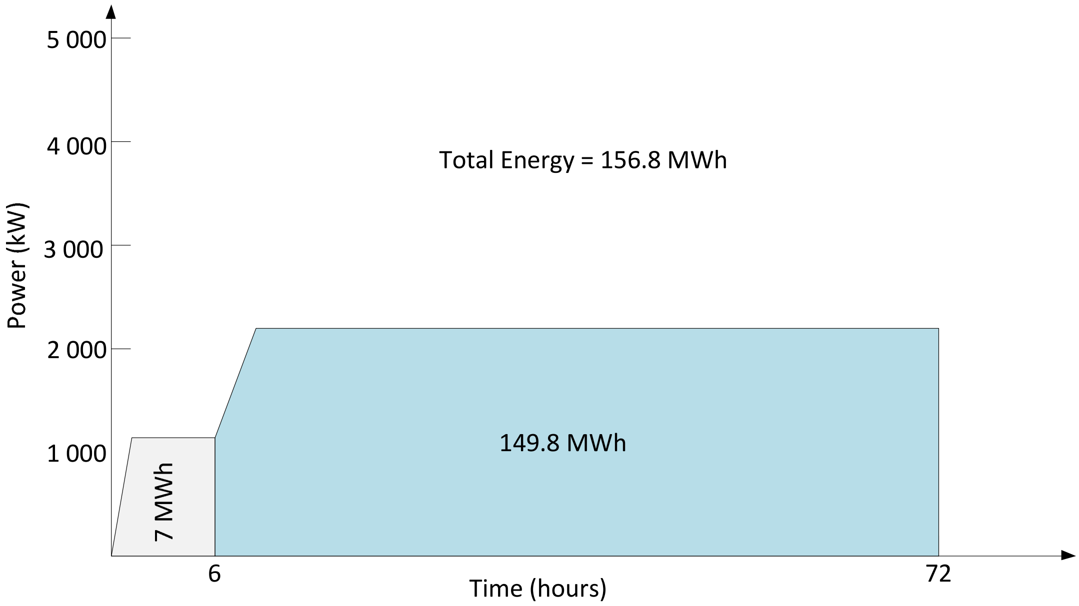

Figure A.2: Energy requirements during LOOP accident

3. Safety Loads Energy Requirements - LOOP Accident with LOCA

The system that is required to remove heat from the reactor core following the loss of offsite power (LOOP) accident combined with the loss of coolant accident (LOCA) is the emergency core cooling system. The emergency core cooling system is illustrated in figure A.3. It is comprised of high-head safety injection pump, intermediate head safety injection system (accumulators), low head safety injection system, containment spray pump, valves, heat exchangers and instrument measurement systems. The high-head safety injection pump supplies borated water to the reactor in situations whether there is a small pipe break and the reactor coolant loop pressure remains relatively high. The supply water is stored in the refuelling water storage tank.

The accumulators inject borated when there is intermediate and large breaks provided the reactor coolant pressure drops below the pressure of water in the accumulators. The low head safety injection pump supplies borated water to the reactor when there is a large pipe break and the pressure in the primary loop has decreased significantly. The pump also supplies water to the suction point of high-head pumps to prevent cavitation. If the pressure in the primary coolant remains high, the low head pump will run in circulation mode. The low head pump also has the connection to the containment sump to continue circulating water through the reactor for long-term residual head removal period (max 72 hours). If the containment pressure increases during the loss of coolant accident (LOCA), the containment spray system is automatically activated to spray cool borated water into the containment.

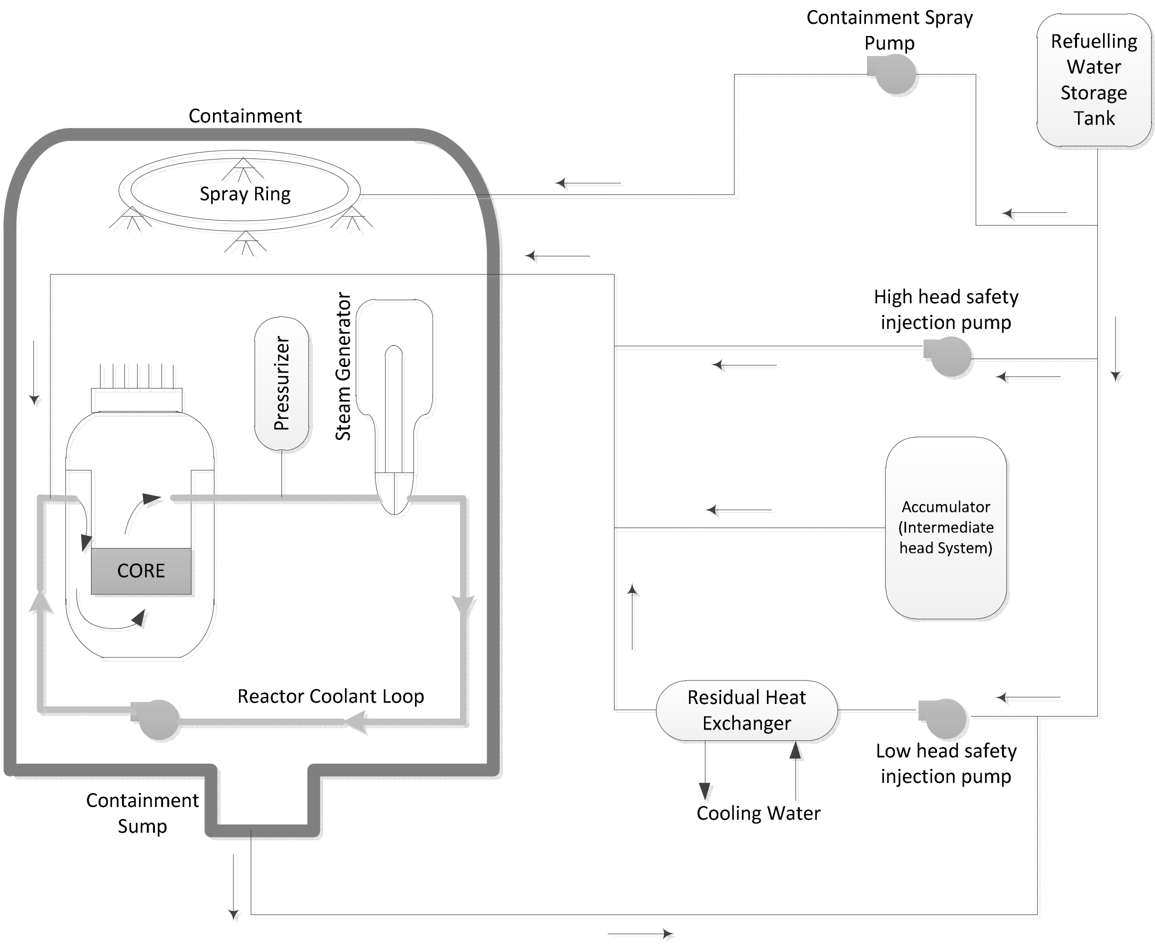

Figure A.3: Emergency core cooling system for pressurized water reactor

The energy requirements for the emergency core cooling system loads are given in table A.3. The loads are supplied continuously for an average period of 72 hours depending on the duration taken to rectify the accident conditions. Figure 6 shows the total energy requirements for the loads following LOOP combined with LOCA accidents. Using the worst case situation (LOOP accident combined with LOCA), the total energy required to be supplied by the micro-grid system is determined as 303 MWh.

Table A.3: Emergency core cooling loads following a LOOP and LOCA accidents

No.	Description of Safeguard Loads	Power Rating
1	Safety loads activated following a LOOP incident	1 725 kW
1	Heat exchangers	710 kW
2	High Head Safety Injection (HHSI) Pump	710 kW
3	Low Head Safety Injection (LHSI Pump	250 kW
4	Containment Spray System (CSS) Pump	450 kW
5	Essential Service Water (ESW) System Pump 2	250 kW
5	Supply to control systems, battery chargers, UPS, radiation monitoring systems	110 kW
	Total kW	4 205 kW

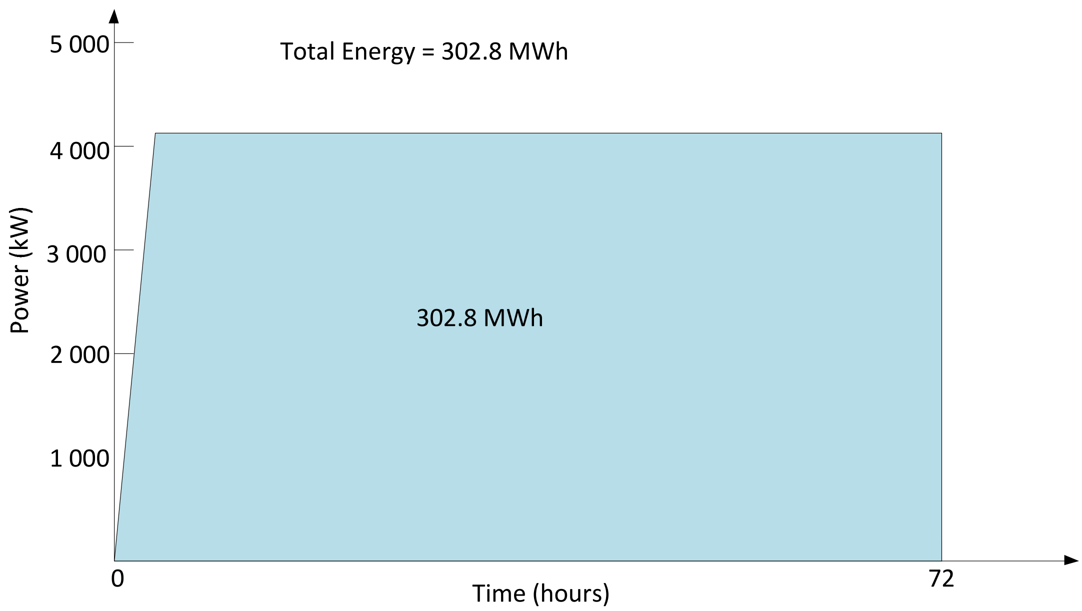

Figure A.4: Energy requirements during LOOP accident with safety injection plus containment spray

10. Appendix B: The Graphs for the Converted Wind Speed

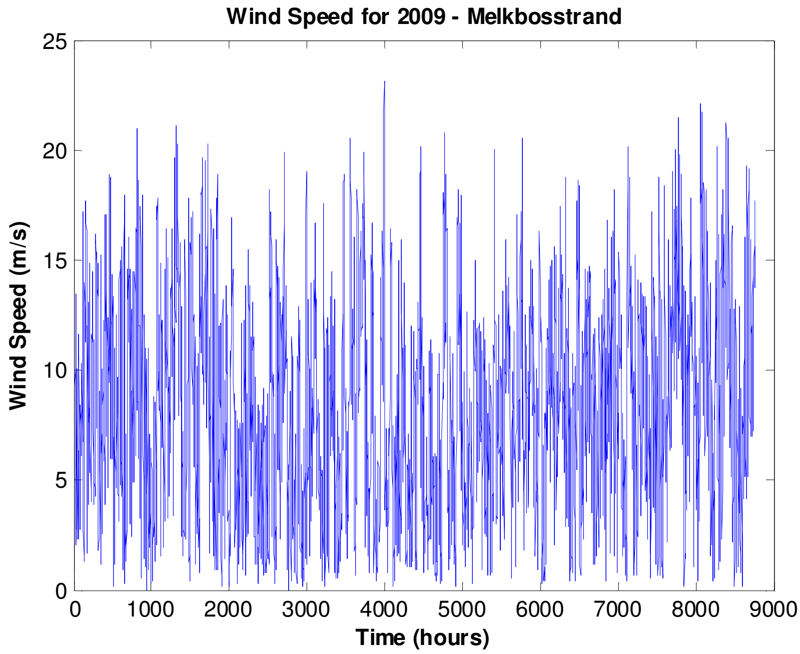

Figure B.1: Wind speed converted from measurement height of 85m to wind generator turbine hub of 91m

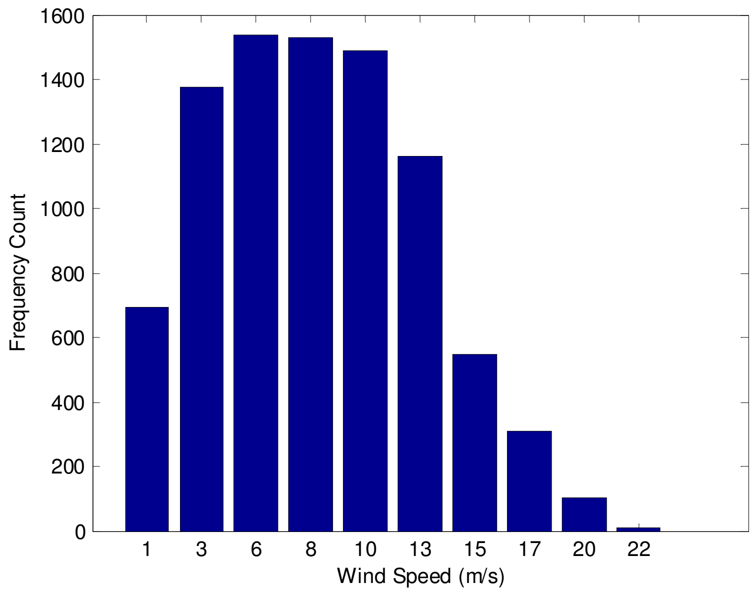

Figure 3.4: Frequency distribution of prominent wind speeds for the converted wind speed

11. Appendix C: MATLAB Code for Capacity Sizing Algorithm

```
%read hours
hours = xlsread('analytical_data2.xlsx' ,
'sheet5','A5:A8764');

%read solar radiation
rad = xlsread('analytical_data2.xlsx' ,
'sheet5','C5:C8764');

%read temperature
temp = xlsread('analytical_data2.xlsx' ,
'sheet5','E5:E8764');

%read Windspeed - converted
winsp = xlsread('analytical_data2.xlsx' ,
'sheet5','K5:K8764');


%Electrical Load for Safety Critical System
loadE = 4.205e06;

%intialize general values
storage1 = zeros(8760,1);
avail = 0;

%Energy storage Capacity variable
Max_Avail_E = 130e06;

%number of PV modules and Wind turbines depends on
constraints
Npv = 51915;
Nw = 1;

while avail < 0.9999

    %increment values depending on simulation objective
    Nw = Nw + 1;
    Npv = Npv + 1;

%initialize values
storage = zeros(8760,1);
solarE = zeros(8760,1);
windE = zeros(8760,1);
netE = zeros(8760,1);
bad_hours = 0;
```

```
for i=1:1:8760

      solarE(i) = 0.95*Npv*355*(rad(i)/1000)*(1-
0.0037*(temp(i)+(0.0325*rad(i))-25));
      if winsp(i)<3
          windE(i)=0;
      elseif winsp(i)>3.1 & winsp(i)<11
          windE(i)= Nw*2.4e06*(winsp(i)^2 - 3^2)/(11^2-
3^2);
      elseif winsp(i)>11
          windE(i)=Nw*2.4e06;
      end

      netE(i)= (solarE(i)+windE(i))-loadE;

      if i == 1
          storage(i)= Max_Avail_E;
      else

      storage(i) = storage(i-1)+netE(i);
      end

      if storage(i)> Max_Avail_E
         storage(i)=Max_Avail_E;
       end

      if storage(i) < 0.05e06
        storage(i) = 0.05e06;
         bad_hours = bad_hours + 1;
      end
end

avail = 1-(bad_hours/8760);
end


%adjust the units
storage1 = storage/1e6;


%Plot the desired trends
plot(hours, storage1)

%Display electrical power availability
avail
```

```
%Provide labels for the desired trends

xlabel({'Time (hours)','(b)'},'FontWeight','bold');
ylabel('Battery Bank Energy (MWh)','FontWeight','bold');
title('Depth of Battery Bank
Discharge','FontWeight','bold');
```

12. Appendix D: Monte Carlo Simulation Algorithm

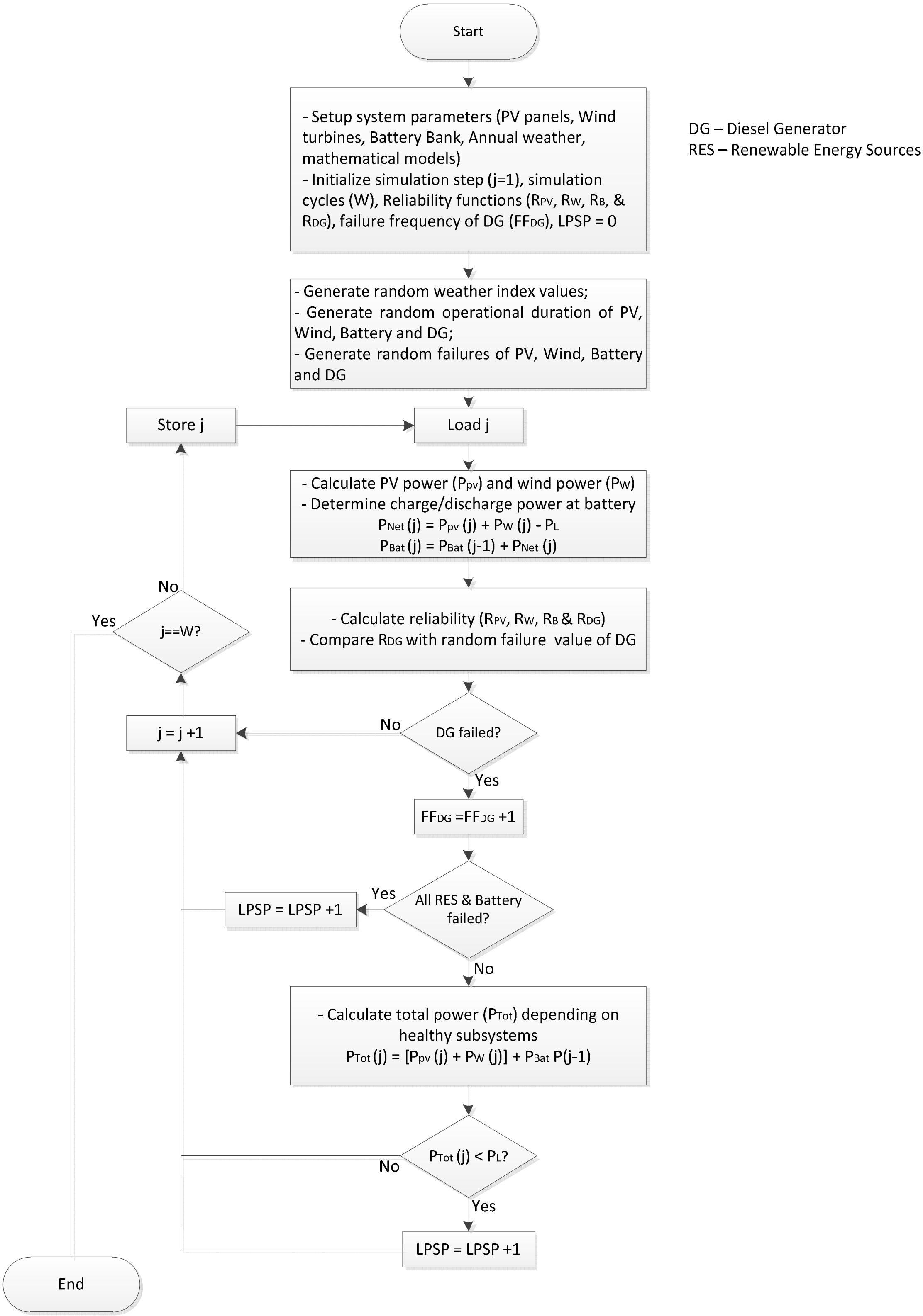

13. Appendix E: MATLAB Code for LPSP Calculation using MCS Algorithm

```
%Loss of power supply probability calculation

%Load weather data

hours = xlsread('analytical_data2.xlsx' ,
'sheet5','A5:A8764'); %Hours
rad = xlsread('analytical_data2.xlsx' ,
'sheet5','C5:C8764'); %Solar radiation
temp = xlsread('analytical_data2.xlsx' ,
'sheet5','E5:E8764');%Temperature
winsp = xlsread('analytical_data2.xlsx' ,
'sheet5','K5:K8764'); %Windspeed - converted

%Setup system parameters
loadE = 4.205e06; %Electrical Load for Safety Critical
System
Npv = 51915; %Number of PV panels
Nw = 10; %Number of wind turbines
B_Max = 80e06;%Intial Battery capacity 80 MWh;
W = 1e06;%Number of simulation cycles
h = 8760; %hours in one year

%Warranty parameters
PvW = 2.19e05; %PV warranty
WdW = 1.752e05; %Wind warranty
BdW = 8.76e04; %Battery warranty
DGW = 6000; %Diesel Generator warranty

%Intialize parameters
storage = zeros(W,1);% Battery storage vector
solarE = zeros(W,1);% Solar energy vector
windE = zeros(W,1);% Wind energy vector
netE = zeros(W,1);% Net energy vector

PV_R = zeros(W,1); %PV reliability function
WD_R = zeros(W,1); %Wind reliability function
BD_R = zeros(W,1); %Battery reliability function
DG_R = zeros(W,1); %Diesel Generator reliability function

F_PV = 0; % Failure frequency count of PV
F_WD = 0; % Failure frequency count of Wind
F_BD = 0; % Failure frequency count of Battery
F_DG = 0; % Failure frequency count of Diesel Generator

LPSP_C = 0; % LPSP counter
```

```
P_TOT = zeros(W,1); %Total power available
P_NET = zeros(W,1); %Net power available

%Generate random samples
OP_PV = randi(PvW,W,1); %Operation duration of PV
OP_WD = randi(WdW,W,1); %Operation duration of Wind
OP_BD = randi(BdW,W,1); %Operation duration of Battery
OP_DG = randi(DGW,W,1); %Operation duration of DG
W_Indx = randi(h,W,1);% random weather index value

R_PV = rand(W,1); %random reliability of PV
R_WD = rand(W,1); %random reliability of Wind
R_BD = rand(W,1); %random reliability of Battery
R_DG = rand(W,1); %random reliability of Diesel generator


for i=1:1:W

    %Calculate power generated by RES
     solarE(i) = 0.95*Npv*355*(rad(W_Indx(i))/1000)*(1-
0.0037*(temp(W_Indx(i))+(0.0325*rad(W_Indx(i)))-25));
     windE(i)= Nw*2.4e06*(winsp(W_Indx(i))^2 - 3^2)/(11^2-
3^2);

    %Store energy in the battery
    if i == 1
        %Set initial Battery value
        storage(i)= B_Max;
    else
        %Store energy in the battery at cycle number i
        P_NET(i) = (solarE(i) + windE(i)) - loadE;
        storage(i) = storage(i-1)+ P_NET(i);
    end

    %Reliability function of PV
    PV_R(i) = 1 - (exp(1)^((-4.57e-
6)*(OP_PV(i)))*exp(1)^((-4.57e-6)*(OP_PV(i)))*exp(1)^((-
6.37e-7)*(OP_PV(i)))*exp(1)^((-1.61e-
7)*(OP_PV(i)))*exp(1)^((-5.93e-7)*(OP_PV(i))));

    %Reliability function of Wind
    WD_R(i) = 1 - (exp(1)^((-2.85e-
5)*(OP_WD(i)))*exp(1)^((-1.43e-5)*(OP_WD(i)))*exp(1)^((-
1.4e-5)*(OP_WD(i)))*exp(1)^((-5.93e-
7)*(OP_WD(i)))*exp(1)^((-1.21e-5)*(OP_WD(i)))*exp(1)^((-
6.73e-7)*(OP_WD(i)))*exp(1)^((-1.61e-7)*(OP_WD(i))));
```

```
    %Reliability function of Battery
    BD_R(i) = 1 - (exp(1)^((-1.14e-
5)*(OP_BD(i)))*exp(1)^((-1.21e-4)*(OP_BD(i)))*exp(1)^((-
6.37e-7)*(OP_BD(i)))*exp(1)^((-5.93e-
7)*(OP_BD(i)))*exp(1)^((-1.61e-7)*(OP_BD(i))));

    %Reliability function of Diesel Generator
    DG_R(i) = 1 - (exp(1)^((-2.74e-3)*(OP_DG(i))));

    %If DG has failed then calculate LPSP for RES
    if DG_R(i) < R_DG(i)
        %Count number of DG failures
        F_DG = F_DG + 1;
        %All RES components have failed
        if PV_R(i) < R_PV(i) & WD_R(i) < R_WD(i) & BD_R(i)
< R_BD(i)
            LPSP_C = LPSP_C+1;
        end
        %All RES components are healthy
        if PV_R(i) > R_PV(i) & WD_R(i) > R_WD(i) & BD_R(i)
> R_BD(i)

            %Calculate Total Power available
            if i == 1
                P_TOT(i) = solarE(i) + windE(i) +
storage(i);
            else
                P_TOT(i) = solarE(i) + windE(i) +
storage(i-1);
            end

               if P_TOT(i) < loadE
                    %Count LPSP for total energy lower than
load
                    LPSP_C = LPSP_C+1;
                end
        end

        %PV and Wind healthy and with Battery failed
        if PV_R(i) > R_PV(i) & WD_R(i) > R_WD(i) & BD_R(i)
< R_BD(i)

               P_TOT(i) = solarE(i) + windE(i);
               if P_TOT(i) < loadE
                    %Count LPSP for total energy lower than
load
```

```
                    LPSP_C = LPSP_C+1;
                end
        end

        %PV healthy, Wind failed and Battery healthy
        if PV_R(i) > R_PV(i) & WD_R(i) < R_WD(i) & BD_R(i)
> R_BD(i)

            %Calculate Total Power available
            if i == 1
                P_TOT(i) = solarE(i) + storage(i);
            else
                P_TOT(i) = solarE(i) + storage(i-1);
            end

               if P_TOT(i) < loadE
                    %Count LPSP for total energy lower than
load
                    LPSP_C = LPSP_C+1;
                end
        end

        %PV failed, Wind healthy and Battery healthy
        if PV_R(i) < R_PV(i) & WD_R(i) > R_WD(i) & BD_R(i)
> R_BD(i)

            %Calculate Total Power available
            if i == 1
                P_TOT(i) = windE(i) + storage(i);
            else
                P_TOT(i) = windE(i) + storage(i-1);
            end

               if P_TOT(i) < loadE
                    %Count LPSP for total energy lower than
load
                    LPSP_C = LPSP_C+1;
                end
        end

        %PV failed, Wind failed and Battery healthy
        if PV_R(i) < R_PV(i) & WD_R(i) < R_WD(i) & BD_R(i)
> R_BD(i)

            %Calculate Total Power available
            if i == 1
                P_TOT(i) = storage(i);
```

```
            else
                P_TOT(i) = storage(i-1);
            end

               if P_TOT(i) < loadE
                    %Count LPSP for total energy lower than
load
                    LPSP_C = LPSP_C+1;
                end
        end

        %PV failed, wind healthy and Battery failed
        if PV_R(i) < R_PV(i) & WD_R(i) > R_WD(i) & BD_R(i)
< R_BD(i)

            %Calculate Total Power available
            P_TOT(i) = windE(i);

               if P_TOT(i) < loadE
                    %Count LPSP for total energy lower than
load
                    LPSP_C = LPSP_C+1;
                end
        end

    end
end

LPSP_V = LPSP_C/W*100; %LPSP for RES
DG_V = F_DG/W*100; %LPSP for DG alone

%Various configurations
c = {'Conf. 1','Conf. 2'};

y = [LPSP_V DG_V];
bar(y)
set(gca,'xticklabel',c)
ylabel('LPSP','FontWeight','bold');
title('LPSP for Nuclear Micro-Grid','FontWeight','bold');
```

14. Appendix F: Flow-Charts for Capacity Sizing Algorithms

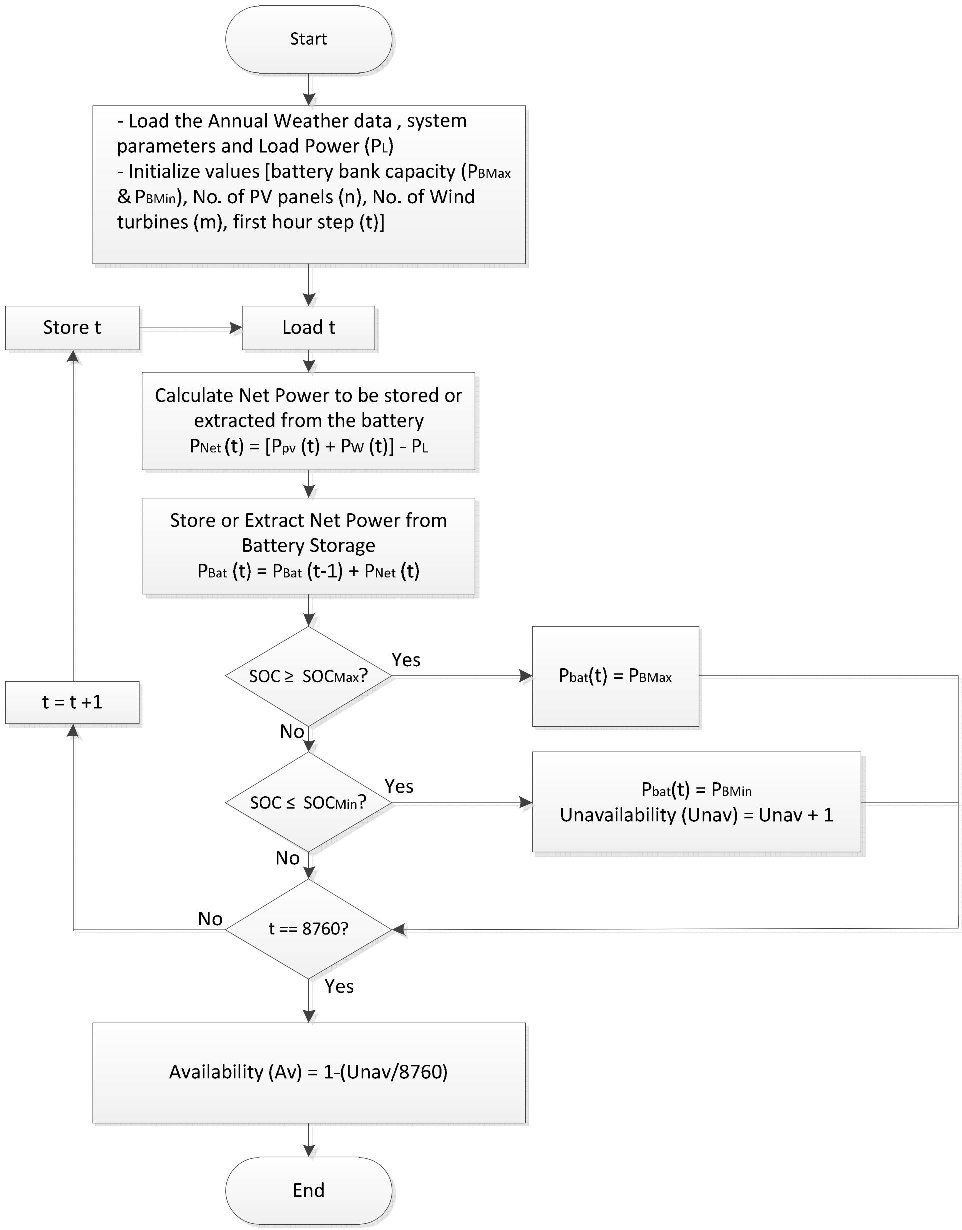

Figure F.1: Flowchart for the availability calculation algorithm

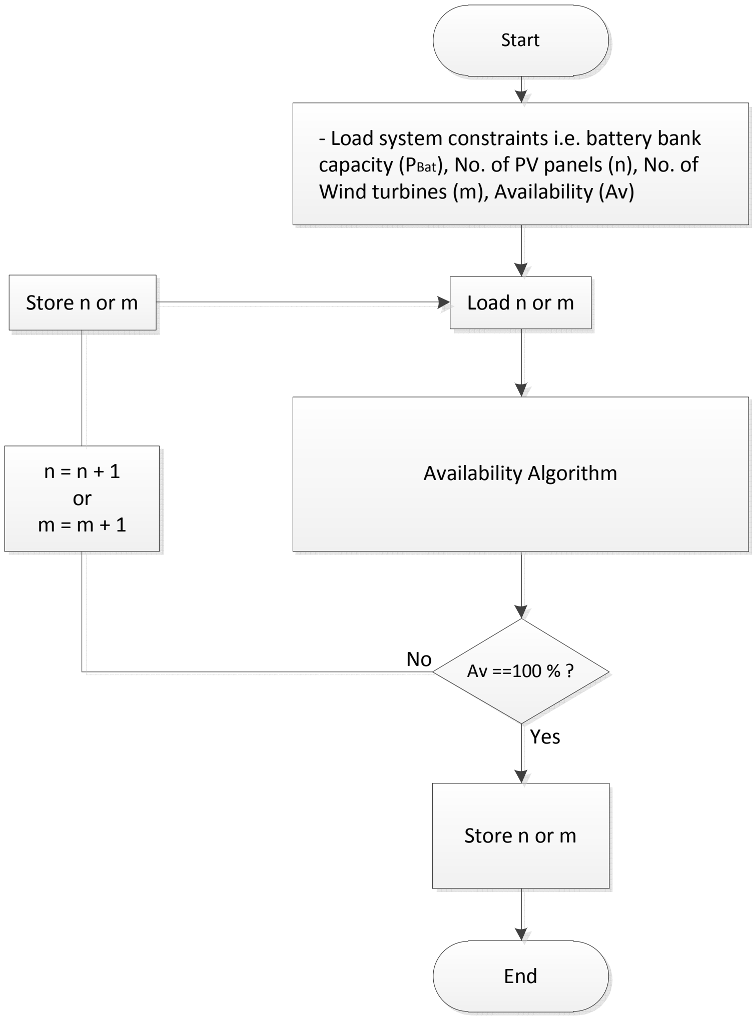

Figure F.2: Flowchart for the sizing algorithm

15. References

[1] International Atomic Energy Agency. *Fundamental Safety Principles;* IAEA Safety Standard Series No: SF-1 IAEA, Vienna 2006

[2] International Atomic Energy Agency. *Safety of Nuclear Power Plants: Design;* IAEA Safety Standard Series No: SSR-2/1 IAEA, Vienna 2012

[3] Zhou J, He L, Li C, Cao Y, Liu X, Geng Y. *What's the difference between traditional power grid and smart grid? — From dispatching perspective*; IEEE PES Asia-Pacific Power and Energy Engineering Conference (APPEEC), 2013, Pg. 1 – 6

[4] Kusko A, Dedad J. *Stored Energy Short-term and long-term energy storage methods*; IEEE Industry Applications Magazine, 2007 Pg. 66-72

[5] International Atomic Energy Agency. *Periodic Safety Review for Nuclear Power Plants;* IAEA Specific Safety Guide No: SSG-25 IAEA, Vienna 2013

[6] Fukushima Accident
http://www.world-nuclear.org/info/Safety-and-Security/Safety-of-Plants/Fukushima-Accident/
Last accessed 14 June 2016

[7] Assessment of DC Backup Power Technology Options for Nuclear Power Generation Stations
http://www.epri.com/abstracts/Pages/ProductAbstract.aspx?ProductId=000000003002001937
Last accessed 14 June 2016

[8] Office for Nuclear Regulation. *Japanese earthquake and tsunami: Implications for the UK nuclear industry*; ONR Report ONR-FR-REP-11-002 Rev 2, United Kingdom, Sept 2011

[9] Nuclear Energy Agency/Organisation for Economic Co-Operation and Development. *The Fukushima Daiichi Nuclear Power Plant Accident: OECD/NEA Nuclear Safety Response and Lessons Learnt;* NEA No. 7161 OECD France, 2013

[10] Olivares D.E, Mehrizi-Sani A, Etemadi, A.H, Canizares C.A, Iravani R, Kazerani, M, Hajimiragha A.H, Gomis-Bellmunt O, Saeedifard M, Palma-Behnke R, Jimenez-Estevez G.A, Hatziargyriou N.D. *Trends in Microgrid Control;* Smart Grid, IEEE Transactions on (Volume:5 , Issue: 4), 20 May 2014, Pg. 1905 – 1919

[11] Gogula R R. *A sustainable hybrid/ off grid power generation systems suitable for a remote coastal area in Oman*; Proceedings of the 8th IEEE GCC Conference and Exhibition, Muscat, Oman, 1-4 February, 2015

[12] Micrograds and Secure Power Supply
http://www.disaster-resource.com/index.php?option=com_content&view=article&id=2337:micrograds-and-secure-power-supply&catid=8:facility-issues
Last accessed 14 June 2016

[13] Lamarsh J R, Baratta A J. *Introduction to Nuclear Engineering,* third edition. Prentice Hall Inc. New Jersey

[14] Santosh B. Bopche S B, Sridharan A. *Experimental investigations on decay heat removal in advanced nuclear reactors using single heater rod test facility: Air alone in the annular gap*; Experimental Thermal and Fluid Science Journal Vol. 34 2010 pp. 1456-1474

[15] International Atomic Energy Agency. *Passive Safety Systems and Natural Circulation in Water Cooled Nuclear Power Plants;* IAEA Technical Document No: IAEA –TECDOC–1624, Vienna 2009

[16] Three Mile Island Accident
http://www.world-nuclear.org/information-library/safety-and-security/safety-of-plants/three-mile-island-accident.aspx
Last accessed 06 July 2016

[17] Lipták Béla. *Automation can prevent the next Fukushima*. International society of Automation, USA, 2014

[18] Fukushima Accident
http://www.world-nuclear.org/information-library/safety-and-security/safety-of-plants/fukushima-accident.aspx
Last accessed 11 July 2016

[19] International Atomic Energy Agency. *The Fukushima Daiichi Accident Technical Volume 1 – Description and Context of the Accident;* IAEA STI/PUB/1710, Austria 2015

[20] International Atomic Energy Agency. *Electric Grid Reliability and Interface with Nuclear Power Plants;* IAEA Nuclear Energy Series No: NS-T-3.8 IAEA, Vienna 2012

[21] Institute of Electrical and Electronics Engineers. *IEEE Standard Criteria for Class 1E Power Systems for Nuclear Power Generating Stations*; Nuclear Power Engineering Society, IEEE Std 308-2001 IEEE New York USA 1 Mar 2002

[22] International Atomic Energy Agency. *Design of Emergency Power Systems for Nuclear Power Plants;* IAEA Safety Guide Series No: NS-G-1.8 IAEA, Austria 2004

[23] United States Nuclear Regulatory Commission. *General Design Criteria for Nuclear Power Plants – Criterion 17: Electric Power Systems;* 10CRF50 Appendix A, USNRC Washington DC USA

[24] Olivares D.E, Mehrizi-Sani A, Etemadi, A.H, Canizares C.A, Iravani R, Kazerani, M, Hajimiragha A.H, Gomis-Bellmunt O, Saeedifard M, Palma-Behnke R, Jimenez-Estevez G.A, Hatziargyriou N.D. *Trends in Microgrid Control;* Smart Grid, IEEE Transactions on (Volume:5 , Issue: 4), 20 May 2014, Pg. 1905 – 1919

[25] Department of Energy Office of Electricity Delivery and Energy Reliability. (2012). *Summary Report: 2012 DOE Microgrid Workshop;* Available Online: http://energy.gov/sites/prod/files/2012%20Microgrid%20Workshop%20Report%2009102012.pdf, Last accessed 05 August 2016

[26] Miveh M. R, Gandomkar M, Mirsaeidi S, Gharibdooost M. R. *A Review on Protection Challenges in Microgrids*; IEEE Proceedings of 17th Conference on Electrical Power Distribution Networks (EPDC), 2-3 May 2012, Pg. 1-5

[27] Majumder Rikwik. *Some Aspects of Stability in Microgrids*; IEEE Transactions on Power Systems, August 2013, Vol. 28, No.3

[28] Soni N, Doolla S, Chandorkar M. C. *Improvement of Transient Response in Microgrids Using Virtual Inertia;* IEEE transactions on Power Delivery, Vol.28, No.3 July 2013

[29] Pecas Lopes J. A, Moreira C. L, Madureira A. G. *Defining Control Strategies for MicroGrids Islanded Operation;* IEEE transactions on Power Systems, Vol.21, No.2, May 2006

[30] Alegria E, Brown T, Minear E, Lasseter R H. *CERTS Microgrid Demonstration with Large Scale Energy Storage and Renewable Generation*; IEEE Transactions on Smart Grid 2013, Pg. 937 – 943

[31] Hirose K, Shimakage T, Reilly J. T, Irie H. *The Sendai Microgrid Operational Experience in the Aftermath of the Tohoku Earthquake: A Case Study;* Available Online: http://www.nedo.go.jp/content/100516763.pdf, Last accessed 05 August 2016

[32] Abbey C, Cornforth D, Hatziargyriou N, Hirose K, Kwasinski A, Kyriakides E, Platt G, Reyes L, Suryanarayanan S. *Powering Through the Storm: Microgrids Operation for More Efficient Disaster Recovery;* IEEE Power and Energy Magazine, Vol.12, No.3 June 2014 Pg. 67-76

[33] Matsuura M, Hisamochi K, Sato S, Moriya K. *Lessons Learned from Fukushima Daiichi Nuclear Power Station Accident and Consequent Safety Improvements;* Hitachi Review Vol. 62, No. 1 2013, Pg. 75 – 80,
Available Online: http://www.hitachi.com/rev/pdf/2013/r2013_01_112.pdf, Last accessed 05 August 2016

[34] Nuclear Energy Agency/Organisation for Economic Co-Operation and Development. *The Fukushima Daiichi Nuclear Power Plant Accident: OECD/NEA Nuclear Safety Response and Lessons Learnt;* NEA No. 7161 OECD France, 2013

[35] Nuclear Energy Institute. *Diverse and Flexible Coping Strategies (FLEX) Implementation Guide;* Aug 2012, Available Online:
http://www.nrc.gov/docs/ML1222/ML12221A205.pdf, Last accessed 05 August 2016

[36] Akkaynak D, *Use of Fuel Cells for Improving On-Site Emergency Power Availability and Reliability at Nuclear Power Plants;* Dissertation for Master of Science in Aeronautics and Astronautics, Massachusetts Institute of Technology, June 2005

[37] Nuclear Energy Agency/Organisation for Economic Co-Operation and Development. *Robustness of Electrical Systems of Nuclear Power Plants in Light of the Fukushima Daiichi Accident (ROBELSYS);* Workshop Proceedings, Paris, France, 1-4 April 2014, NEA No. NEA/CSNI/R(2015)4, Available Online:
https://www.oecd-nea.org/nsd/docs/2015/csni-r2015-4.pdf, Last accessed 05 May 2017

[38] Solar Energy
http://www.energy.gov.za/files/esources/renewables/r_solar.html
Last accessed 26 August 2016

[39] Rashad M, El-Samahy A. A, Daowd M, Amin A. M. A. *A comparative Study on Photovoltaic and Concentrated Solar Thermal Power Plants*

[40] Renewables 2016 Global Status Report
http://www.ren21.net/wp-content/uploads/2016/10/REN21_GSR2016_FullReport_en_11.pdf
Last accessed 12 February 2017

[41] NERSA Monitoring of Renewable Energy Performance
http://www.nersa.org.za/Admin/Document/Editor/file/Electricity/SustainableEnergy/MONITORING%20RE%20PERFORMANCE%20ISSUE%207%20APRIL_2016.pdf
Last accessed 12 February 2017

[42] Electric Research Institute (EPRI) White Paper. *Solar Photovoltaics: Status, Costs, and Trends*; December 2009

[43] Martin A. Green1, Keith Emery, Yoshihiro Hishikawa, Wilhelm Warta,Ewan D. Dunlop. *Solar cell efficiency tables (version 47)*; Progress in Photovoltaics: Research and Applications, Wiley Online Library, 24 November 2015

[44] Özge Demir Başak, Bekir Sami Sazak. *Effect of developments on a PV system efficiency*; 2013 4th International Symposium on Electrical and Electronics Engineering (ISEEE), Pages: 1 - 6

[45] Steiner M, Siefer G, Schmidt T, Wiesenfarth M, Dimroth F, Bet W. A. *43% Sunlight to Electricity Conversion Efficiency Using CPV*; IEEE Journal Of Photovoltaics, VOL. 6, NO. 4, JULY 2016

[46] PV Installation Professional Resource Guide – NABCEP
http://www.nabcep.org/wp-content/uploads/2013/08/NABCEP-PV-Guide-7-16-13-W.pdf
Last accessed 12 February 2017

[47] Rautenbach K. F. *Characterisation of a solar roof tile (SunSlates™) with focus on local applicability and conditions*; Project report for the degree of Master of Engineering, University of Stellenbosch, December 2008

[48] Boxwell M. *Solar Electricity Handbook*; Greenstream Publishing, United Kingdom, 2011

[49] Sassine E. *Optimal solar panels positioning for Beirut*; 7th International Renewable Energy Congress (IREC), 2016, Pages: 1 - 5

[50] Patel M. R. *Wind and Solar Power Systems Design, Analysis and Operation*; 2^{nd} Ed. Tylor & Francis Group, New York, USA, 2006

[51] Wind Atlas for South Africa
http://www.wasaproject.info/
Last accessed 12 February 2017

[52] Onshore Geared Wind Turbine SWT-2.3-101
http://www.energy.siemens.com/nl/en/renewable-energy/wind-power/platforms/g2-platform/wind-turbine-swt-2-3-101.htm#content=Technical%20Specification
Last accessed 12 February 2017

[53] List of ocean plants
https://en.wikipedia.org/wiki/List_of_wave_power_stations
Last accessed 12 February 2017

[54] Frick J. *Implementation Plan for the Stellenbosch Wave Energy Converter on the South-West Coast of South Africa*; Master's thesis, Energy Research Center, University of Cape Town, May 2014

[55] Todreas N. E,Kazimi M. S. Nuclear Systems: Thermal Hydraulic Fundamentals, Second Edition, Volume 1; 2nd Ed, Tylor & Francis Group, New York, USA, 2012

[56] Thermionic converter
https://en.wikipedia.org/wiki/Thermionic_converter
Last accessed 12 February 2017

[57] New generator creates electricity directly from heat
http://physicsworld.com/cws/article/news/2013/dec/09/new-generator-creates-electricity-directly-from-heat
Last accessed 12 February 2017

[58] Institute of Electrical and Electronics Engineers. *IEEE Standard Criteria for Diesel Generator Units Applied as Standby Power Supplies for Nuclear Power Generating Stations*; Nuclear Power Engineering Committee, IEEE Std. 387-1995 IEEE New York USA 12 December 1995

[59] Thermoelectric generator
https://en.wikipedia.org/wiki/Thermoelectric_generator
Last accessed 12 February 2017

[60] Rowe D, M. *Thermoelectric Waste Heat Recovery as a Renewable Energy Source*; International Journal of Innovations in Energy Systems and Power, Vol. 1, no. 1 (November 2006)

[61] Xuan X.C,Li D. Optimization of a combined thermionic–thermoelectric generator; Journal of Power Sources 115, 2003, Pg. 167–170

[62] US Nuclear Regulatory Commission. *Fuel-oil Systems for Standby Diesel Generators*; Regulatory guide 1.137, October 1979

[63] Institute of Electrical and Electronics Engineers. *IEEE Recommended Practice for Emergency and Standby Power Systems for Industrial and Commercial Applications*; Power Systems Engineering Committee, IEEE Std. 446-1995 IEEE New York USA 20 April 2001

[64] List of countries by proven oil reserves
https://en.wikipedia.org/wiki/List_of_countries_by_proven_oil_reserves#cite_note-OPEC-11
Last accessed 12 February 2017

[65] Worldwide reserves, oil production post modest rise
http://www.ogj.com/articles/print/volume-111/issue-12/special-report-worldwide-report/worldwide-reserves-oil-production-post-modest-rise.html
Last accessed 12 February 2017

[66] Biodiesel Vehicle Emissions
http://www.afdc.energy.gov/vehicles/diesels_emissions.html
Last accessed 12 February 2017

[67] Power Stations and Pumped Storage Schemes
http://www.eskom.co.za/Whatweredoing/ElectricityGeneration/PowerStations/Pages/Power_Stations_And_Pumped_Storage_Schemes.aspx
Last accessed 12 February 2017

[68] Ingula Pumped Storage Scheme
http://www.eskom.co.za/Whatweredoing/NewBuild/IngulaPumpedStorage/Pages/Ingula_Pumped_Storage_Scheme.aspx
Last accessed 12 February 2017

[69] Poullikkas, A. A comparative overview of large-scale battery systems for electricity storage; Available at http://www.sciencedirect.com

[70] Luo X, Wang J, Dooner M, Clarke J. *Overview of current development in electrical energy storage technologies and the application potential in power system operation*; Applied Energy, Volume 137, 1 January 2015, Pages 511–536

[71] Chena H, Conga T. N, Yanga W, Tanb C, Lia Y, Ding Y. *Progress in electrical energy storage system: A critical review*; Progress in Natural Science, Volume 19, Issue 3, 10 March 2009, Pages 291–312

[72] Gnanapragasam N, Ryland D, Suppiah S. *Status of energy storage options for electricity from nuclear power plants*; IEEE International Conference on Smart Energy Grid Engineering , 2013, Pages: 1 - 11

[73] Hacker V, Nestl S, Friedrich T. *Progress in hydrogen production and storage technologies*; International Conference on the Domestic Use of Energy (DUE), 2016, Pages: 1 - 6

[74] Hydrogen Energy Storage
http://energystorage.org/energy-storage/technologies/hydrogen-energy-storage
Last accessed 12 February 2017

[75] Mekhilefa S, Saidur R, Safari A. *Comparative study of different fuel cell technologies*; Renewable and Sustainable Energy Reviews, Volume 16, Issue 1, January 2012, Pages 981–989

[76] Divya1 K.C, Østergaard J. *Battery energy storage technology for power systems—An overview*; Electric Power Systems Research Volume 79, Issue 4, April 2009, Pages 511–520

[77] Hadjipaschalis I, Poullikkas A, Efthimiou V. *Overview of current and future energy storage technologies for electric power applications*; Renewable and Sustainable Energy Reviews, Volume 13, Issues 6–7, August–September 2009, Pages 1513–1522 –

[78] Toshiba Completes Delivery of World's largest Lithium-ion Battery Energy Storage System in Operation
https://www.toshiba.co.jp/sis/en/topics/2016/20160226.htm
Last accessed 12 February 2017

[79] Krieger E. M, Cannarella J, Arnold C. B. *A comparison of lead-acid and lithium-based battery behavior and capacity fade in off-grid renewable charging applications*; Energy, Volume 60, 1 October 2013, Pages 492–500

[80] Tesla to deploy 'largest li-ion battery project in the world' with 80 MWh in Powerpacks
https://electrek.co/2016/09/15/tesla-to-deploy-largest-li-ion-battery-project-in-the-world-with-80-mwh-in-powerpacks/
Last accessed 12 February 2017

[81]AES to Help SCE Meet Local Power Reliability with PPA for 100 MW of Energy Storage in California
http://aesenergystorage.com/2014/11/05/aes-help-sce-meet-local-power-reliability-20-year-power-purchase-agreement-energy-storage-california-new-facility-will-provide-100-mw-interconnected-storage-equivalent-200-mw/
Last accessed 12 February 2017

[82] 38,000 Tesla Powerwall Reservations In Under A Week
https://cleantechnica.com/2015/05/07/38000-tesla-powerwall-reservations-in-under-a-week-tesla-elon-musk-transcript/
Last accessed 12 February 2017

[83] Kumagai K. *A battery as big as the grid*; IEEE Spectrum, 2012 Volume: 49, Issue: 1, Pages: 45 - 46

[84] Alotto P, Guarnieri M, Moro F, Stella A. *Redox flow batteries for large scale energy storage*; IEEE International Energy Conference and Exhibition (ENERGYCON), 2012 Pages: 293 - 298

[85] Hossain E, Kabalci E, Bayindir R, Perez R. *A Comprehensive Study on Microgrid Technology*; International Journal Of Renewable Energy Research, Ramazan Bayindir et al. ,Vol. 4, No. 4, 2014

[86] Lopes J. A. P, Moreira C. L, Madureira A. G, Resende F. O, Wu X, Jayawarna N, Zhang Y, Jenkins N, Kanellos F, Hatziargyriou N. *Control strategies for microgrids emergency operation;* IEEE International Conference on Future Power Systems 2005, Pages: 6

[87] Chandorkar M. C, Divan D. M, Adapa R. *Control of parallel connected inverters in standalone AC supply systems*; IEEE Transactions on Industry Applications, Volume: 29, Issue: 1, 1993, Pages: 136 – 143

[88] Du W, Jiang Q, Erickson M. J, Lasseter R. H. *Voltage-Source Control of PV Inverter in a CERTS Microgrid*; IEEE Transactions on Power Delivery, Volume: 29, Issue: 4, 2014, Pages: 1726 - 1734

[89] Guerrero J. M, Loh P. C, Lee T, Chandorkar m. *Advanced Control Architectures for Intelligent Microgrids—Part II: Power Quality, Energy Storage, and AC/DC Microgrids*; IEEE Transactions on Industrial Electronics, Volume: 60, Issue: 4, 2013, Pages: 1263 - 1270s

[90] Guerrero D. Wu, Guerrero J. M, Vasquez J. C, Dragicevic T, Tang F. *Coordinated power control strategy based on primary frequency-signaling for islanded microgrids*; Proc. Energy Conversion Congress and Exposition (ECCE), pp.1033,1038, 15-19 Sept. 2013

[91] Olivares D E, Canizares C. A, Kazerani M, *A centralized optimal energy management system for microgrids*; 2011 IEEE Power and Energy Society General Meeting, pp.1-6, 24-29 July 2011.

[92] Wu D, Tang F, Guerrero J. M, Vasquez J. C, Chen G, Sun L. *Autonomous active and reactive power distribution strategy in islanded microgrids*; IEEE Applied Power Electronics Conference and Exposition - APEC 2014, Pages: 2126 - 2131

[93] Belmilia H, Haddadib M, Bachac S, Almia M. F, Bendiba B. *Sizing stand-alone photovoltaic–wind hybrid system: Techno-economic analysis and optimization;* Renewable and Sustainable Energy Reviews Volume 30, February 2014, Pages 821–832

[94] Han H, Hou X, Yang J, Wu J, Su M, Guerrero J. M. *Review of Power Sharing Control Strategies for Islanding Operation of AC Microgrids*; IEEE Transactions On Smart Grid, VOL. 7, NO. 1, JANUARY 2016

[95] Institute of Electrical and Electronics Engineers. *IEEE Guide for Design, Operation and Integration of Distributed Resource Island Systems with Electric Power Systems*; IEEE Std. 1547.4-2011. IEEE New York USA 20 July 2011

[96] Kennedy S. *Reliability evaluation of islanded microgrids with stochastic distributed generation*; 2009 IEEE Power & Energy Society General Meeting, Pages: 1 - 8

[97] Gan L. K, Shek J. K. H, Mueller M. a. *Hybrid wind–photovoltaic–diesel–battery system sizing tool development using empirical approach, life-cycle cost and performance analysis: A case study in Scotland*; Energy Conversion and Management, Volume 106, December 2015, Pages 479–494

[98] He J, Li Y. W, Guerrero J. M, Blaabjerg F, Vasquez J. C. *An Islanding Microgrid Power Sharing Approach Using Enhanced Virtual Impedance Control Scheme*; IEEE Transactions on Power ElectronicsVolume: 28, Issue: 11, 2013, Pages: 5272 - 5282

[99] Zhanga P, Lib w, Lia S, Wanga Y, Xiaod W. *Reliability assessment of photovoltaic power systems: Review of current status and future perspectives*; Applied Energy, Volume 104, April 2013, Pages 822–833

[100] Harb S, Kedia M, Zhang H, Balog R. S. *Microinverter and string inverter grid-connected photovoltaic system — A comprehensive study*; 2013 IEEE 39th Photovoltaic Specialists Conference (PVSC), Pages: 2885 - 2890e s

[101] Pregelj A, Begovic M, Rohatgi A. *Impact of inverter configuration on PV system reliability and energy production*; Conference Record of the Twenty-Ninth IEEE Photovoltaic Specialists Conference, 2002, Pages: 1388 - 1391

[102] Variable speed versus fixed speed
http://easywindenergy.blogspot.co.za/2013/02/variable-speed-versus-fixed-speed.html
Last accessed 12 February 2017

[103] Tang Y, Xu L. *Adaptive Fuzzy Control of a Variable Speed Power Generating System with Doubly Excited Reluctance Machine*; IEEE Power Electronics Specialists Conference, Taipei 1994, p. 377 – 384

[104] Carroll J, McDonald A, McMillan D. *Reliability Comparison of Wind Turbines with DFIG and PMG Drive Trains*; IEEE Transactions on Energy Conversion 2015, Pages: 663 - 670

[105] Chen W. Comparison of doubly-fed Induction generator and Brushless doubly-fed Reluctance generator for Wind energy applications; Thesis for degree of Doctor of Philosophy, School of Electrical Engineering, Newcastle University, June 2014

[106] Polinder H, Van der Pijl F. F. A, De Vilder G. J, Tavner P. J. *Comparison of direct-drive and geared generator concepts for wind turbines*; IEEE Transactions on Energy Conversion, 2006, Pages: 725 - 733

[107] R. Koffler Transformer or transformerless UPS; Power Engineer Volume: 17, Issue: 3, June/July 2003, Page(s): 34 – 36, 28 July 2003

[108] Xu L, Ruan X, Mao C, Zhang B, Luo Y, *An Improved Optimal Sizing Method for Wind-Solar-Battery Hybrid Power System*; IEEE Transactions on Sustainable Energy, 2013, Volume: 4, Issue: 3, Pages: 774 - 785

[109] Hameed A. H, Elhagri M. T, Shaltout A. A, Aziz M. M. A. *Optimum sizing of hybrid WT/PV systems via open-space particle swarm optimization*; 2012 Second Iranian Conference on Renewable Energy and Distributed Generation, Pages: 55 – 60

[110] Patel M. R. *Wind and Solar Power Systems Design, Analysis and Operation*; 2nd Ed. Tylor & Francis Group, New York, USA, 2006

[111] SunPower® SunPowerPerformance Series | P17 ® Performance Series | P17
https://us.sunpower.com/sites/sunpower/files/media-library/data-sheets/ds-sunpower-p17-355-commercial-solar-panels.pdf
Last accessed 12 February 2017

[112] – Nordex N117/2400
http://www.nordex-online.com/fileadmin/MEDIA/Gamma/Nordex_Gamma_en.pdf
Last accessed 12 February 2017

[113] POWERPACK Utility and Business Energy Storage
https://www.tesla.com/powerpack
Last accessed 12 February 2017

[114] Kimball J W, Kuhn B T, Balog R S, *A System Design Approach for Unattended Solar Energy Harvesting Supply*; IEEE Transactions on Power Electronics, 2009 Pages: 952 - 962

[115] Ghahderijani M M, Barakati S M, Tavakoli S, *Reliability Evaluation of Stand-Alone Hybrid Microgrid Using Sequential Monte Carlo Simulation*; 2012 Second Iranian Conference on Renewable Energy and Distributed Generation, Pages: 33 - 38

[116] Wei H, Zijun H, Li F, Hongliang T, Li Z, *Reliability evaluation of Microgrid with PV-WG hybrid system*; 2011 4th International Conference on Electric Utility Deregulation and Restructuring and Power Technologies (DRPT), Pages: 1629 – 1632

[117] Guocheng S, Jingtao Z, Xiaoyan Z, Cheng L, Yusen Z, Xiangyu K, Xinpeng L. *Reliability Analysis Method for Microgrid with Intermittent Distributed Generations*; 2016 China International Conference on Electricity Distribution (CICED), Pages: 1 - 5

[118] Cepin M. *Assessment of power systems reliability methods and applications*; Springer-Verlag London Limited 2011

[119] Shi X. Micro-grid Reliability Modeling and Analysis Approaches; Thesis for Degree of Master of Science, University of Connecticut Graduate School, 2015

[120] Review of Failures of Photovoltaic Modules; Report No. IEA-PVPS T13-01:2014
http://www.isfh.de/institut_solarforschung/files/iea_t13_review_of_failures_of_pv_modules_final.pdf
Last accessed 12 February 2017

[121] Institute of Electrical and Electronics Engineers, *IEEE Recommended Practice for the Design of Reliable Industrial and Commercial Power Systems;* Power Systems Engineering Committee, IEEE Std. 493-2007 IEEE New York USA 7 February 2007

[122] SunPower® Module Degradation Rate
https://us.sunpower.com/sites/sunpower/files/media-library/white-papers/wp-sunpower-module-degradation-rate.pdf
Last accessed 12 February 2017

[123] AlMuhaini M, Tuffaha T. *Reliability assessment of a microgrid distribution system with pv and storage*; International Symposium on Smart Electric Distribution Systems and Technologies (EDST), 8-11 September 2015, Pg. 195 - 199

[124] Zhou D, Blaabjerg F, Franke T, Tønnes M, Lau M. *Comparison of Wind Power Converter Reliability with Low-Speed and Medium-Speed Permanent-Magnet Synchronous Generators*; IEEE Transactions on Industrial Electronics, vol. 62, no. 10, October 2015

[125] Echavarria E, Hahn B, Van Bussel G. J, Tomiyama T. Reliability of Wind Turbine Technology through Time; Journal of Solar Energy Engineering, ASME Vol. 130/ 031005-1

[126] Reliability Study:Emergency Diesel Generator Power System, 1987-1993 U.S. Nuclear Regulatory Commission NUREG/CR-5500, Vol. 5

[127] South African National Standards. *Protection against Lightning—Part 1: General Principles;* SANS 62305-1:2011SABS Standards Division, Pretoria, 2011